THE INTERACTION BETWEEN GAMMA-SECRETASE AND ITS INHIBITORS AND MODULATORS – STRUCTURAL INSIGHTS

A Dissertation

Presented to the Faculty of the Weill Cornell Graduate School

of Medical Sciences

in Partial Fulfillment of the Requirements for the Degree of

Doctor of Philosophy

by

Natalya Gertsik

May 2016

THE INTERACTION BETWEEN GAMMA-SECRETASE AND ITS INHIBITORS AND MODULATORS – STRUCTURAL INSIGHTS

Natalya Gertsik, Ph.D.

Cornell University, 2016

γ-Secretase is a four subunit, 20-pass transmembrane aspartyl protease that has sustained a great deal of scientific scrutiny due to its role in disease: γ-Secretase cleaves amyloid precursor protein, catalyzing the formation of amyloid plaques, which contribute to Alzheimer's disease (AD) pathogenesis, and it also cleaves Notch, the abnormal signaling of which can lead to cancer. γ-Secretase has been reported to process over 90 other substrates, all of which are type 1 transmembrane proteins. As a result of γ-secretase's enzymatic promiscuity and role in many pivotal cellular processes, it is a difficult target for drug development. γ-Secretase inhibitors (GSIs), which pan-inhibit γ-secretase so that it cannot cleave any of its substrates, are poor candidates for AD therapy as they cause toxicity. Still, GSIs are promising candidates for cancer. γ-Secretase modulators (GSMs), which reduce formation of the amyloidogenic Aβ42 without affecting Notch signaling, are promising therapeutics for AD, as they avoid the Notch-associated toxicities seen with GSI treatment. In order to develop safe and effective therapies for AD and cancer we must gain a deeper understanding of γ-secretase biology and the mechanism of action of GSIs/GSMs.

To understand the process of γ-secretase activation we developed CBAP-BPyne, a clickable photoaffinity probe that inhibits not only γ-secretase activity, but also endoproteolysis, an event required for formation of an active γ-secretase complex. We found that CBAP-BPyne specifically labels PS1-NTF and signal peptide peptidase

(SPP). Endoproteolysis is not well characterized and CBAP-BPyne is a valuable tool with which to further explore its mechanism.

To provide insight into the mechanism of action of GSIs/GSMs, we studied the impact of these compounds on the active sites of their target enzyme, γ-secretase, and on an off-target enzyme, SPP. We found that GSIs/GSMs impact the active site architecture of not only γ-secretase, but also SPP, suggesting that they may lead to a change in SPP activity and function, potentially causing toxicity in the clinic. Furthermore, we identified the binding site of BMS-708163, a clinically relevant GSI, on γ-secretase, marking the first time that a GSI/GSM was mapped onto its target with high precision.

BIOGRAPHICAL SKETCH

Natalya was born in Moscow, Russia and arrived in New York in 1995, at the age of seven. As a high school student, she worked for a summer at NYU Langone Medical Center in the Clinical Microbiology and Pathology laboratory of Dr. Philip M. Tierno. She performed her undergraduate studies in New York University on nearly a full scholarship, with a major in Biochemistry and a minor in English, and conducted her honors thesis in the laboratory of Dr. David Stokes at NYU Langone Medical Center, where she studied the erythrocyte cytoskeleton through electron microscopy. She won several Dean's Undergraduate Research Fund grants and was named a NYU Margaret and Herman Sokol Chemistry Scholar.

Natalya obtained her Ph.D. from Weill Cornell Graduate School under the mentorship of Dr. Yueming Li at Memorial Sloan Kettering Cancer Center. During her time as a doctoral student she published several academic and general interest articles, traveled to and presented at more than ten conferences and symposia, TAed graduate courses, and mentored students. Throughout college and up until her fourth year in graduate school, Natalya Ballroom danced. Later she danced only in lab, between incubation breaks, and at Pharmacology retreats. She continues to be an avid yoga and acroyoga practitioner.

For Raisa, my grandmother, who made the best mille feuilles

ACKNOWLEDGEMENTS

I'd like to thank Dr. Yueming Li for being a mentor, a friend, a confidante, and a pork-bun virtuoso. You have taught me not only how to think critically (so critically, in fact, that we basically don't believe anything), but also how to write cleverly, manage failure gracefully, and see the future hopefully. Your door was always open, whether it was to discuss scientific questions, manuscript revisions, or the state of the lab sorority union. I'm so grateful to have been a part of your group, where we did great science and drank Chinese liquor to celebrate.

Thank you to the Li lab members for their collaborative, friendly, fun-loving spirit. Thank you for lending a helping hand when I needed your expertise and a helping ear when I needed to vent about protein purification. Six years in your company has helped me grow as a scientist and human. I'd also like to thank all the people of the 19th floor of Zuckerman for the graduation parties, Christmas parties, pie days, BBQs, happy hours, and late-night science binges in the conference room. There's no floor like ours.

Thank you to Pascale Presendor for helping me do everything but science, which is a surprisingly large number of things! I can't imagine how our lab would function without you. From finding last minute recommendation letters for a grant to planning group outings and providing life advice, thank you.

I'm grateful to my committee members, Drs. Marilyn Resh and Andrew Koff, who persevered from my ACE exam to graduation, guiding and supporting along the way. Andy, your *Logic and Critical Analysis* course gave me the courage to stand up in a crowded auditorium and ask a question as a second year graduate student. I haven't stopped asking questions since.

I thank Drs. Douglas S. Johnson, Kieran F. Geoghegan, Christopher W. am Ende, and Thomas Eric Ballard for a long and fruitful collaboration. I began working with your group in 2011 and we have continued to publish together, culminating in a very exciting recent finding that is the cherry on top of my doctoral studies. Thank you, Doug, for your unwavering dedication to both basic science and drug development.

I'm forever indebted to my parents, Ellen Gertsik, Dr. Boris Gertsik, and Dr. Serge Resnick, for supporting me in every way. Ellen, you gave me the confidence to be a dancing scientist; you told me I could do anything so many times that eventually I believed you. Boris, you said I would end up with a Ph.D. in both biochemistry and dance. I have yet to obtain the latter, but I'm working on it. Serge, thank you for teaching me calculus in a week – you not only saved my GPA, but also showed me that even the most complex subjects are manageable. I've been trying my hand at things that don't come naturally ever since.

I'd like to thank Dr. David B. Iaea for being first a teacher, then a colleague, next a friend, later a boyfriend, and finally all of the above. You provided not only a shoulder to cry on when experiments failed, but also detailed instructions describing how to fix the problem. For helping me do great science, reading all my manuscripts (and thesis!) and providing brilliant insights, believing in me, and always having peanut butter and Scotch ready after a long day, thank you.

TABLE OF CONTENTS

LIST OF FIGURES

LIST OF ABBREVIATIONS

αCTF: α-Secretase cleaved C terminal fragment of APP
βCTF: β-Secretase cleaved C terminal fragment of APP
AD: Alzheimer's disease
ADAM: A disintegrin and metalloproteinase
AICD: APP intracellular domain
ANP24: HEK293 cells overexpressing 3 components of γ-secretase (Aph1, Nct, PS)
ANPP8: HEK293 cells overexpressing 4 components of γ-secretase (Aph1, Nct, PS, Pen2)
APH1: Anterior pharynx defective 1
APOE: Apolipoprotein E
APP: Amyloid precursor protein
Aβ: β-Amyloid peptide
BACE-1/β-secretase: β-Site APP Cleaving Enzyme 1
BMS-708163: Same compound as GSI-495, also known as avagacestat
CHAPSO: 3-[(3-Cholamidopropyl)dimethylammonio]-2-hydroxy-1-propanesulfonate
COX: cyclooxygenase
CSF: Cerebrospinal fluid
CSL: CBF1/Su(H)/Lag-1, also known as RBP-Jκ family
CuAAC: Copper(I)-catalyzed Azide-Alkyne Cycloaddition, also called Azide-Alkyne Huisgen Cycloaddition
DMSO: Dimethyl sulfoxide
EM: Electron microscopy
ER: Endoplasmic reticulum
FAD: Familial Alzheimer's disease
FLIM: Fluorescence-lifetime imaging microscopy
GSAP: γ-Secretase activating protein
GSI: γ-Secretase inhibitor
GSM: γ-Secretase modulator
HLA-E: Histocompatibility antigen, alpha chain E, also called MHC class I antigen E
L458: L-685,458
L505: L-852,505
L646: L-852,646
LY450139: Also called semagacestat
MBP: Maltose binding protein
NCT: Nicastrin
NFT: Neurofibrillary tangles
NICD: Notch intracellular domain
NSAIDs: Non-steroidal anti-inflammatory drugs

PBS: Phosphate buffered saline
PEN2: Presenilin enhancer 2
PMSF: Phenylmethanesulfonyl fluoride
PS: Presenilin
PS1-CTF: Presenilin1 carboxy-terminal fragment
PS1-NTF: Presenilin1 amino-terminal fragment
PS1ΔE9: Presenilin1 exon 9 removed
PSase: The enzyme responsible for endoproteolysis of presenilin
PS-FL: Full length presenilin
PVDF: polyvinylidene difluoride
RIP: Regulated intramembrane proteolysis
RIPA: Radioimmunoprecipitation assay buffer
sAPPα: Soluble APP, cleavage product of α-secretase
sAPPβ: Soluble APP, cleavage product of β-secretase
SAR: Structure-activity relationship
SCAM: Surface cysteine accessibility method
SDS: Sodium dodecyl sulfate
SDS-PAGE: SDS-polyacrylamide gel
SPP: Signal peptide peptidase, also known as minor histocompatibility antigen H13
SPPL: SPP-like
TAMRA: 5-carboxytetramethylrhodamine
TBTA: Tris[(1-benzyl-1H-1,2,3-triazol-4-yl)methyl]amine
TCEP: Tris(2-carboxyethyl)phosphine hydrochloride
TMD: Transmembrane domain
UV: Ultra-violet

LIST OF SYMBOLS

α: Alpha
β: Beta
γ: Gamma
Δ: Delta
ε: Epsilon
κ: Kappa
μ: Mu, for micro
Å: Angstrom
°: Degree

CHAPTER 1

Introduction (Gertsik et al., 2014b)

1.1 The discovery and importance of γ-secretase

Proteolysis is a process by which proteins are cleaved into smaller fragments through hydrolysis of the peptide bond. This process is catalyzed by enzymes, which have evolved to quickly and efficiently cleave target proteins to enable signaling, transcription, degradation, clearance, etc. Until the mid 1990s, proteolysis was believed to be carried out by soluble proteases, as a water molecule is required for hydrolysis. However, three classes of transmembrane proteases – metallo, aspartyl, and serine – were discovered between 1997 and 2001 (Rawson et al., 1997;Esler et al., 2000;Li et al., 2000b;Urban et al., 2001). Moreover, these proteases were shown to have active sites deep within the lipid membrane, where they hydrolyze transmembrane regions. This was revolutionary at the time of its discovery, as it was hard to imagine how a reaction that requires a water molecule can take place in a region as hydrophobic as the membrane. We now know that these enzymes can coordinate a water molecule in a hydrophilic pocket in order to catalyze cleavage. It is no surprise then that the enzymes all have multiple transmembrane domains (TMDs) which can arrange to form a local environment conducive to hydrolysis.

Regulated intramembrane proteolysis (RIP) is a highly conserved mechanism that controls many cellular processes. The presence of intramembrane-cleaving proteases in the genomes of evolutionarily distinct species underscores the highly conserved nature of the process they catalyze (Freeman, 2008). There has been much speculation regarding the fundamental, overarching role of γ-secretase in RIP. Because it was discovered in a genetic linkage Familial Alzheimer's disease (FAD) study, γ-secretase was initially associated with amyloid precursor protein (APP) cleavage and

amyloidogenic Aβ42 production in the brain. Later, when γ-secretase was shown to cleave Notch, forming Notch intracellular domain (NICD) that travels to the nucleus to induce transcription (De Strooper et al., 1999), scientists became excited by the idea that γ-secretase cleavage of its substrates may generally result in the release of transcriptional regulators. However, this idea was thwarted by the lack of evidence for the function of APP intracellular domain (AICD) as a transcriptional regulator. Next, scientists adopted a more general hypothesis that γ-secretase substrates are involved in signaling. Again this hypothesis needed further examination, as some ectodomain shedding and subsequent γ-secretase cleavage events, like APP proteolysis, appear to be constitutive and many ICDs are rapidly degraded (Cupers et al., 2001;Edbauer et al., 2002). Another hypothesis for the physiological relevance of γ-secretase is that it initially functioned as a "proteasome of the membrane," clearing the transmembrane region of unwanted proteins; some of the released fragments evolved to become signaling molecules while others are still destined for degradation (reviewed in (Kopan and Ilagan, 2004)).

APP and Notch are the most widely studied γ-secretase substrates. APP undergoes sequential proteolytic processing by β-secretase, a membrane bound aspartyl protease called β-site APP cleaving enzyme 1 (BACE-1), and γ-secretase to generate amyloid beta (Aβ) peptides. Notch, a protein that resides on the surface of signal-receiving cells as a heterodimeric receptor, is also subject to a series of proteolytic cleavages that result in NICD nuclear translocation and subsequent transcription (Figure 1.1). The scientific scrutiny sustained by both APP and Notch results from their role in disease: aberrant γ-secretase cleavage of APP and Notch can lead to Alzheimer's disease (AD) and cancer, respectively. γ-Secretase is an important potential drug target

for both diseases and γ-secretase inhibitors (GSIs) and modulators (GSMs) are in clinical trials for cancer and AD, respectively.

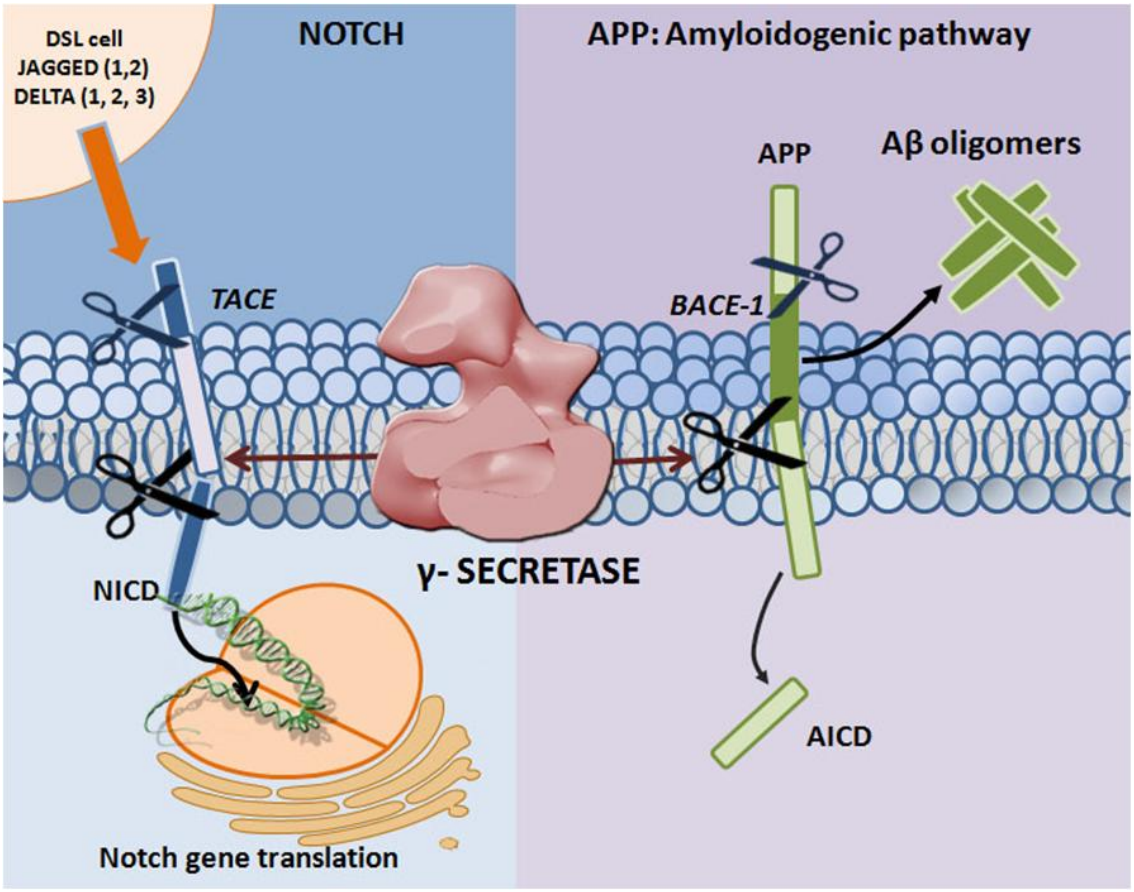

Figure 1.1. Proteolytic processing of APP and Notch. Mature Notch receptors are activated by binding to ligands (Jagged-1, -2 and Delta-like -1, -3, -4) located on adjacent signal-presenting cells. An induced conformational change exposes a cleavage site (S2) for ADAM family metalloproteases that cleave Notch at an extracellular, membrane-proximal region. The membrane-bound Notch segment that results from this cleavage, known as Notch Intracellular Truncation domain (NEXT), is a γ-secretase substrate (Kopan and Ilagan, 2009). γ-Secretase performs the subsequent cleavage at S3 (De Strooper et al., 1999), releasing Notch intracellular domain (NICD) from the membrane and allowing for signal transduction through binding with the CSL (CBL-1, Su(H), Lag-1) (Schroeter et al., 1998;Struhl and Adachi, 1998) family of DNA binding proteins. APP undergoes sequential proteolytic processing first by β-secretase (BACE-1, aspartyl protease) and then by γ-secretase, in the amyloidogenic pathway. The first cleavage results in ectodomain shedding in which the amino-terminal of APP is removed, yielding a soluble APP derivative (sAPPβ) and a carboxy-terminal membrane stub known as βCTF (C99). βCTF is a substrate for γ-secretase, and is cleaved in its transmembrane domain to form AICD and the potentially toxic Aβ. Mutations in PS (the catalytic subunit of γ-secretase) and APP can lead to increases in the Aβ42 to Aβ40 ratio, resulting in Aβ deposition and plaque formation.

1.2 Alzheimer's disease – its causes and risk factors

Alzheimer's disease

AD, the most common form of dementia, causes dysfunctions of memory, judgment, and daily tasks. In today's rapidly aging population AD has become a major public health concern. It is the 6th leading cause of death in the U.S., and while deaths from other major diseases have been on the decline, AD related deaths continue to climb, affecting 5.3 million Americans, of whom 5.1 million are over 65 (Alzheimer's Association, 2015). By 2050, 13.8 million people over 65 are expected to have the disease. AD cost the nation $226 billion in 2015 alone, and this number takes into account only direct cost of care, without considering the many indirect losses associated with the disease. There is no cure for AD and no way to slow disease progression. Current treatments include cholinesterase inhibitors and NMDA antagonists.

Histopathologically, AD is characterized by the presence of extracellular amyloid plaques (Glenner and Wong, 1984a;b) and intracellular neurofibrillary tangles (NFTs) (Grundke-Iqbal et al., 1986;Nukina and Ihara, 1986) in the brain. The amyloid plaques are mainly composed of β-amyloid peptides (Aβ), which are cleavage products of amyloid precursor protein (APP). These peptides can begin to aggregate when the production of the highly amyloidogenic Aβ42 (42 amino acids) increases with respect to production of Aβ40 (40 amino acids). The NFTs are composed of hyperphosphorylated tau, a microtubule-binding protein that forms insoluble filaments (reviewed in (Morris et al., 2011)).

The amyloid cascade hypothesis

According to the amyloid cascade hypothesis, AD is driven by Aβ accumulation (Hardy and Allsop, 1991). Specifically, Aβ accumulation is believed to be the upstream event that leads to plaque and NFT formation, neuronal cell death, the inflammatory response, and cognitive impairment (Figure 1.2). Aβ can exist in many forms, including monomers, dimers, oligomers, fibrils, and plaques. Although insoluble plaques were initially considered to be the culprit of the disease, it is now generally recognized that soluble Aβ may actually be the pathogenic species (Selkoe, 2002).

Strong genetic evidence for the amyloid cascade hypothesis exists. An abundance of autosomal dominant AD mutations have been identified in APP (Goate et al., 1991) and PS (Levy Lahad et al., 1995;Sherrington et al., 1995), which are key players in the pathway that leads to Aβ formation. We now know of 30 APP mutations, 9 APP duplications, 211 PS1 mutations, and 33 PS2 mutations that lead to early onset FAD (Cruts et al., 2012) (www.molgen.ua.ac.be/ADMutations) (Figure 1.2). It is tempting to hypothesize that these mutations lead to an overall increase in Aβ, because such a finding would directly link increased Aβ to AD. However, not all of these mutations are gain of function (where "gain of function" means increased Aβ). In fact, many of them cause decreased levels of overall Aβ. Significantly, all of these mutations increase the Aβ42:Aβ40 ratio (Scheuner et al., 1996) (www.molgen.ua.ac.be/ADMutations). This suggests that the toxic event is an increase in the Aβ42:Aβ40 ratio, and not necessarily in total Aβ. Aβ42 is more hydrophobic than the shorter Aβ peptides and is enriched in Aβ plaques (Iwatsubo et al., 1994). Small increases in Aβ42:Aβ40 without changes in total Aβ enhance aggregation of the neurotoxic peptides (Kuperstein et al., 2010). Similarly, decreases

in Aβ40 increase Aβ42:Aβ40 and may result in amyloidogenesis (Deng et al., 2006;Kumar-Singh et al., 2006;Wang et al., 2006;Kim et al., 2007;Yan and Wang, 2007;Jan et al., 2008;Murray et al., 2009).

A recent genome-wide association study (GWAS) of an Icelandic population revealed the existence of a mutation in APP that protects against AD (Jonsson et al., 2012). The A673T mutation is adjacent to the β-secretase cleavage site on APP and reduces the amount of β-cleavage, thereby reducing Aβ production. This discovery has cemented the importance of Aβ in AD, revealing that changes in Aβ production can mean the difference between early onset disease and immunity.

Risk factors

While the autosomal dominant mutations detailed above have provided insight into disease etiology, they account for a very small fraction of AD cases. Most commonly, AD presents as a late onset, sporadic, multi-factorial condition. The biggest risk factor for AD is age. The second biggest is the APOE4 allele (Corder et al., 1993) (Figure 1.2). The APOE gene has three common alleles (e2, e3, e4) with e3 being the most frequent (Ward et al., 2012). The APOE proteins derived from these alleles differ by only one or two amino acids, yet they have strikingly different impacts on disease. Homozygotes for APOE4 have a higher risk of AD than do heterozygotes, and heterozygotes have a higher risk than non-carriers. Conversely, APOE2 may be protective (Berlau et al., 2009). While the mechanism of action is poorly understood, one possibility is that APOE4 induces increased aggregation and impaired clearance of Aβ while APOE2 has the opposite effect (Holtzman et al., 2000;Kim et al., 2009). An additional risk factor for AD is being a female. Interestingly, the reverse is true of Parkinson's disease.

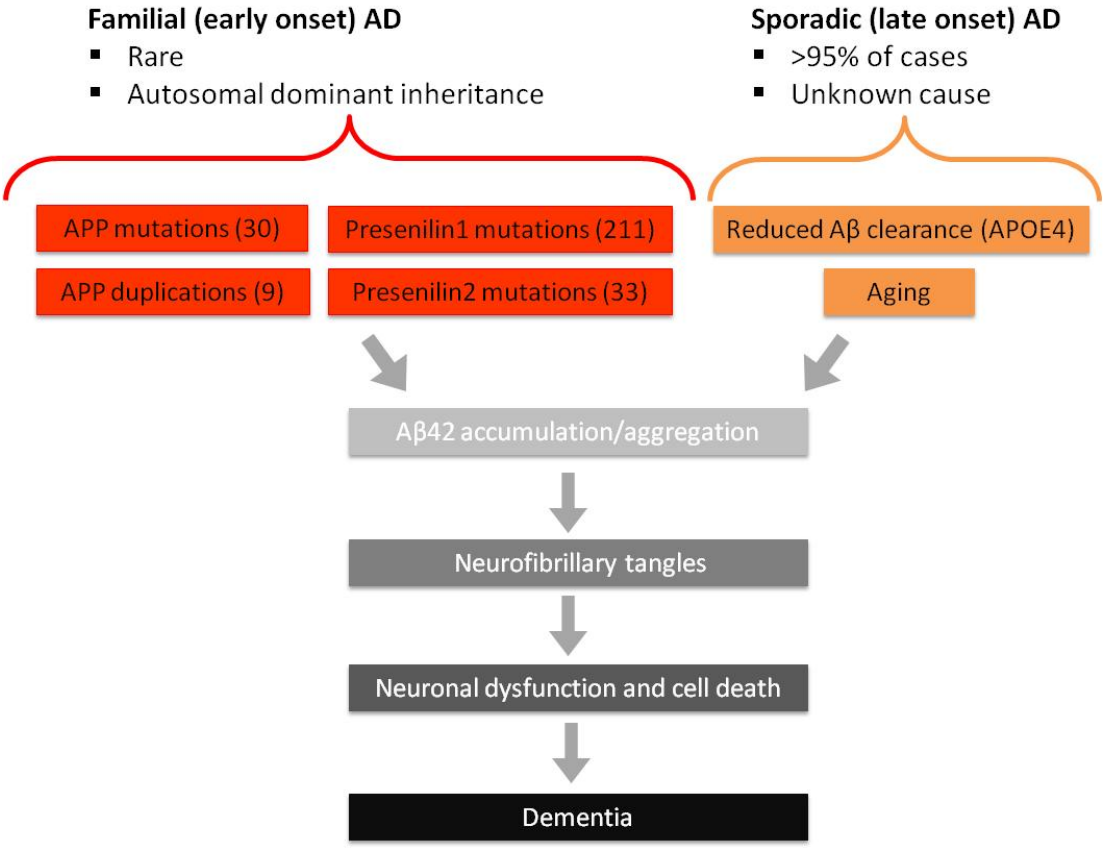

Figure 1.2. The Aβ cascade hypothesis. Mutations in APP and presenilin (PS) (red) are fully penetrant and cause FAD. The number of FAD mutations discovered in each of these proteins is shown in parentheses. The number of mutations is large, but the percentage of FAD cases compared to total AD cases is small. Risk factors such as APOE4 alleles, age, and gender contribute to over 95% of all AD cases. AD is believed to be driven by an imbalance/overabundance of Aβ, which leads to downstream consequences such as NFT formation, neuronal cell death, and dementia. Today's treatments focus on the symptoms and not on the processes involved in early disease progression.

1.3 γ-Secretase cleaves APP

APP proteolysis falls into one of two pathways: either APP is cleaved sequentially by α and γ-secretase in the nonamyloidogenic pathway, generating P3, sAPPα, and AICD, or it is cleaved by β and γ-secretase in the amyloidogenic pathway, generating Aβ, sAPPβ, and AICD (Figure 1.3). α-Secretase cleavage of APP occurs in the Aβ region, which precludes Aβ production, so the choice to preferentially undergo more α cleavage can mean the difference between healthy and disease states. What factors determine the decision to participate in one pathway over the other? It has been suggested that α-secretase competes with β-secretase for the APP substrate, thereby lowering Aβ formation (Lammich et al., 1999;Skovronsky et al., 2000;Postina et al., 2004). However, compelling evidence exists for an alternate mechanism in which α-secretase cleavage results in formation of a substrate inhibitory domain (ASID) within αCTF that binds to an allosteric site in γ-secretase, thereby inhibiting γ-secretase processing of βCTF and ultimate Aβ production (Tian et al., 2010b). In this model, α-secretase plays a dual anti-amyloidogenic role: first, it cleaves APP in the Aβ region, thereby directly precluding Aβ formation, and second, it initiates a feedback loop in which αCTF binds γ-secretase and acts as a γ-secretase modulator which specifically lowers Aβ production. ASID is also present in βCTF, suggesting that the product of β-secretase cleavage is imbued with γ-secretase-regulating capacity as well. The Flemish FAD mutation, located in the ASID domain, interferes with βCTF's inhibitory potency, leading to increased Aβ (Tian et al., 2010a). ASID is the first example of a substrate's inherent ability to regulate γ-secretase, but it is probably not the last (reviewed in(Zhang and Xu, 2010)).

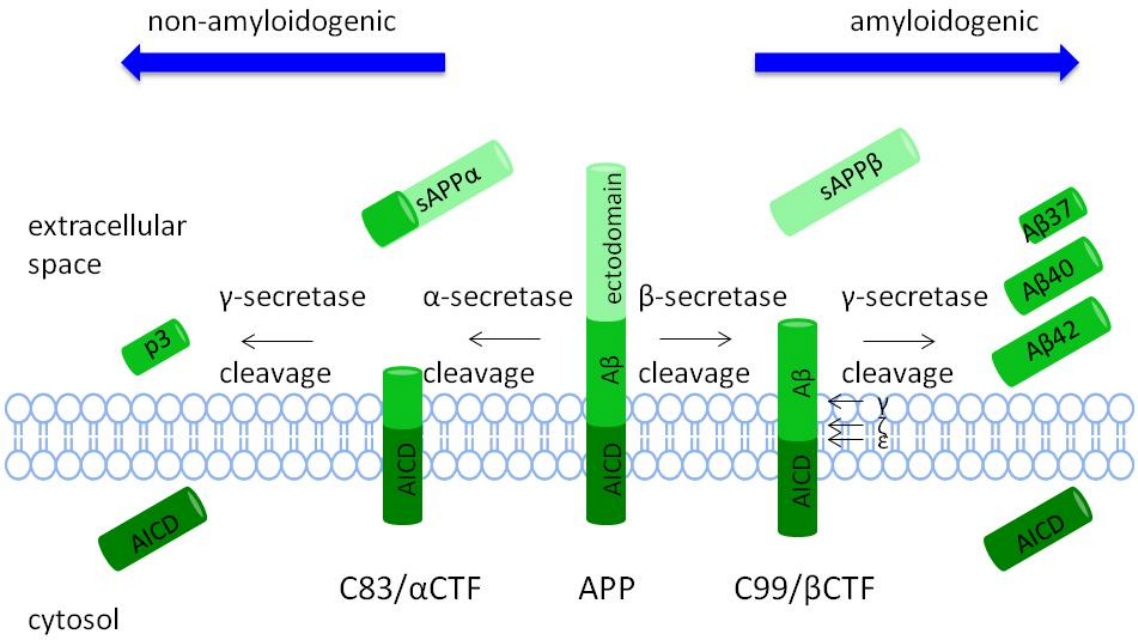

Figure 1.3. γ-Secretase cleavage of APP can follow either the amyloidogenic or non-amyloidogenic pathway. Amyloidogenic pathway: The ectodomain of APP is cleaved by β-secretase, which results in production of sAPPβ and βCTF. βCTF is then cleaved by γ-secretase to produce Aβ peptides of various lengths and AICD. Non-amyloidogenic pathway: The ectodomain of APP is cleaved by α-secretase, which results in production of sAPPα and αCTF. αCTF is then cleaved by γ-secretase to produce the non-amyloidogenic p3 species and AICD.

1.4 The γ-secretase complex: composition and regulation

Biochemical studies indicated that γ-secretase activity is catalyzed by the presenilin (PS)-containing macromolecular complex (Li et al., 2000b). The search for other components of the complex revealed three additional proteins: nicastrin (Nct), anterior pharynx-defective-1 (Aph1), and presenilin enhancer-2 (Pen2) (Yu et al., 2000;Francis et al., 2002;Goutte et al., 2002). It has since been established that these four proteins constitute the mature γ-secretase complex (De Strooper, 2003;Selkoe and Wolfe, 2007), and their stepwise assembly, followed by endoproteolysis of PS into amino-terminal (PS-NTF) and carboxy-terminal fragments (PS-CTF), is necessary for active

complex formation (Takasugi et al., 2003) (Figure 1.4). Recent reports of high resolution cryo-electron microscopy structures of intact human γ-secretase and identification of novel γ-secretase modulating mechanisms have provided insight into the flexibility and complexity of this enzyme (Lu et al., 2014;Bai et al., 2015a;Bai et al., 2015b).

γ-Secretase processing of its substrates produces distinct amino and carboxy termini with variable functions; some products of γ-secretase cleavage function as transcriptional regulators while others are thought to play roles in signaling, cell adhesion, and cytoskeletal dynamics. As the list of putative γ-secretase substrates continues to grow, now reaching over 90 reported proteins (Haapasalo and Kovacs, 2011), the lack of homology between these substrates becomes increasingly apparent: other than the fact that they are all type I transmembrane proteins that have undergone ectodomain shedding, γ-secretase substrates are surprisingly dissimilar (Beel and Sanders, 2008;Lleo, 2008). (Of note, how many of these substrates are actually processed by γ-secretase *in vivo* remains to be investigated.) Not only are the substrates themselves widely variable, but cleavage of some substrates (i.e. CD44 and Notch1) (Lammich et al., 2002;Okochi et al., 2002) leads to release of peptides with variable carboxy-terminal ends, further confirming γ-secretase's astounding promiscuity. In short, γ-secretase not only cleaves many substrates, but it cleaves the same substrate in many places. The permutation is daunting, and may be evolutionary evidence for γ-secretase's initial function in regulated degradation of transmembrane proteins (Kopan and Ilagan, 2004). However, even if γ-secretase was ever simply a "proteasome of the membrane," its function now is certainly much more complex. As a result, γ-secretase regulation must be at least as intricate and diverse as its function.

γ-Secretase activity is regulated by the assembly of its four essential subunits as well as at the level of the entire complex. Extensive investigation of the former revealed that each of the four essential γ-secretase subunits is tightly and independently controlled. More recently, the importance of regulation of the entire complex has emerged, suggesting additional levels of modulation in γ-secretase function. CD147, phospholipase D1, TMP21, GPR3, γ-secretase activating protein (GSAP), syntaxin-1, Arc, voltage-dependent anion channel 1 (VDAC1), contactin-associated protein 1 (CNTNAP1), TPPP, NDUFS7, Erlin-2, β-arrestin-1, β-arrestin-2, Hif-1α, and Nexin 27 have all been implicated as nonessential γ-secretase interacting partners that modulate γ-secretase activity (Zhou et al., 2005;Cai et al., 2006;Chen et al., 2006;Thathiah et al., 2009;He et al., 2010;Teranishi et al., 2010;Wu et al., 2011;Frykman et al., 2012;Hur et al., 2012;Teranishi et al., 2012;Liu et al., 2013;Thathiah et al., 2013;Villa et al., 2014;Wang et al., 2014). However, some of this work is controversial and it remains to be seen whether many of these proteins play a specific and functionally significant role in γ-secretase regulation (Vetrivel et al., 2007;Vetrivel et al., 2008;Hussain et al., 2013). Despite the uncertainty, much can be learned from the way in which a promiscuous enzyme is spatially and temporally modulated by its essential subunits and nonessential cofactors.

γ-Secretase is regulated by its four essential subunits

γ-Secretase's enzymatic promiscuity may on first glance suggest a kind of rampant cleavage activity that indiscriminately chops up anything in its way. Actually, the opposite is true. γ-Secretase may be flexible in its choice of substrate and cleavage site, but its activity is controlled in the cell by a variety of mechanisms, not the least of which is regulation of active complex formation. Perhaps the most basic evidence for this is the finding that γ-secretase activity cannot be increased through the

overexpression of PS alone (Levitan et al., 2001), and can be reconstituted only when all four γ-secretase subunits are present (Edbauer et al., 2003). Put another way, the selective ablation of any one of the essential subunits leads to a loss of active complex and enzymatic activity (De Strooper, 2003). This implies that each subunit must be in the proper place at the right time in order for γ-secretase to form. However, the presence of all four essential subunits does not guarantee active complex formation. This is evidenced by the fact that only a small fraction of steady-state γ-secretase in the cell is actually catalytically active (Beher et al., 2003;Lai et al., 2003;Gu et al., 2004). Furthermore, while overexpression of wild type PS1 in mice is sufficient to increase the amount of γ-secretase complex and protease activity in brains, this is not the case in cellular studies (Li et al., 2011). The implication is that even when all four subunits are in complex with one another, additional events may be necessary to render that complex catalytically active. Some of these events are initiated by modulatory proteins, discussed briefly in the "γ-secretase is regulated by modulatory proteins" section below.

The issue is further complicated by the fact that active complexes fall into a wide range of activities with respect to both catalytic efficiency and substrate specificity. Despite the deceptive language used here to describe γ-secretase as "active" and "inactive," γ-secretase activity is far from a simple on/off switch. Assuming γ-secretase complexes have a 1:1:1:1 ratio of all essential subunits (Sato et al., 2007), at least four different complexes can be theoretically constructed, keeping in mind the existence of PS and Aph1 (PS1/PS2 and Aph1a/Aph1b) isoforms and the finding that these isoforms do not co-exist in the same complexes (Lai et al., 2003;Shirotani et al., 2004). Identification of the Aph1a splice variants (Aph1aS and Aph1aL) increased the permutation further, to a total of six (Shirotani et al., 2004). Experimentally, different

γ-secretase complexes have indeed been identified and shown to vary in catalytic activity (Lai et al., 2003). Some tissue specificity has been observed in the expression of Aph1 and PS variants, but this alone cannot account for determining which complex gets formed and which does not, especially since different variants of the γ-secretase complex exist dynamically in the same tissue, and even in the same cell line (Placanica et al., 2009a;Placanica et al., 2009b). More complicated mechanisms of regulating complex formation pervade, such as the ability of one isoform/mutant to outcompete the other for limiting factors (Placanica et al., 2009a).

The inherent complexity of γ-secretase can be put into perspective by comparing it to signal peptide peptidase (SPP), the only other family of intramembrane aspartyl proteases. Unlike γ-secretase, SPP appears to function alone without the participation of other protein co-factors (Weihofen et al., 2002), although it does form higher order oligomers (Nyborg et al., 2004b;Nyborg et al., 2006;Miyashita et al., 2011). SPP's simpler structure fits its function as a processor of signal peptides in the membrane, which may not require the same extent of regulation as γ-secretase. Below I discuss each essential γ-secretase subunit individually, paying particular attention to its role in regulating activity.

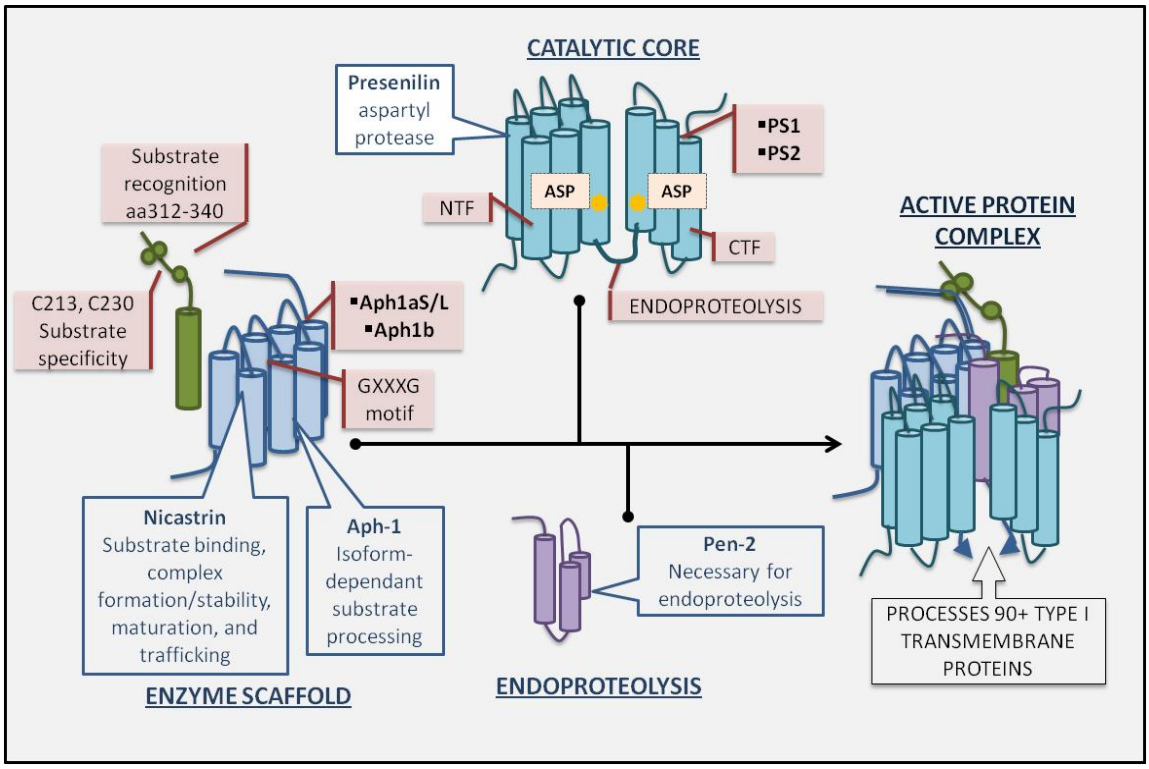

Figure 1.4. The γ-secretase complex is formed by the sequential assembly of Aph1, nicastrin (Nct), presenilin (PS), and Pen2. First, Aph1 and Nct come together to form the scaffold. Next, PS-FL is incorporated. Last, Pen2 is recruited and PS-FL is endoproteolysed into PS-NTF/CTF, activating the enzyme. Nct, a heavily glycosylated single-pass transmembrane protein, plays a role in scaffolding, enzyme stabilization, substrate recognition, and trafficking. Nct's amino acids 312-340 are important for substrate recognition and deletion of these residues reduces γ-secretase activity and Nct's interaction with APP and Notch. Furthermore, mutation of Nct's C213 and C230 leads to different impact on processing of APP and Notch, underscoring Nct's role in substrate selectivity. Aph1, a 7-pass transmembrane protein with 3 human isoforms, is crucial for scaffolding and stability, and may have an additional role in determining length of Aβ species produced depending on which isoform is incorporated into the γ-secretase complex. The GXXXG motif in Aph1 is critical for γ-secretase complex assembly. PS, a 9-pass transmembrane protein with 2 isoforms, is the catalytic subunit of γ-secretase, and PS-FL is a zymogen that must be endoproteolysed into PS-NTF/CTF to be enzymatically active. Mutations in PS1 and PS2-encoding genes account for the majority of genetic mutations leading to Familial Alzheimer's disease. Pen2, a 3-pass transmembrane protein, is required for PS endoproteolysis and γ-secretase activation, but also may play an endoproteolysis-independent role in γ-secretase regulation. Active γ-secretase constitutes a small percentage of total γ-secretase and resides primarily in the plasma membrane.

Presenilin

PS1 and its less abundant isoform PS2, are ~50 kDa multipass transmembrane proteins that contain the catalytic core of the γ-secretase complex. These proteins were implicated in γ-secretase function when knock-out of PS1 resulted in severely reduced γ-secretase activity (De Strooper et al., 1998). For a long time it was unclear whether PS contains the active site of γ-secretase or is a chaperone involved in γ-secretase activity or colocalization to substrate. Several seminal studies indicated that PS is indeed the catalytic subunit of γ-secretase. First, mutation of the two conserved aspartates in both PS1 (Wolfe et al., 1999) and PS2 (Steiner et al., 1999a) significantly reduced Aβ production, suggesting that the aspartates are catalytic or essential residues for γ-secretase activity. Second, aspartyl protease transition-state analogues were shown to directly label and inhibit γ-secretase activity through covalent binding to PS, providing compelling evidence for PS as the catalytic core of γ-secretase (Esler et al., 2000;Li et al., 2000b). Finally, recombinant PS reconstituted into proteoliposomes was shown to be catalytically active even in the absence of other γ-secretase subunits (in contrast to cellular activity which requires all four subunits), providing conclusive evidence for PS's role as the catalytic subunit of γ-secretase (Ahn et al., 2010).

PS is synthesized as a full length (FL) protein but PS-FL is unstable and is quickly either endoproteolysed or degraded (Ratovitski et al., 1997;Thinakaran et al., 1997;Zhang et al., 1998). Endoproteolysis, a process required for γ-secretase activation, results in the formation of PS1-NTF/CTF, which remain associated as a stable heterodimer (Podlisny et al., 1997). In fact, the requirement for endoproteolysis is an onerous one to meet, as evidenced by the fact that in cells it is dependent on the assembly of all four subunits. Furthermore, the ability of FAD mutant PS1ΔE9

(Thinakaran et al., 1996) to be constitutively active despite its inability to be endoproteolysed suggests that evolution has found a way to increase enzymatic activity by circumnavigating an important requirement. A parallel can again be drawn to the PS-like enzyme SPP, which is not endoproteolysed and is active in its FL form, suggesting a simpler form of regulation. The exact molecular mechanism of γ-secretase endoproteolysis remains unclear, but one approach to study it is through the use of active-site directed probes (Gertsik et al., 2014a).

As mentioned previously, the formation of an active complex is only the first hurdle in regulating γ-secretase activity in the cell. An added layer of regulation resides in the choice to form PS1 versus PS2-containing complexes. Different PS variants play different, albeit overlapping, roles as evidenced by genetic knock out studies (De Strooper et al., 1998;Herreman et al., 1999). Later biochemical studies showed that PS1 complexes display a much higher activity than PS2 complexes for a truncated APP substrate (Lai et al., 2003).

PS1 is not only the more active of the two isoforms, but also may be the more amyloidogenic. A reconstitution study in which four γ-secretase isoforms (PS1–aph-1a, PS1–aph-1b, PS2–aph-1a, PS2–aph-1b) were analyzed showed that PS1 complexes form more aggregation-prone Aβ42 (relative to Aβ40) compared to PS2 complexes (Lee et al., 2011). This provides further evidence that the 67% homologous PS isoforms may have different cleavage-site preferences. It would be interesting to investigate whether the PS isoforms also have different substrate preferences. For example, do PS1/PS2 complexes differentially cleave APP/Notch? The decision to form PS1 versus PS2 complexes probably determines not only “how much” but also “what” is cleaved.

Pen2

Presenilin enhancer 2 (Pen2), a ~10 kDa protein with three TMDs (Bai et al., 2015b), was discovered as a gene product that can interfere with PS activity in a genetic study involving *C. elegans* (Francis et al., 2002). Pen2 is required for endoproteolysis of PS-FL into PS-NTF/CTF and for γ-secretase activity. The following evidence supports that Pen2 is indispensable for endoproteolysis of PS: first, knock-down of Pen2 by RNAi resulted in a decrease of PS1-NTF/CTF and a stabilization of the PS1 holoprotein in the Nct-Aph1 complex, while transient overexpression of Pen2 in Pen2 deficient cells led to the recovery of PS fragments (Takasugi et al., 2003). Second, coincorporation of recombinant PS1 and Pen2 in liposomes showed Pen2 to be necessary and sufficient for endoproteolysis of PS1 (Ahn et al., 2010). Pen2 is also required for γ-secretase activity: Pen2 knockdown in mammalian cells resulted not only in an accumulation of the PS1 holoprotein, but also in a drastic decrease in γ-secretase activity (Takasugi et al., 2003). Pen2$^{-/-}$ mouse embryos exhibited a Notch-deficiency phenotype and Pen2$^{-/-}$ MEFs displayed no γ-secretase activity toward APP processing (Bammens et al., 2011). Furthermore, overexpression of human Pen2 in Pen2 deficient mice recapitulated AD-like symptoms such as increase in Aβ42, behavioral dysfunctions, and feeding defects, underscoring the importance of Pen2 in γ-secretase activity and AD pathogenesis (Nam et al., 2011).

The roles of Pen2 in PS endoproteolysis and γ-secretase activity raised the question – is Pen2 necessary for γ-secretase activity *per se,* or is Pen2-inspired endoproteolysis of PS the only requirement for activity? To answer this question the catalytically active PS1ΔE9 endoproteolysis deficient mutant was expressed in Pen2$^{-/-}$ MEFs and found to have no activity, suggesting that Pen-2 is required for γ-secretase activity *per se*, and not just for endoproteolysis of PS (Bammens et al., 2011). This implies that Pen2

regulates γ-secretase on multiple levels. We already discussed that Pen2 dictates activity, as PS-FL is a zymogen that relies on Pen2-dependent endoproteolysis. This type of regulation is close to being an "on" switch, since lack of WT PS endoproteolysis precludes γ-secretase activity. However, Pen2 is also capable of more subtle regulation in which it modulates the composition of the γ-secretase complex: overexpression of Pen2 shifted the equilibrium from PS1 containing complexes to PS2 containing complexes and increased the Aβ42:Aβ40 ratio (Placanica et al., 2009a). Clearly, Pen2 regulates γ-secretase through a variety of mechanisms, not the least of which are endoproteolysis of PS and complex assembly.

Nicastrin

In the search for cofactors required for γ-secretase activity, Nct, a type I transmembrane glycoprotein, was the first to be discovered through coimmunoprecipitation with PS1-directed antibody (Yu et al., 2000). A 1.95 Å-resolution crystal structure of Nct from an amoeboid eukaryote *Dictyostelium purpureum* has been solved (Xie et al., 2014). Four hydrophilic residues in the proximal one third of the N-terminal portion of the Nct TMD are critical for interaction between Nct and the rest of the γ-secretase complex (Capell et al., 2003). Nct interacts initially with Aph1, followed by the incorporation of PS and Pen2 (LaVoie et al., 2003). Not only does Nct, together with Aph1, provide a scaffold for the γ-secretase complex, but it also may recognize γ-secretase substrates by binding to their amino termini. Particularly, Nct's ectodomain has been shown to bind the extracellular regions of APP and Notch after they undergo ectodomain shedding, with Nct's residues 312-340, and especially Glu333, being most important for substrate recognition (Shah et al., 2005). This finding branded Nct as the substrate-recruiting subunit of γ-secretase. Further confirmation came from work with anti-Nct antibodies:

the monoclonal antibody A5226A binds the extracellular domain of Nct causing both a disruption in Nct binding to Notch-based substrate (N100) and a decrease in γ-secretase activity (Hayashi et al., 2011). Additionally, the use of synthetic antibodies showed that a certain structured region in Nct, homologous to the TPR domain involved in peptide recognition, is critical for substrate binding (Zhang et al., 2012). However, several studies had called the "substrate-binding" capacity of Nct into question: mutation of mouse Nct-Glu332 (equivalent to human Glu333) to alanine or glutamine was reported to hinder assembly of the γ-secretase complex but not its specific activity, suggesting that substrate recognition/binding was not affected (Chavez-Gutierrez et al., 2008). Furthermore, Nct-independent, L-685,458 specific, γ-secretase activity has since been detected in two separate MEF lines, suggesting that Nct is in fact not required for substrate recognition (Zhao et al., 2010). These results support Nct's role in complex assembly and maturation, but not substrate recognition. A subsequent study reexamined the role of Nct and Glu333 in substrate recognition, overturning the previous finding and suggesting once again that Nct is indeed involved in substrate binding (Dries et al., 2009).

While Nct's role as the substrate-binding subunit of γ-secretase may be controversial, its importance in γ-secretase regulation is uncontested: mutation of two conserved cysteine residues to serine (C213S and C230S) in Nct's ectodomain resulted in differential γ-secretase processing of APP and Notch in MEF cells lacking endogenous Nct. In particular, APP processing was reduced compared to Notch, suggesting that Nct plays a role in substrate selectivity, although the exact mechanism was not identified (Pamren et al., 2011). Furthermore, synthetic anti-Nct antibodies were shown to impact substrate selectivity by changing γ-secretase sub-cellular localization (Zhang et al., 2014). Quite possibly Nct regulates γ-secretase activity, and particularly

substrate selectivity, through a variety of mechanisms including direct substrate binding, complex formation/stabilization, maturation, and trafficking.

Aph1

Aph1, a ~29 kDa protein with seven TMDs, was discovered in the same genetic screen as Pen2 (Francis et al., 2002). The GXXXG motif of Aph1's TMD4 is crucial for assembly into the γ-secretase complex as it plays a major role in intramembrane helix-helix interactions. Mutation of Gly123 and Gly122 to aspartic acid in *C. elegans* and humans, respectively, results in a loss-of-function phenotype (LOF). The *C. elegans* LOF phenotype gave Aph1 its name: anterior-pharynx-defective (Goutte et al., 2002). In mammals, mutation of Gly122 to aspartic acid renders Aph1 incapable of associating with the γ-secretase complex, thereby leading to deficiency in Notch cleavage (Lee et al., 2004).

Humans have two Aph1 genes that give rise to three versions of the Aph1 protein (Aph1aS, Aph1aL, Aph1b) due to alternative splicing of the Aph1a gene (Shirotani et al., 2004). Rodents have an additional isoform, Aph1c, which is a duplication of the Aph1b gene. Aph1 isoforms have been reported to differ in their production of longer and shorter Aβ peptides. Particularly, when Aph1a, Aph1b, and Aph1c were individually reintroduced into an Aph1-$a^{-/-}b^{-/-}c^{-/-}$ mouse, Aph1a rescue of γ-secretase activity resulted in production of shorter Aβ peptides while Aph1b and Aph1c rescue led to formation of longer Aβ species. A potential mechanism for this variability may stem from the structural changes evident in PS upon binding to one or the other Aph isoform: fluorescence lifetime imaging microscopy showed that PS may adopt a more closed conformation upon binding to Aph1b compared to its more open conformation when in complex with Aph1a (Serneels et al., 2009). This data implies that the choice

to incorporate one Aph1 isoform over another can have a profound impact on Aβ production and plaque formation.

γ-Secretase is regulated by modulatory proteins

γ-Secretase is regulated not only by its four essential subunits, but also by other pathways and proteins, many of which have been identified through LCMS analysis (Teranishi et al., 2010;Frykman et al., 2012;Teranishi et al., 2012). However, it is unclear whether most of these putative γ-secretase-interacting partners actually bind the active complex and impact γ-secretase activity. Two γ-secretase-interacting partners, GSAP (He et al., 2010;Chu et al., 2014;Zhu et al., 2014) and Hif-1α (Villa et al., 2014), have been reproducibly shown to bind *active* γ-secretase and modulate γ-secretase activity, rendering them both biologically interesting and potentially clinically relevant.

Implications of γ-secretase regulation

γ-Secretase is regulated at many levels, including but not limited to regulation by "essential" subunits, complex formation, "nonessential" subunits, substrates, and lipid composition (Holmes et al., 2012;Walter and van Echten-Deckert, 2013). Although the importance of PS in γ-secretase activity is well established, it appears that the other essential subunits also notably contribute to regulating activity and substrate specificity beyond just their roles in complex assembly. Furthermore, nonessential subunits like GSAP and Hif-1α fine-tune modulation of the already stringently-regulated enzyme, thereby presenting potential therapeutic opportunities for modulating γ-secretase activity without the mechanism-based toxicities that result from γ-secretase inhibition (i.e. GSIs). The multifaceted levels of γ-secretase

regulation that are now emerging may improve our ability to develop targeted therapies for AD and cancer.

1.5 γ-Secretase inhibitors (GSIs) (Hur et al., 2016)

Small molecule inhibition of γ-secretase was explored as a potential therapy for AD. γ-Secretase inhibitors (GSIs) are intended to block γ-secretase cleavage of APP, thereby lowering the amount of toxic Aβ produced and slowing neurodegeneration. However, these GSIs also block γ-secretase cleavage of other substrates, including the critical signaling molecule Notch. A wide range of GSIs have been tested in animals and humans, but none have successfully passed clinical trials due to toxicity. A deeper understanding of γ-secretase structure and function would help to develop safe and effective γ-secretase-based therapies.

GSIs have extensively been developed as molecular probes and therapeutic agents (Josien, 2002;Wolfe, 2012;Golde et al., 2013). Distinct classes of small molecules that target γ-secretase have been reported (Josien, 2002;Wolfe, 2012;Crump et al., 2013;Golde et al., 2013). Complete inhibition of γ-secretase, as achieved by nonselective GSIs, abolishes all γ-secretase activity so that there is a decrease in Aβ production and Notch signaling. "Notch-sparing" GSIs, on the other hand, are intended to inhibit Aβ production while leaving some Notch signaling intact (Kreft et al., 2008;Mayer et al., 2008).

Active site-directed GSIs

Wolfe et al. found that a substrate-based difluoro ketone peptidomimetic compound (IC_{50} = 13 ± 5 μM) inhibited γ-secretase activity in APP-expressing cells (Wolfe et al., 1998). Shearman et al. reported a potent GSI, L458, which contains a hydroxyethylene dipeptide isostere directed to the active site of aspartyl proteases (Shearman et al.,

2000) (Figure 1.5A). Active site-directed small molecule inhibitors have been developed as activity-based probes for identification, localization, and isolation of γ-secretase and detection of conformational changes within the active site (Li et al., 2000a;Li et al., 2000b;Beher et al., 2003;Kimberly et al., 2003;Chun et al., 2004;Tarassishin et al., 2004;Vetrivel et al., 2007;Vetrivel et al., 2008;Placanica et al., 2009a;Placanica et al., 2009b;Shelton et al., 2009;Yang et al., 2009;Placanica et al., 2010;Teranishi et al., 2010;Tian et al., 2010a;Crump et al., 2011;Chau et al., 2012;Gertsik et al., 2015). These probes interact with the PS-NTF/PS-CTF heterodimer, but not with PS-FL (Li et al., 2000b;Ahn et al., 2010).

First-generation GSIs

Compound E, DAPT, and LY-411,575 are early first-generation GSIs that continue to be used for investigation of γ-secretase (Figure 1.5A). Compound E (IC_{50} = 300 pM) was shown to inhibit Aβ production by binding to PS1 and PS2 (Seiffert et al., 2000). DAPT (IC_{50} = 20 nM) was one of the first compounds to show reduction of Aβ *in vivo* (Dovey et al., 2001). When DAPT was orally administered to PDAPP mice (harbouring human APP with the 'Indiana' mutation [V717F]), brain Aβ levels decreased in a dose-dependent manner and APP-CTFs accumulated (Dovey et al., 2001). Similarly, DAPT decreased Aβ levels in the plasma and CSF of Tg2576 mice (harbouring human APP with the 'Swedish' mutation) (Lanz et al., 2003). Administration of LY-411,575 (IC_{50} = 30 pM) for 15 days in a murine model of AD also led to a reduction in Aβ levels (Wong et al., 2004). However, side effects on lymphocyte development and the intestine were observed due to the inhibition of Notch signaling by this GSI (Wong et al., 2004).

Clinical GSIs for AD

Nonselective GSIs

LY450139 (semagacestat, Eli Lilly) is a potent GSI that pan-inhibits γ-secretase cleavage of its substrates and was the first GSI to enter phase 3 clinical trials (Figure 1.5B). The most surprising outcome of the clinical trial of semagacestat was the worsening of memory in patients (Doody et al., 2013). The other major adverse effect of the trial was the increased risk of skin cancer, which likely resulted from inhibition of Notch signaling (Xia et al., 2001;Nicolas et al., 2003). While the Notch-associated side effects are somewhat understood, the mechanism of cognitive decline is elusive.

"Notch-Sparing" GSIs

GSI-953 (begacestat, Wyeth [now Pfizer]) is a thiophene sulfonamide GSI (Martone et al., 2009) (Figure 1.5B). It is 16 times more potent for inhibition of APP cleavage versus Notch cleavage in the assays used and was optimized for improved stability in humans ($t_{1/2}$ > 90 min) compared to other Wyeth compounds (Martone et al., 2009;Hopkins, 2012). Begacestat was reported to decrease plasma, brain, and CSF Aβ levels in Tg2576 mice overexpressing APP and also reduce plasma Aβ levels in a dose-dependent manner in healthy humans (Martone et al., 2009). While begacestat appeared to have a higher selectivity for APP over Notch than semagacestat, it was discontinued in the phase 1 trial in 2010 for unknown reasons.

BMS-708163 (avagacestat, Bristol-Myers Squibb) is a sulfonamide-based GSI that has a preference for inhibition of APP processing over Notch processing (Gillman et al., 2010)(Figure 1.5B). Initially, avagacestat was reported to have 193-fold selectivity for APP over Notch in cell culture (Gillman et al., 2010). Although the major adverse effects of the avagacestat phase 2 trial were gastrointestinal and dermatologic

complications, which probably stemmed from Notch inhibition, the 100 mg and 125 mg dose arms also led to a trend for cognitive worsening (Coric et al., 2012), suggesting that avagacestat may share a common mechanism of toxicity with semagacestat. While avagacestat was initially reported as a Notch-sparing inhibitor (Gillman et al., 2010), two groups were unable to reproduce this result using different assay formats (Chavez-Gutierrez et al., 2012;Crump et al., 2012b). Therefore, the toxicity can be partially attributed to the inhibition of Notch signaling (Chavez-Gutierrez et al., 2012;Crump et al., 2012b;De Strooper, 2014). A recent study suggested that the worsening in cognition by treatment with semagacestat and avagacestat could be due to the accumulation of APP-CTF in the presynaptic terminals of the hippocampus (Mitani et al., 2012).

1.6 γ-Secretase modulators (GSMs)

GSMs are compounds that have numerous attributes favorable for AD treatment. Specifically, GSMs reduce amyloidogenic Aβ42, do not affect quantity of total Aβ, and do not inhibit Notch signaling. What makes GSMs different from GSIs is their ability to keep total Aβ constant, by raising amounts of shorter Aβ species, and their ability to interfere with APP processing without interfering with Notch processing. By maintaining total Aβ constant, these compounds prevent the accumulation of the toxic βCTF, and by maintaining Notch processing, GSMs allow for normal cell signaling to continue in pathways unrelated to Aβ formation.

First generation GSMs

GSMs were discovered when some NSAIDS, such as ibuprofen, indomethacin, and sulindac sulfide, were found to reduce Aβ42 and increase Aβ38 without inhibiting Notch1 signaling (Weggen et al., 2001). Moreover, these properties were dissociated

from their cyclooxygenase (COX) activity. For the first time it seemed that γ-secretase activity could be modulated, not just inhibited, but the low *in vitro* (Aβ42 IC_{50} >10 μM) potency and brain penetration of these compounds precluded them from becoming promising clinical candidates (with the exception of R-flurbiprofen which made it to phase III trials but did not achieve statistically significant outcomes (Green et al., 2009)).

Second generation GSMs

Second generation GSMs, which are either NSAID-derived carboxylic acids, non-NSAID-derived heterocyclic GSMs, or natural product-derived GSMs, were developed with the goal of improving potency and brain penetration.

NSAID-derived heterocyclic GSM: GSM-1 is a piperidine acetic acid GSM that increases Aβ38 at the expense of Aβ42 and does not impact Aβ40 and NICD levels. When WT and Tg2576 mice were treated with GSM-2 (a piperidine acetic acid), LY450139, or BMS-708163, the only compound to recover cognition as shown by the Y-maze test was GSM-2 (Mitani et al., 2012). In fact, LY450139 (Figure 1.5B) actually impaired cognition in WT mice, suggesting that accumulated β-CTF may be toxic and non-selective inhibition of γ-secretase is not a viable AD therapy.

Non-NSAID-derived heterocyclic GSM: E2012 (Figure 1.5C) is an imidazole compound, developed by Eisai, that enhanced Aβ37 and 38 at the expense of Aβ42, 40, and 39 (Portelius et al., 2010;Borgegard et al., 2012). It entered phase I clinical trials (Nagy et al., 2010), was dropped for an improved version called E2212, and has not been heard from since (clinicaltrials.gov identifier NCT01221259).

GSM mechanism of action

How do GSMs reduce Aβ42 without affecting overall Aβ production and Notch signaling? Three mechanisms of action were proposed by different groups: 1. GSMs bind γ-secretase (Takahashi et al., 2003;Beher et al., 2004;Clarke et al., 2006) 2. GSMs bind APP, the substrate of γ-secretase or (Kukar et al., 2008;Botev et al., 2011) 3. GSMs bind both γ-secretase and APP (Lleo et al., 2004;Uemura et al., 2010). However, all of these studies were performed with low potency NSAID GSMs, which required compounds in high micromolar concentrations. It was shown that sulindac sulfide aggregates above 50 μM (Barrett et al., 2011). As a result of high compound concentrations, many of these studies identified unspecific GSM-interacting proteins that were mistaken for true targets. The literature filled with contradictory findings and most data was difficult to interpret. With the advent of second generation GSMs, the search for GSM targets finally began to yield clearer results. Despite their structural diversity, all second generation GSMs known to date were shown to bind γ-secretase and not APP (Crump et al., 2011;Ebke et al., 2011;Ohki et al., 2011;Jumpertz et al., 2012;Pozdnyakov et al., 2013). One of the most convincing pieces of evidence for PS as the target of GSMs is the finding that a probe form of GSM-1 specifically binds to reconstituted PS1ΔE9 in liposomes without substrate (Ahn et al., 2010). Although second generation GSMs were all found to target γ-secretase, a series of reciprocal labeling experiments showed that GSM binding occurs in different regions of PS (Figure 1.5C). Not surprisingly, GSMs have been found to induce conformational changes in γ-secretase (Uemura et al., 2010;Crump et al., 2011;Ohki et al., 2011;Gertsik et al., 2015).

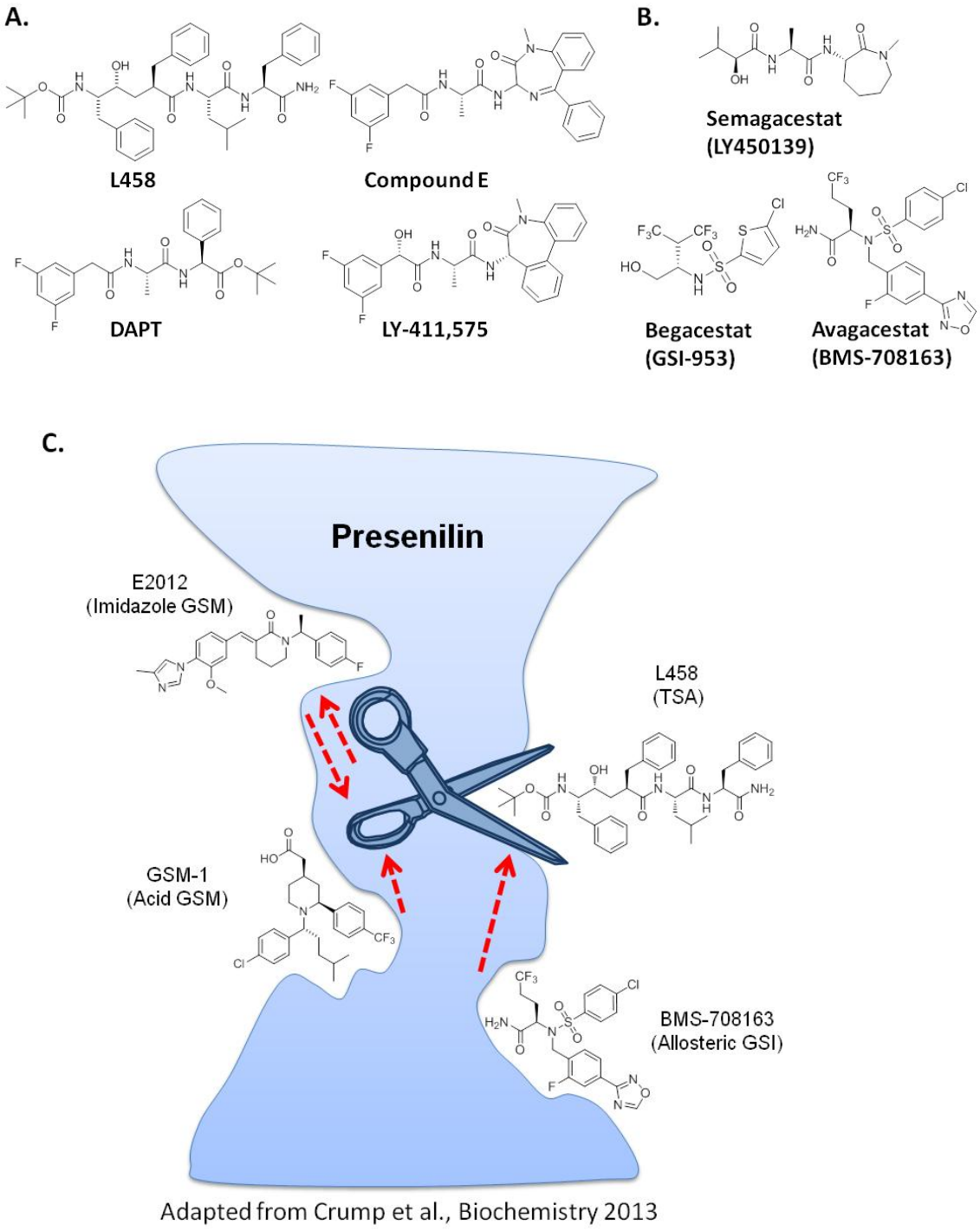

Figure 1.5. A. Structures of L458 and first generation GSIs B. Structures of GSIs that have advanced into clinical studies for AD. C. Schematic showing that structurally diverse GSIs/GSMs bind in different allosteric regions on PS and have an impact on the enzyme active site.

1.7 Activity-based protein profiling (ABPP)

ABPP is a chemical proteomic strategy that profiles the activity of enzymes and contributes to inhibitor development and functional understanding (Niphakis and Cravatt, 2014). ABPP can be used to study the mechanism of catalysis, the mechanism of action of other small molecules that target the enzyme of interest, or in conjunction with gene disruption to trace biological pathways. ABPP also allows us to become a lot more sophisticated in drug development, as we can use the information gleaned from activity-based probes' (ABPs) interaction with the proteome to make compounds that are increasingly more specific for our target of interest. ABPP relies on the ability of compounds to distinguish between active and inactive forms of an enzyme. ABPs, which have been developed for a wide array of enzymes with aspartate, glutamate, cysteine, lysine, tyrosine, and serine catalytic residues, consist of a reactive group for covalent linkage, a binding group for affinity, and a reporter tag for isolation. We use a photoactive benzophenone for covalent linkage, an aspartyl protease active site-directed transition state peptidomimetic with a hydroxyethylene isostere (L458) (Li et al., 2000b) for affinity and a biotin (or clickable alkyne) for isolation.

1.8 Thesis overview: insights into drug development for AD using chemical probes

While all clinical trials for treating AD with GSIs have failed to date, there is reason to believe that a successful Aβ-reducing therapy is around the corner. Recent analyses and discussion questioned whether GSIs, such as semagacestat or avagacestat, were the best candidates for clinical studies (Chavez-Gutierrez et al., 2012;Crump et al., 2012b;De Strooper, 2014), and suggested that the failed clinical trials do not disqualify γ-secretase as a target for AD drug development (De Strooper, 2014;Alzforum, 2015;De Strooper and Chavez Gutierrez, 2015). Past failures with

GSIs appear to have been a result of suboptimal compound selection and poorly designed trials. For example, the once-a-day dosing regimen of semagacestat resulted in abrupt inhibition of γ-secretase followed by a rebound in activity and Aβ production. This not only led to spikes in Aβ, but also may have interfered severely with Notch signaling. A constant, moderate dose treatment may have improved trial results. Moreover, both semagacestat and avagacestat are non-selective GSIs that caused severe Notch-associated toxicities. As a result, the cognitive worsening observed with these compounds may have been a result of making patients very sick. By taking into account the lessons we have learned, it will be possible to design efficacious, minimally toxic drug candidates to slow or arrest disease progression. In fact, clinical investigation of aducanumab (BIIB037) suggests that targeting Aβ is a valid strategy for AD drug development (BioGen, 2015).

To create effective Aβ-reducing therapies, we must delve deeper into disease mechanism through a better understanding of the structure and function of γ-secretase (De Strooper, 2014;Alzforum, 2015;De Strooper and Chavez Gutierrez, 2015). One major challenge lies in obtaining a clearer picture of γ-secretase biology, and in particular, the processes by which the zymogen is converted into its active form. In this work we developed CBAP-BPyne, a tool to study the process of γ-secretase activation. Insights into enzyme endoproteolysis and activation, a set of events about which much has been written but little is understood, will not only teach us about the basic biology of this protein, but can also inform drug development as we intervene in specific enzymatic formation/activation events. An understanding of endoproteolysis can shed light on the mechanism by which PS1ΔE9, an FAD mutation that is endoproteolytically deficient but enzymatically active, causes an accumulation of Aβ and subsequent neurodegeneration. Rational drug design will be well served by a

recognition for the physiological and pathological processes by which γ-secretase is activated.

Another challenge of AD drug development lies in retaining the physiological activity of γ-secretase while decreasing its pathological activity, a feat that can be attained through development of selective GSIs or GSMs, compounds that lower formation of the toxic Aβ42 without affecting formation of other γ-secretase cleavage products. While we and others have developed GSMs that fit this profile and appear to have minimal mechanism-based toxicity, we know little about their potential off-target effects. Here we extend our understanding of structurally distinct GSMs by determining their impact on the active site architecture of an off-target protein, SPP. SPP cleaves transmembrane signal peptides after they have been cleaved off the protein by signal peptidase (SP) and SPP is required in eukaryotes. The modulation of SPP may result in off-target toxicities that need to be thoroughly understood before another attempt at GSI/GSM clinical development.

Yet a third challenge is in obtaining a high resolution understanding of drug-γ-secretase interaction. Because there is no crystal structure of γ-secretase, we have a limited understanding of where GSIs/GSMs bind and how the location of binding impacts the modulation profile. Whether the recent high resolution electron microscopy (EM) structure of γ-secretase (Bai et al., 2015b) illustrates an active enzyme complex is questionable. We have taken the first step toward a structure-function understanding of GSIs/GSMs and their enzyme target by identifying the binding site of BMS-708163, a GSI that was in clinical trials. This work combines probe development with the study of γ-secretase biology, the union of which we hope brings us another step closer to safe and effective AD therapies.

CHAPTER 2

Development of CBAP-BPyne, a probe for γ-secretase and presenilinase (PSase)

(Gertsik et al., 2014a)

2.1 Introduction

γ-Secretase activity is required for development, as PS1 knock-out mice are embryonic lethal (Shen et al., 1997;Wong et al., 1997). Endoproteolysis of PS, or as we will interchangeably call it, presenilinase (PSase), is required for γ-secretase activation (Figure 2.1). This logically leads to the supposition that PSase is required for development. As a result, reports of familial Alzheimer's disease (FAD) mutations that abolish PSase are very surprising. In fact, the existence of an endoproteolytically dead PS1 FAD mutant – PS1ΔE9, in which amino acids 290-319 are deleted – appears to invalidate the above conclusion that PSase is required for development. Deletion of the exon 9 encoded peptide loop of PS1, found between transmembrane domains (TMDs) 6 and 7 (Laudon et al., 2005), results in an active γ-secretase that does not depend on endoproteolysis for its activation.

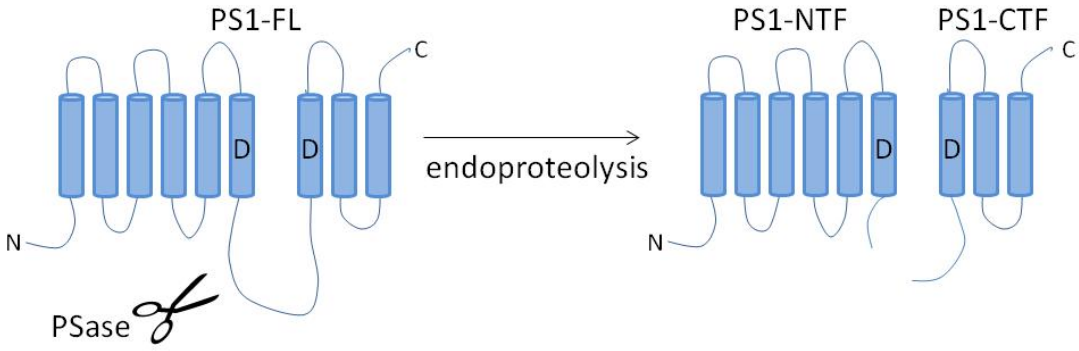

Figure 2.1. Endoproteolysis of PS1. PS1-FL (full-length) is endoproteolysed by PSase in a hydrophobic stretch of the cytoplasmic loop, to form a ~27 kDa NTF and ~16 kDa CTF. Endoproteolysis and subsequent PS1-NTF/CTF heterodimer formation are required for γ-secretase activity, as PS1-FL is a zymogen, activated by autocleavage. (D: catalytic Asp residues)

Under wild-type (WT) conditions, endoproteolysis and concurrent PS1-NTF/CTF fragment formation are required for γ-secretase activity, as full length PS (PS1-FL) is a zymogen, activated by autocleavage (Li et al., 2000b;Ahn et al., 2010;Lessard et al., 2010). PS is synthesized in the ER as a full length, 467 amino acid protein, but PS-FL is unstable ($T_{1/2}$~1 hour) and is quickly either endoproteolysed or degraded (Ratovitski et al., 1997;Thinakaran et al., 1997;Zhang et al., 1998). Endoproteolysis occurs between amino acids 298 and 299, or 292 and 293, in a hydrophobic stretch of the cytoplasmic loop to form a ~27 kDa amino terminal fragment (NTF) and ~16 kDa carboxy terminal fragment (CTF) (Thinakaran et al., 1996;Podlisny et al., 1997;Steiner et al., 1999b). The two fragments, each of which donates an aspartate residue to form the active site (D257 and D385), go on to generate a stable heterodimer with a long biological half-life ($T_{1/2}$~12 hours) (Zhang et al., 1998). However, mutations in PS can also activate γ-secretase, as evidenced by PS1ΔE9, which results in an uncleavable, constitutively active PS1 variant (Thinakaran et al., 1996). This mutant causes an increase in the Aβ42:Aβ40 ratio and early onset AD (Cruts et al., 2012). Mutagenesis studies have further shown that a single M292D amino acid substitution is sufficient to form an endoproteolytically deficient and catalytically active PS1 (Steiner et al., 1999b). Additional PS FAD mutations that have little endoproteolysis but retain γ-secretase activity exist (Godbolt et al., 2004). The function of these mutations may be explained by studies that have shown that PS1-FL can support γ-secretase activity. For example, a random mutagenesis screen identified endoproteolytically deficient PS1 mutants that had increased activity for longer Aβ production (Aβ43) (Nakaya et al., 2005). Clearly, endoproteolysis is just one of a variety of ways in which the γ-secretase complex can be activated. This is not surprising, as we now know that γ-secretase is regulated on many levels by a variety of complex formation events and interacting partners (see introduction). Understanding

the mechanism of PSase will clarify γ-secretase activation under WT conditions, and may also serve as a model for γ-secretase activating mutations in disease conditions.

γ-Secretase and PSase have much overlap but are not the same

Before the enzyme responsible for the endoproteolytic cleavage of PS was known, it was termed "presenilinase" (PSase). Current evidence suggests that PSase is actually PS itself, and endoproteolysis is an autocatalytic cleavage event. This is illustrated by the following observations: 1. Mutation of PS's catalytic aspartate residues not only blocks γ-secretase activity, but also PSase activity (Wolfe et al., 1999). 2. Pepstatin A, an aspartyl protease inhibitor, suppresses PSase activity, further suggesting that PSase is an aspartyl protease (Campbell et al., 2002). 3. PSase is an integral membrane protein, as its activity is not lost upon washing membrane vesicles with sodium carbonate (Campbell et al., 2002). 4. The coexpression of WT PS1 with PS1 D257A (a γ-secretase and PSase deficient mutant) does not restore endoproteolysis of the mutant (Brunkan et al., 2005a), indicating that endoproteolysis occurs *in cis* and is an autocatalytic event. 5. An *in vitro* reconstitution study showed that bimolecular interaction of PS1 and Pen2 is necessary and sufficient for PS1 endoproteolysis (Ahn et al., 2010). Pen2 is unlikely to be PSase, and is probably required to orient PS in a conformation that facilitates autocatalytic cleavage.

γ-Secretase and PSase are intimately tied, as both are aspartyl proteases (Campbell et al., 2003) and PSase is necessary for formation of mature, active γ-secretase under WT conditions. However, γ-secretase and PSase are not identical (Figure 2.2). This is illustrated by the following observations: 1. Some endoproteolysis deficient PS1 mutants have γ-secretase activity (PS1ΔE9 and M292D), so PSase is not strictly required for γ-secretase (Steiner et al., 1999b). 2. Some PS1 mutations, including PS1 FAD mutations, that alter γ-secretase activity have no effect on PSase (Steiner et al.,

2000;Campbell et al., 2002;Laudon et al., 2004;Brunkan et al., 2005b). 3. The active site-directed, peptidomimetic γ-secretase inhibitor L685,458 (L458) binds and inhibits γ-secretase without inhibiting PSase (Beher et al., 2001). These findings, summarized in Figure 2.2, suggest that while endoproteolysis is required for γ-secretase activity in most cases, other activating mechanisms, such as deletions/mutations in PS1, do exist. Furthermore, it appears that, given the right tools, γ-secretase and PSase can be dissociated and studied separately in order to better understand the mysterious process of endoproteolysis.

Bio-orthogonal probe development – "click" chemistry

In order to perform activity-based protein profiling (ABPP) we needed an active site-directed probe that could be covalently crosslinked to target proteins and pulled-down for protein isolation. While a biotin moiety could be directly attached to the probe for enrichment, this would result in a bulky protrusion that may modulate or attenuate the probe's activity. To avoid this, we took advantage of copper-catalyzed azide-alkyne cycloaddition (CuAAC), which is bio-orthogonal to the system in which it is carried out, meaning the precursors do not react with biomolecules but do react with each other at high efficiency (Rostovtsev et al., 2002;Tornoe et al., 2002). We introduced an alkyne into the probe, which can be "clicked" to biotin-azide (or TAMRA-azide) after the probe bound target proteins. Next, the protein-probe-biotin complex can be pulled-down with streptavidin beads for protein isolation and identification. This clickable probe approach facilitates the design of functional probes that can selectively label and detect proteins in complex cellular systems with minimal modification to the original compound (Crump et al., 2011;Crump et al., 2012a;Crump et al., 2012b;Pozdnyakov et al., 2013;Gertsik et al., 2014a).

A.

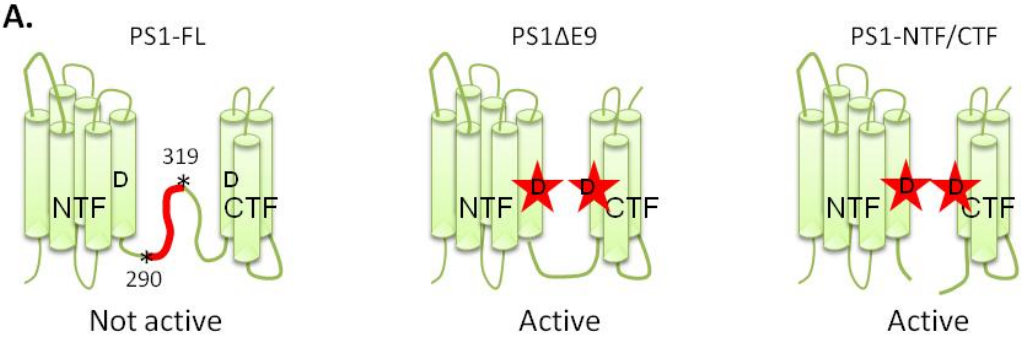

B.

PS1 FAD mutation	Effect on PSase
M139I, L250S, Y115H	No affect
M146L, A246E, C263R, P264L, P267S, E280A, L286V	Partial inhibition
V96F, M146V, A246E, E280G, C410Y	Inhibition

C.

	γ-secretase	PSase
L458	inhibition	minimal inhibition
Pepstatin A	inhibition	inhibition

Figure 2.2. γ-Secretase and presenilinase (Psase) are not the same. A. Some endoproteolysis deficient PS1 mutants have γ-secretase activity (i.e. PS1ΔE9), so PSase is not strictly required for γ-secretase Left: PS1-FL does not have γ-secretase activity. Middle: The FAD mutant PS1ΔE9, which lacks amino acids 290-319 and does not undergo endoproteolysis, has γ-secretase activity. Right: PS1-NTF/CTF fragments, which form as a result of PS-FL endoproteolysis, have γ-secretase activity. B. PS1 FAD mutations with different effects on PSase. Some PS1 mutations, including PS1 FAD mutations, that alter γ-secretase activity have no effect on PSase. C. The active site-directed, peptidomimetic γ-secretase inhibitor L458 inhibits γ-secretase but not PSase. Conversely, the aspartyl protease inhibitor pepstatin A inhibits both γ-secretase and PSase.

How can we separate the highly interdependent but separate activities of γ-secretase and PSase?

Notwithstanding findings that PS possesses γ-secretase and PSase activities, it has been a formidable challenge to characterize both activities and understand their differences due to their complex interdependence. While many γ-secretase active site-based inhibitors exist to directly probe γ-secretase, no successful PSase-directed probes exist to date. CBAP (Figure 2.3A) is a γ-secretase inhibitor that also causes a "pharmacological knock-down" of PS1 NTF/CTF with a concomitant accumulation of PS1-FL in the cell (Beher et al., 2001). However, the mechanism of action of CBAP in γ-secretase and PSase remains to be investigated. Here, we have synthesized CBAP-BPyne, a clickable, photoreactive form of CBAP, as a tool to understand the mechanism of PSase (Figure 2.3).

2.2 Results

CBAP, a potent γ-secretase inhibitor, is a chimeric compound containing a transition state isostere similar to L458 and a benzodiazepine group similar to the GSI Compound E (Seiffert et al., 2000). CBAP was found to accumulate PS1-FL with concomitant PS1 NTF/CTF fragment depletion in SH-SY5Y cells that were treated for 7 days (Beher et al., 2001). CBAP offers a unique opportunity for probe development and PSase mechanistic studies.

Synthesis of CBAP-BPyne

The CBAP intermediate TBS-protected alcohol (**4**) was synthesized by coupling amino benzodiazepinone **3** to carboxylic acid **1** as previously reported (Beher et al., 2001). To synthesize CBAP-BPyne, we initially investigated the selective removal of the NHBoc group from **4**, but all conditions examined resulted in poor product

formation where removal of the silyl and Boc protecting groups occurred at competitive rates. It was determined that selective Boc group removal or one-pot global deprotection strategies were not viable to produce the CBAP-BPyne in sufficient yields and purity. CBAP-BPyne was ultimately synthesized by removing the silyl protecting group in **4** with TBAF to yield CBAP followed by a rapid deprotection of the NHBoc group at 0 °C in dilute TFA to produce the fully deprotected scaffold. The crude amino alcohol was then immediately coupled with the NHS ester of propargyl benzophenone **2** to afford CBAP-BPyne [‡] (van Scherpenzeel et al., 2009) (Figure 2.3B).

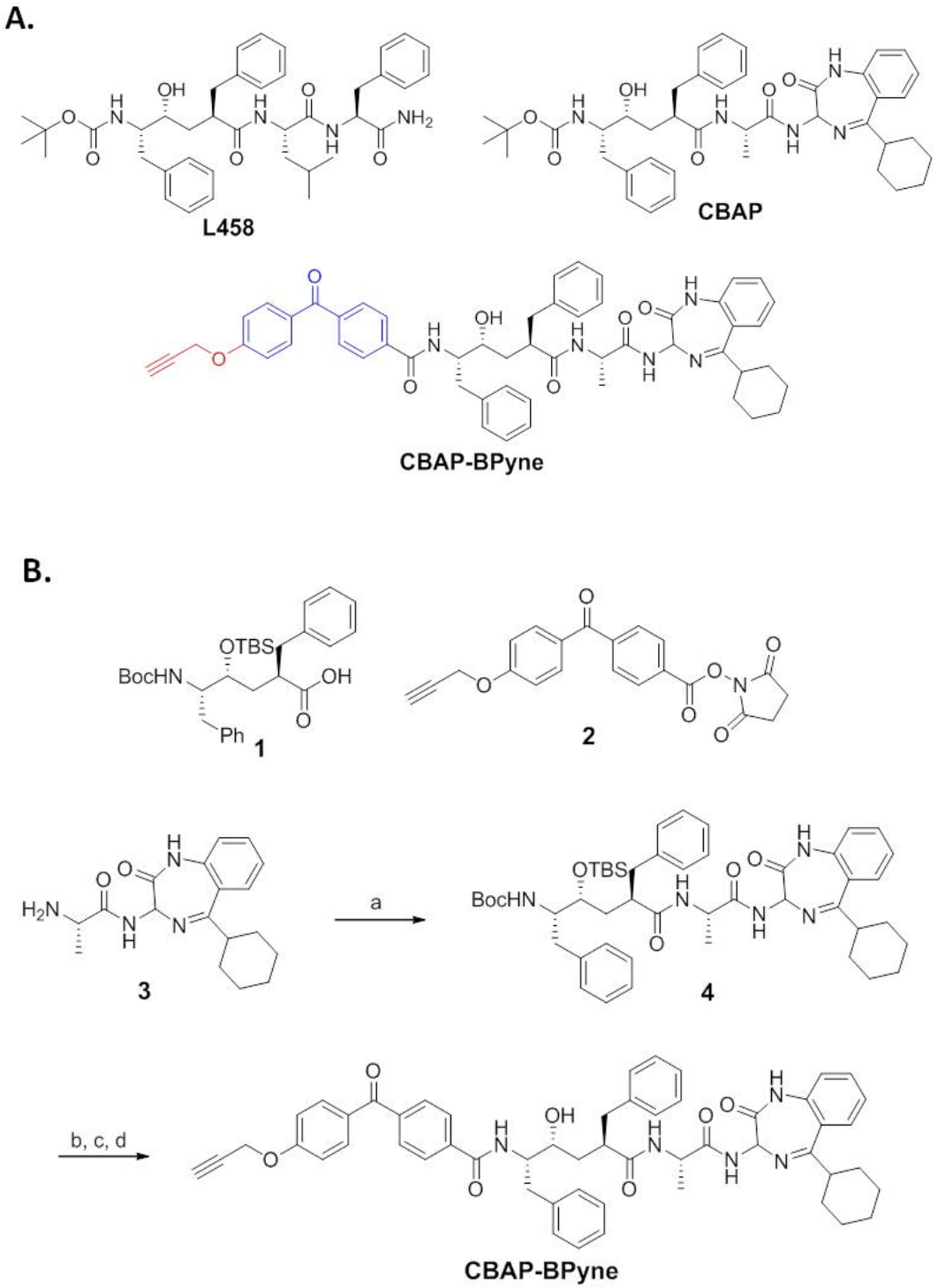

Figure 2.3. A. Structures of L458, CBAP, and CBAP-BPyne. Red: clickable alkyne; blue: crosslinkable benzophenone B. Reagents and conditions for synthesis of CBAP-BPyne. a) **1**, HATU, DIPEA, DMF, 24 h, RT, 83%; b) TBAF, THF, 6 h, RT, 84%; c) TFA, CH_2Cl_2, 5 min, 0 °C; d) **2**, DIPEA, DMF, 18 h, 79%.

CBAP-BPyne inhibits both γ-secretase and PSase

CBAP-BPyne contains a photophore for photoaffinity labeling and an alkyne for CuAAC. First, using our *in vitro* γ-secretase activity assay with recombinant APP and Notch1 substrates (Placanica et al., 2009b;Shelton et al., 2009;Tian et al., 2010a;Chau et al., 2012;Chau et al., 2013), we determined that both CBAP and CBAP-BPyne are equipotent γ-secretase inhibitors. Specifically, both compounds potently inhibit γ-secretase activity for the production of Aβ40 and Notch1-NICD (Figure 2.4A, left). Next, we examined CBAP and CBAP-BPyne's cellular activity in inhibiting PS1 processing. HeLa cells were treated for four days in a 12-well plate with CBAP, CBAP-BPyne, L458, or vehicle control at concentrations of 1, 3, or 10 μM and lysates were Western blotted for PS1-NTF. CBAP and CBAP-BPyne caused a much greater accumulation of PS1-FL at the expense of PS1-NTF/CTF than did L458 (Figure 2.4B for PS1-NTF and data not shown for PS1-CTF). We saw a very similar effect when SH-SY5Y cells were treated with 10 μM of all the same compounds for seven days and Western blotted, probing with anti PS1-NTF antibody (Figure 2.4C). This indicates that CBAP and CBAP-BPyne are capable of inhibiting PSase activity, while L458 has little effect on PSase activity under these conditions. CBAP is a more potent PSase inhibitor than CBAP-BPyne as seen by the nearly complete depletion of PS1-NTF in CBAP treated cells compared to the incomplete PS1-NTF depletion in CBAP-BPyne treated cells (Figure 2.4B, C). This effect is not due to a difference in the ability of the compounds to permeate the cell membrane because CBAP and CBAP-BPyne were equipotent in a cell-based γ-secretase activity assay in CHO-APP cells (Aβ42 IC_{50} = 28 nM and 20 nM, for CBAP and CBAP-BPyne, respectively) and in N2A-APP cells (Aβ40 IC_{50} = 95 nM, 167 nM, and 330 nM for CBAP, CBAP-BPyne, and L458, respectively) (Figure 2.4A, right). The ~2X difference between the Aβ40

IC_{50}s of CBAP and CBAP-BPyne is negligible as Aβ40 IC_{50} for L458 was 330 nM, suggesting the differences are due to natural variation in the cell-based activity assay.

A.

In vitro IC_{50} (nM)		
	Aβ40	Notch1
CBAP	0.70	0.56
CBAP-BPyne	0.91	1.0

Cell-based IC_{50} (nM)		
	Aβ40 (N2A-APP)	Aβ42 (CHO-APP)
CBAP	95	28
CBAP-BPyne	167	20
L458	330	

B.

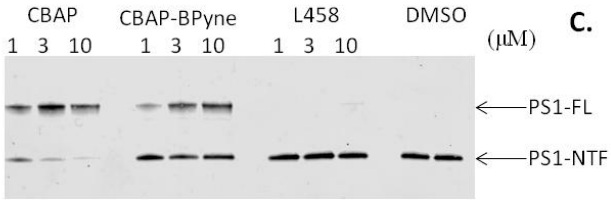

C.

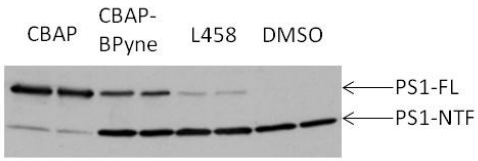

Figure 2.4. A. *In vitro* and cell-based inhibitory potency (IC_{50}) of CBAP and CBAP-BPyne. B. HeLa cells were treated with 1, 3, and 10 μM of CBAP, CBAP-BPyne, and L458, or vehicle control (DMSO), for 4 days. Protein concentration was determined and same amount of cell lysate (15 μg) was run on SDS-PAGE. Western blot analysis was performed with an anti PS1-NTF antibody. C. SH-SY5Y cells were treated with 10 μM of various compounds for 7 days and Western blotted as in B.

CBAP-BPyne labels γ-secretase

We determined that CBAP-BPyne is a functional probe, as photoaffinity labeling followed by CuAAC, biotin pull-down, and Western blot showed that CBAP-BPyne specifically labels PS1-NTF (Figure 2.5A, left). CBAP-BPyne was also found to label signal peptide peptidase (SPP), a protein structurally similar to PS (Figure 2.5A, right). Photoaffinity labeling studies followed by CuAAC with TAMRA-azide confirmed the specific labeling of PS1-NTF and SPP, and showed that CBAP-BPyne binds additional proteins, although PS1-NTF is the primary target (Figure 2.5B). The

additional unidentified proteins that are specifically labeled (denoted with a star) may play a role in endoproteolysis and should be studied further for their identity and function. Whether bands that migrated in the range of high molecular weight represent aggregated PS1-NTF, SPP, or novel proteins also remains to be investigated.

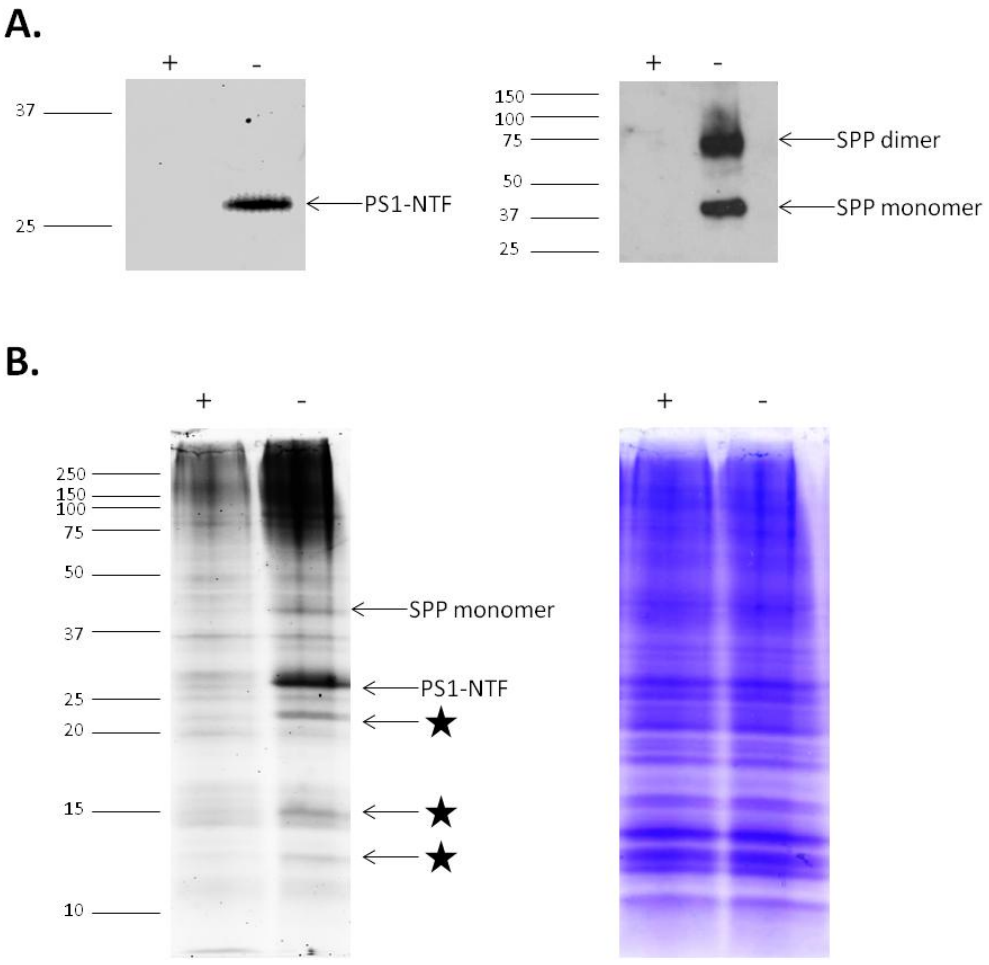

Figure 2.5. HeLa membranes were photolabeled with CBAP-BPyne (20 nM) in the presence (+) or absence (-) of CBAP (2 μM), followed by click chemistry with: A. biotin-azide, streptavidin pull-down, and Western blot analysis with either anti PS1-NTF (left), or SPP (right) antibody or B. TAMRA-azide, in-gel fluorescence (left) and Coomassie blue gel staining (right). Stars represent unidentified proteins that are specifically labeled by CBAP-BPyne.

CBAP-BPyne does not label PS1-FL

We hypothesized that PS-NTF/CTF has γ-secretase activity and PS-FL has PSase activity. As a result, we expected that CBAP inhibits γ-secretase by binding to PS-NTF/CTF and that it inhibits PSase by binding to PS-FL. In the previous section, through the use of CBAP-BPyne, we confirmed that CBAP does in fact label γ-secretase. In this section we set out to determine whether it also binds PS-FL.

We could not look for PS1-FL labeling in HeLa cell membrane because PS1-FL that is not endoproteolysed is rapidly degraded, so HeLa has no detectable PS1-FL. To circumvent this problem, we looked for labeling of PS1-FL in ANP24 and ANPP8 cell membranes, which are HEK293 overexpressing cells with high levels of PS1-FL (Kim et al., 2003) (Figure 2.6A). ANP24 cells have little endoproteolysis as they overexpress all γ-secretase components except Pen2. As a result, these cells have more PS-FL than PS-NTF/CTF. ANPP8 cells overexpress all four γ-secretase components. As a result, these cells have more PS1-NTF/CTF than PS-FL. Both cell lines have ample PS1-FL. First, we photolabeled both ANP24 and ANPP8 cell membranes with various concentrations of CBAP-BPyne (20 nM–500 nM, only 500 nM labeling of ANP24 shown here) (Figure 2.6B). While we found robust PS1-NTF labeling, we were unable to detect any specific PS1-FL labeling. We considered the possibility that additional factors may be required for successful CBAP-BPyne labeling of PS1-FL and performed live-cell labeling experiments in which CHAPSO permeabilized ANP24 and ANPP8 cells were photolabeled with 500 nM CBAP-BPyne in the presence (+) or absence (-) of 10 μM CBAP (Figure 2.6C). Again, no PS1-FL labeling was detected but PS1-NTF was clearly labeled. PS1-NTF in ANPP8 is more robustly labeled than that in ANP24 because there is more active γ-secretase in ANPP8, which expresses all four components of γ-secretase, than there is in ANP24, which does not

have Pen2. We hypothesized that the γ-secretase complex in the overexpressing cells may not be in the proper conformation for labeling by CBAP-BPyne due to artifacts of overexpression. To test this, we treated SH-SY5Y cells, which have endogenous levels of γ-secretase, with 1 μM CBAP-BPyne for 48 hours in order to accumulate PS1-FL, switched the cells into new media with fresh 1 μM CBAP-BPyne, and photocrosslinked (Figure 2.6D). Switching the cells into media with fresh compound was critical because when we removed the media and did not add any fresh compound, we did not see any PS1-NTF labeling. This is probably because CBAP-BPyne degraded over the course of the incubation at 37 ˚C. Again, we observed labeling of PS1-NTF but not PS1-FL. These and other experiments convinced us that CBAP-BPyne is not labeling PS1-FL.

CBAP-BPyne is not acting through the proteasome pathway

Since CBAP-BPyne did not label PS1-FL, we recognized that there is a possibility that CBAP accumulates PS1-FL through some other mechanism, such as proteasome inhibition. To rule this out, we treated SH-SY5Y cells either with 1 μM CBAP-BPyne for 48 hours, 20 μM MG132 (a proteasome inhibitor) for 2 hours, or both (Figure 2.6E). Treatment of SH-SY5Y cells with MG132 did not accumulate PS1-FL, suggesting that the mechanism of PS1-FL accumulation is not through inhibition of the proteasome.

CBAP-BPyne does not impact the levels of other γ-secretase subunits

Another potential pathway through which CBAP may be accumulating PS1-FL is by downregulating γ-secretase subunits other than PS. For example, if CBAP downregulates Pen2, a protein required for endoproteolysis, then cleavage of PS-FL cannot occur. Similarly, the downregulation of either Nct or Aph1 would impair

complex formation and inhibit endoproteolysis, which occurs exclusively in mature complexes that have all four subunits. We checked the levels of Nct and Pen2 in SH-SY5Y cells treated for four days with 10 μM CBAP, L458, and vehicle control (Figure 2.6F). The levels of these proteins were not changed compared to DMSO control, illustrating that CBAP does not accumulate PS1-FL through downregulation of these γ-secretase subunits. This was confirmed by the finding that CBAP-BPyne does not label PS1-CTF or any of the other three subunits (Nct, Pen2, Aph1) of γ-secretase (Figure 2.6G). Specifically, when HeLa membrane was photolabeled with 20 nM CBAP-BPyne +/- 2 μM CBAP there was no labeling of Pen2, Aph1, or Nct especially when compared to positive control labeling by GSI-877 (163-BP3), a probe that pulls-down all components of the γ-secretase complex. To confirm that CBAP does not target Pen2, we used a higher concentration of compound for labeling of ANPP8 membrane: ANPP8 membrane was photolabeled with 500 nM CBAP-BPyne, followed by click chemistry and Western blot for Pen2 (data not shown). Again, there was no Pen2 labeling. Similarly, when ANP24 membrane was photolabeled with 20 nM CBAP-BPyne +/- 2 μM CBAP there was no labeling of PS1-CTF, especially when compared to positive control labeling by GSI-256, which is an active site-directed probe that labels both PS1-NTF and PS1-CTF.

Figure 2.6. A. Relative levels of PS1-NTF/CTF and PS1-FL in ANP24 (3 γ-secretase subunits) and ANPP8 (4 γ-secretase subunits) cell lysate shown in duplicate. B. ANP24 membrane (600 μg) or C. live ANP24 and ANPP8 cells were photolabeled with CBAP-Bpyne (500 nM) in the presence (+) or absence (-) of CBAP (10 μM), followed by click chemistry and Western blot, probing for PS. Input=5 ug ANP24 membrane. D. SH-SY5Y cells were treated with 1 uM CBAP-BPyne for 48 hours and crosslinked with fresh 1 μM CBAP-BPyne followed by click chemistry and Western blot, probing for PS. Input=lysate from SH-SY5Y cells that were treated with CBAP-BPyne. E. SH-SY5Y cells were treated with 1 uM CBAP-Bpyne (48 hrs), 20 μM MG132 (2 hrs), or both. Cells were lysed and Western blotted. Input=5 μg ANP24 membrane. F. SH-SY5Y cells treated for 4 days with 10 μM indicated compound, lysed, and Western blotted for Pen2 and Nct. Experiment shown in duplicate. G. Top panel: structures of GSI-877 and GSI-256. Bottom left panel: HeLa membrane photolabeled with 20 nM GSI-877 +/- 2 μM GSI-495 or 20 nM CBAP-BPyne +/- 2 μM CBAP, followed by click chemistry and Western blot for Pen2, Aph1, or Nct. Bottom right panel: ANP24 membrane photolabeled with 20 nM GSI-256 +/- 2 μM L458 or 20 nM CBAP-BPyne +/- 2 μM CBAP, followed by click chemistry and Western blot for PS1-CTF.

Figure 2.6

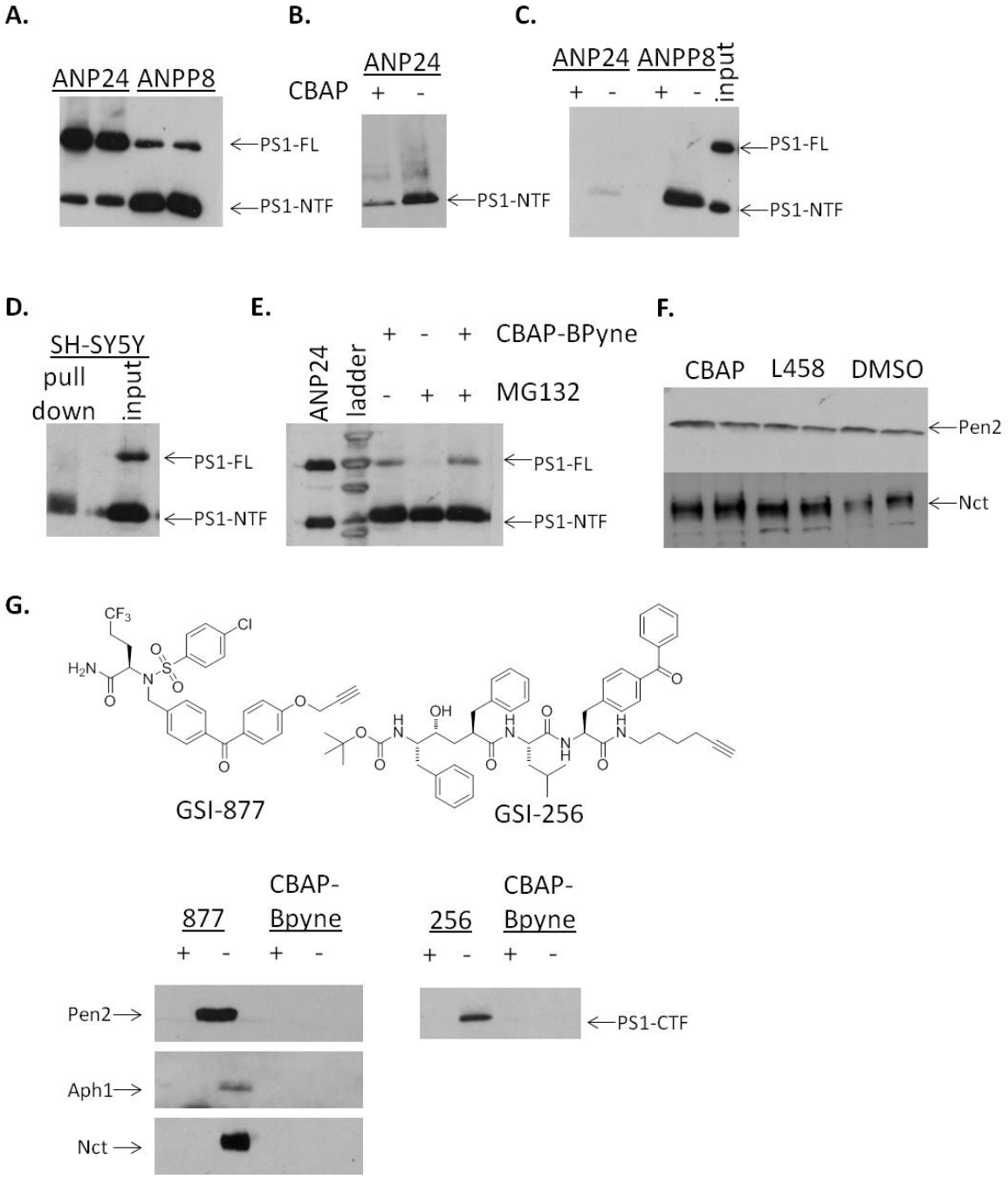
A.
ANP24 ANPP8
PS1-FL
PS1-NTF
B.
CBAP
ANP24
+ -
PS1-NTF
C.
ANP24 ANPP8
+ - + - input
PS1-FL
PS1-NTF
D.
SH-SY5Y
pull down
input
PS1-FL
PS1-NTF
E.
+ - + CBAP-BPyne
- + + MG132
ANP24
ladder
PS1-FL
PS1-NTF
F.
CBAP L458 DMSO
Pen2
Nct
G.
GSI-877
GSI-256
877 CBAP-Bpyne
256 CBAP-Bpyne
+ - + -
Pen2
Aph1
Nct
PS1-CTF

2.3 Conclusion and Discussion

CBAP-BPyne is the first clickable, photoreactive probe that inhibits both γ-secretase and PSase activities (Figure 2.7A). However, CBAP-BPyne labels γ-secretase but not PSase. This may be because 1. CBAP-BPyne does not bind PS1-FL or 2. CBAP-BPyne binds PS1-FL, but the crosslinking efficiency is low. If scenario one is correct and CBAP-BPyne has a target other than PS1-FL, then large scale pull-down, LC-MS, and validation studies can identify this protein and confirm its role in endoproteolysis. As the TAMRA gel illustrates, CBAP-BPyne certainly has targets other than PS, but whether these proteins play a role in endoproteolysis remains unknown. We confirmed that these candidate proteins are *not* Pen2, Aph1, PS1-CTF or Nct. This begs the question, can another, yet unknown protein be playing a role in endoproteolysis? While unlikely, this possibility is worth exploring. Scenario two seems more plausible because our data shows that the potency of CBAP-BPyne for γ-secretase inhibition is much higher than it is for PSase inhibition. Consequently, the probe used in labeling experiments may be binding PS1-NTF tightly without having a chance to significantly interact with and bind PS1-FL. If this is the case, then SAR can help improve the efficiency of probe binding to PS1-FL. We have previously found that the location of the crosslinkable moiety on a probe is critical for efficient labeling. Particularly, steric issues and amino acid/benzophenone distances play a major role in crosslinking efficiency. This is illustrated by the observation that all four of our L458 analogue probes (L646, GY4, JC8, L505) have similar IC_{50}s, but label the active site of γ-secretase with different efficiencies (Tian et al., 2010a;Gertsik et al., 2015). Additionally, FAD mutations in PS1 hinder the labeling efficiency of some probes while having no perceptible impact on others (Chau et al., 2012). These findings suggest that all four active site-directed probes actually label different sub-sites of the

γ-secretase active site. Similarly to the L458 based probes, I propose to design additional CBAP-based probes by moving the benzophenone (or another photocrosslinking group) to other sites on the compound. This technique is known as "photophore walking." It is likely that synthesis of additional CBAP-based probes using the photophore walking approach will allow us to characterize the various sub-sites of the γ-secretase active site, and more importantly, the PSase active site. The synthesis of distinct, photoreactive, clickable, CBAP-based probes that differ only in the location of the crosslinkable moiety can generate compounds that are optimized to label PS1-FL. My first recommendation is to make CBAP analogues that incorporate a benzophenone in the P1' and P1 positions and to use these probes to pull-down PS1-FL (Figure 2.7B).

Based on current clinical investigation of non-selective γ-secretase inhibition (i.e. the case of semagacestat), PSase may not be a viable drug target for the treatment of AD since PSase inhibition also blocks γ-secretase activity, leading to toxicity (Doody et al., 2013). However, PSase could serve as a target for cancer therapy. Furthermore, CBAP-BPyne can be used to investigate PSase and γ-secretase activation, which appear to play a role in disease states, as evidenced by reports that some FAD PS1 mutations affect PSase activity (Mercken et al., 1996;Murayama et al., 1999;Brunkan et al., 2005b). CBAP-BPyne provides a novel means to investigate the mechanism of PSase as it has the capacity not only to bind and inhibit γ-secretase, but also to inhibit the endoproteolysis of PS1-FL, a novel function not observed in other γ-secretase probes. CBAP-BPyne may aid in the identification and characterization of PSase, revealing the mechanism of γ-secretase activation and uncovering PSase as a potential target in cancer therapy.

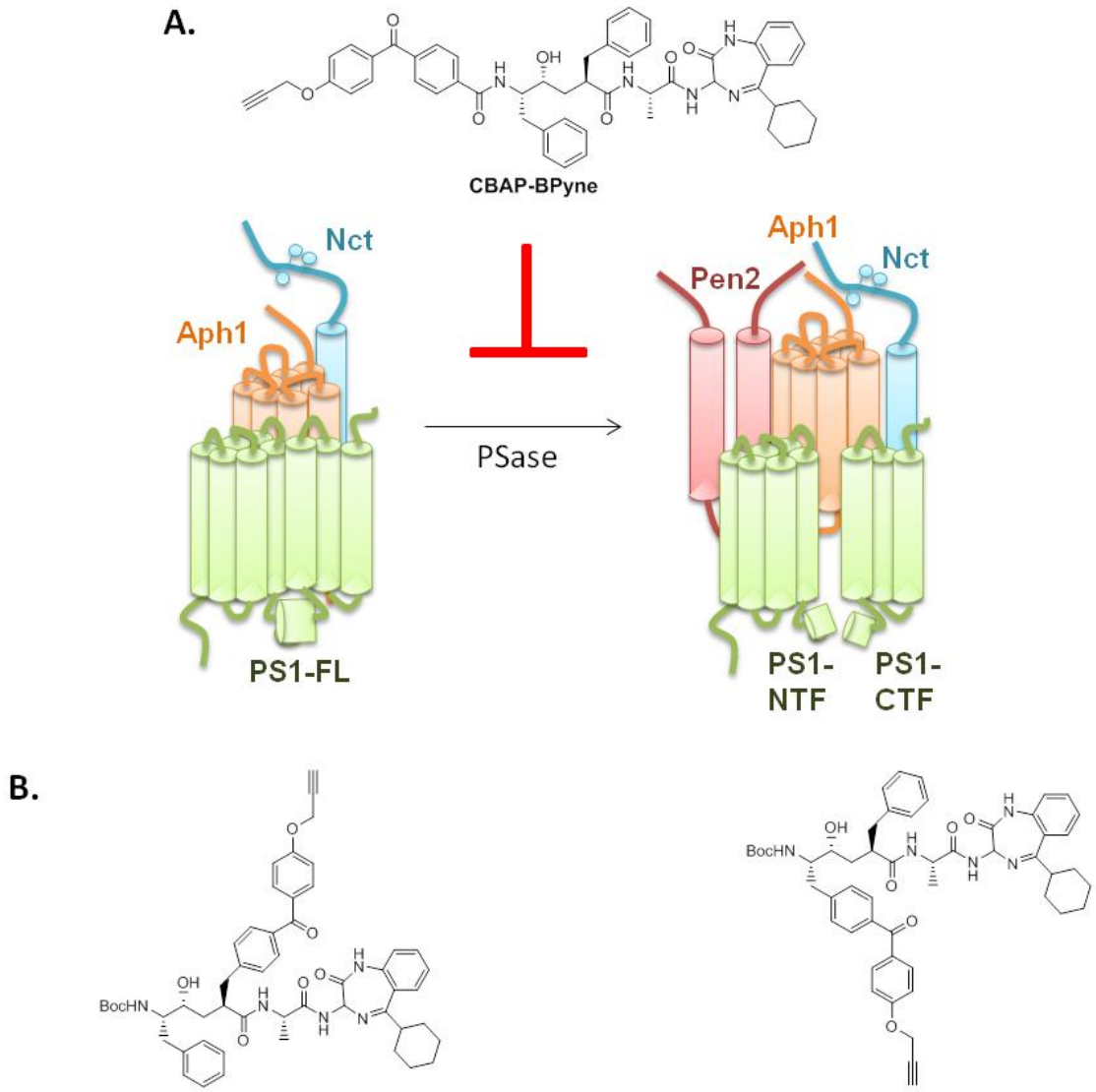

Figure 2.7. A. CBAP-BPyne, a dual γ-secretase and PSase clickable probe, inhibits both activities and provides a novel means to investigate the mechanism of endoproteolysis. B. Generation of alternative CBAP-based probes using the photophore walking approach. Each probe, with its benzophenone moiety on a different P position, crosslinks to a different sub-site of the enzyme active site. Left: clickable benzophenone is in the P1' position. Right: clickable benzophenone is in the P1 position.

2.4 Methods

Treatment of cells with compound followed by lysis and Western blot

Cells were treated with compound at indicated concentration for 4-7 days, maintaining a final DMSO concentration of 0.1% (v/v). Cells were lysed with RIPA buffer (50 mM Tris base pH 8.0, 150 mM NaCl, 0.1% SDS, 1% NP-40, 0.5% deoxycholate), and equal amounts of cell lysate was separated on a 12% Bis-Tris or a 4-20% TGX gel. Proteins were transferred to Immobilon-FL PVDF membrane, probed with indicated antibody, and imaged on Odyssey.

Photoaffinity labeling followed by biotin pull-down and Western blot

600 μg of HeLa cell membrane, diluted with PBS to a volume of 500 μL in a 12-well plate, was incubated with either 2 μM CBAP or vehicle control for 20 min at 37° C. 20 nM CBAP-BPyne was added for 1 hour at 37° C followed by UV irradiation at 350 nm for 45 min to promote benzophenone-protein crosslinking. Membrane was pelleted by centrifugation at 100,000 ×*g* for 30 min and resuspended in PBS using Qiagen TissueLyser. Click chemistry reagents [1 mM tris(2-carboxyethyl)phosphine, 1 mM $CuSO_4$, 0.1 mM tris-(benzyltriazolylmethyl)amine, and 0.1 mM biotin azide in 5% *t*-butyl alcohol with 1% DMSO] were added and the mixture was rotated for 1 hour at room temperature. Membranes were pelleted by centrifugation at 100,000 ×*g* for 30 min, resuspended in 500 μL PBS, and solubilized with the addition of RIPA buffer. Samples were centrifuged at 15,700 ×*g* and supernatant was added to Pierce Streptavidin Plus UltraLink Resin and rotated overnight at 4° C. Proteins were eluted with 2 mM biotin in SDS sample buffer at 70° C for 10 min, separated on a 12% Bis-Tris gel or a 4-20% TGX gel, transferred to Immobilon-FL PVDF, probed with the relevant antibody, and visualized on Odyssey.

Photoaffinity labeling followed by CuAAC with TAMRA-azide

See introduction for detailed method

Live-cell photolabeling

SH-SY5Y cells were plated to 60% confluence in 100x20 mm tissue culture dish. Next day cells were treated with 1 μM CBAP-BPyne (0.1% DMSO in media, v/v). After 24 hours, cells were split and half the cells were seeded in fresh media + 1 μM CBAP-BPyne. 24 hours later the media was removed and fresh media with 1 μM CBAP-BPyne was added. Samples were UV irradiated at 350 nm for 45 minutes on an ice block. Plate with samples was washed 2X with 5 ml cold PBS. Cells were scraped into Eppendorf tube in 1 ml PBS and spun down at 100 x*g* for 5 minutes. Supernatant was discarded. Cells were lysed in 1 mL cold PBS + PI by sonication, 6 x 0.5 second pulses. Low speed spin removed nuclear debris and supernatants were ultracentrifuged at 53,000 x*g* for 30 minutes. Supernatant from this spin was discarded and pellet was resuspended in 0.25% CHAPSO in PBS with TissueLyser. CuACC was performed as in 6.4. Samples were ultracentrifuged at 100,000 x*g* for 1 hour and pellets were resuspended with 1X RIPA in TissueLyser. Samples were spun down at 15,700 x*g* for 10 min to pellet insoluble matter. The supernatants were transferred to a dolphin-nosed tube with 20 μl Streptavidin Plus UltraLink Resin and biotinylated proteins were pulled-down with rotation at 4˚ C overnight. The next day, samples were spun down at 100 x*g* and supernatant was removed. The streptavidin slurry pellet was washed 3X with RIPA and once with tris buffered saline, 0.1% tween-20. Proteins were eluted with 40 μl of 2 mM biotin in Laemmli sample buffer at 70˚ C for 10 minutes and 20 μl of eluate was loaded and separated on SDS-PAGE. Proteins were transferred to PVDF membrane and probed with necessary antibodies. Similar protocol, without the 4-7 day pretreatment with CBAP-BPyne, was performed for ANP24 and ANPP8 cell labeling.

‡ Characterization of CBAP-BPyne: ^{1}H NMR (400 MHz, CD_3OD) δ 8.61 - 8.43 (m, 1H), 8.26 (d, *J* = 8.8 Hz, 1H), 8.18 (t, *J* = 7.9 Hz, 1H), 7.82 - 7.75 (m, 2H), 7.73 - 7.67 (m, 5H), 7.55 - 7.48 (m, 1H), 7.29 (t, *J* = 7.7 Hz, 1H), 7.24 - 7.08 (m, 13H), 7.08 - 7.00 (m, 1H), 5.15 - 5.08 (m, 1H), 4.85 (2H, buried in solvent), 4.49 (dt, *J* = 13.5, 6.9 Hz, 1H), 4.34 - 4.22 (m, 1H), 3.76 (td, *J* = 8.5, 4.3 Hz, 1H), 3.12 - 3.03 (m, 1H), 3.01 (t, *J* = 2.3 Hz, 1H), 3.00 - 2.93 (m, 1H), 2.88 (d, *J* = 9.2 Hz, 1H), 2.82 - 2.69 (m, 2H), 2.04 - 1.74 (m, 4H), 1.69 - 1.54 (m, 2H), 1.49 - 1.21 (m, 8H), 1.15 (d, *J* = 10.4 Hz, 1H), 1.08 - 0.94 (m, 1H); LRMS calcd for $C_{54}H_{55}N_5O_7$ (M+H) 886.4, found 886.5; HPLC Purity: 99.9%.

CHAPTER 3

γ-Secretase inhibitors (GSIs) and modulators (GSMs) induce distinct conformational changes in the active sites of γ-secretase and signal peptide peptidase (SPP) (Gertsik et al., 2015)

3.1 Introduction

γ-Secretase and signal peptide peptidase (SPP) are aspartyl proteases that catalyze regulated intramembrane proteolysis, a process that controls the activity and function of membrane proteins in all living systems studied to date (Brown et al., 2000). You can read Chapter 1 for a detailed introduction to γ-secretase. In this chapter we introduce SPP and the overlap between the two enzymes.

The differences and similarities between γ-secretase and SPP

SPP proteolyses signal peptides in their transmembrane (TM) region after they have been cleaved off from the protein by signal peptidase. The signal peptide fragments released by SPP are required for important cellular events such as immune surveillance by HLA-E epitopes and HCV polyprotein cleavage critical for viral lifecycle (Lemberg et al., 2001;McLauchlan et al., 2002). γ-Secretase and SPP are multi-span TM proteins that share the same YD/GXGD catalytic motif (Fluhrer et al., 2009), but are structurally and functionally distinct (Figure 3.1). The key differences between the two proteins are: first, γ-secretase is a multi-subunit protein complex that includes Aph1, Nct, Pen2, and presenilin (PS, the catalytic subunit) (De Strooper, 2003;Edbauer et al., 2003;Takasugi et al., 2003;Gertsik et al., 2014b). Unlike γ-secretase, SPP appears to function alone without the participation of other protein co-factors (Weihofen et al., 2002). Second, SPP and PS have opposite orientations within the membrane (Weihofen et al., 2002;Friedmann et al., 2004;Nyborg et al., 2004a). As

a consequence, γ-secretase cleaves type 1 TM substrates while the substrates of SPP are type 2. Third, endogenous, wild type PS is expressed as a full-length protein that is activated by endoproteolytic cleavage during protein maturation (Thinakaran et al., 1996;Takasugi et al., 2003). Endoproteolysis results in the formation of two fragments, PS-NTF and PS-CTF, which remain associated within active γ-secretase complexes. Conversely, SPP functions as a full-length protein (Weihofen et al., 2002;Nyborg et al., 2004b;Nyborg et al., 2006). There is evidence to suggest that SPP forms dimers and tetramers within the cell (Nyborg et al., 2004b;Nyborg et al., 2006;Miyashita et al., 2011).

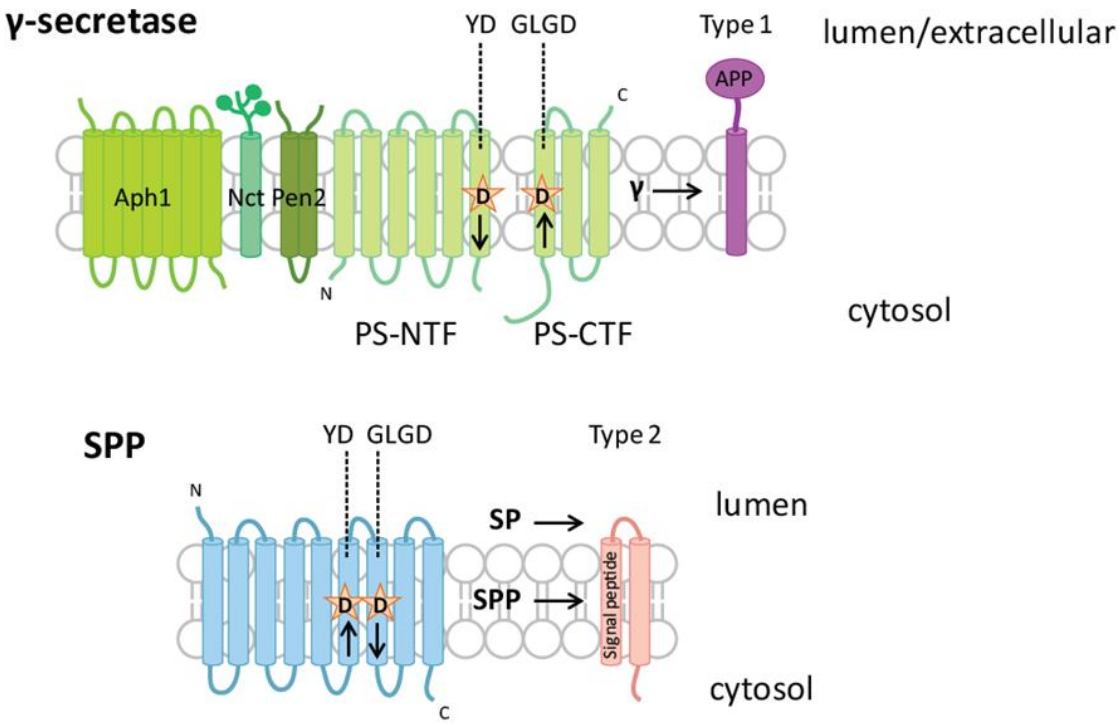

Figure 3.1. Structural and functional similarities/differences between γ-secretase and SPP. γ-Secretase and SPP are similar in that they are both multipass transmembrane enzymes that share the YD/GXGD catalytic motif and cleave their respective substrates in the transmembrane region. SPP and PS, the catalytic subunit of γ-secretase, both transverse the membrane nine times. The differences between the enzymes include their limited sequence homology, their inverse orientation in the membrane, and their specificity for either type 1 or type 2 substrates. Additionally, SPP functions without protein cofactors while PS requires at least 3 additional proteins (Aph1, Nct, and Pen2) for γ-secretase activity.

Although PS and SPP have opposite topologies with limited sequence homology, they share pharmacological characteristics: transition-state γ-secretase inhibitor L458 inhibits SPP activity (Weihofen et al., 2003;Iben et al., 2007) and L458-based photoaffinity probes L852,646 (L646) and CBAP-BPyne specifically label SPP (Weihofen et al., 2003;Crump et al., 2012a;Gertsik et al., 2014a). These data suggest structural similarity within the active sites of SPP and γ-secretase.

Our approach to studying the highly similar active sites of these distinct enzymes

Because there is no crystal structure of either γ-secretase or SPP, scant information exists regarding the active site architecture of these enzymes. Moreover, a comparison study exploring the effect of γ-secretase inhibitors (GSIs) and modulators (GSMs), which are being developed for cancer and AD treatment, on the active sites of SPP and γ-secretase has not been reported. We use a chemical biology approach to probe the active sites of PS1 and SPP. Particularly, we employ active site-directed photoprobes, in a method called photophore walking, to target the various sub-pockets of the enzyme active site (see Chapter 1 for detailed introduction to this technique) (Shelton et al., 2009;Tian et al., 2010a;Crump et al., 2011;Chau et al., 2012;Crump et al., 2013) (Figure 3.2A). Comparison of the photolabeling profiles of PS1 and SPP demonstrated that the active sites of these proteins are similar, yet some differences are apparent in specific active site sub-pockets. Furthermore, we used the photophore walking approach to determine the effects of GSIs and GSMs on the active site conformations of γ-secretase and SPP, which is an important step toward understanding off-target effects of GSI and GSM treatment. In addition, we provide evidence that active SPP exists as a stable homodimer.

3.2 Results

PS1 and SPP active site conformations are similar yet distinct

L458 has been a valuable tool in the study of γ-secretase (Shearman et al., 2000). We incorporated a photoreactive benzophenone moiety into different side chain positions of L458 (P and P' sites) to generate a series of photoprobes. These photoprobes, JC8, L646, GY4, and L505, photocrosslink to S1', S2, S1, or S3' subsites within the γ-secretase active site, respectively (Li et al., 2000b;Shelton et al., 2009;Yang et al., 2009;Tian et al., 2010a) (Figure 3.2A). A biotin linker was attached for isolation of the labeled species. This photophore walking approach facilitates the comparison of active site conformational changes of target enzymes, as the photocrosslinking efficiency is determined by the distance and orientation between contact residues of the enzyme active site and the benzophenone moiety of the photoprobes. By comparing the photocrosslinking efficiency of each probe to PS1 and SPP, we can gain insight into the conformational differences between the active sites of these enzymes.

Total membrane isolated from HeLa cells was used as the source of endogenous γ-secretase and SPP. First, we confirmed that JC8, L646, GY4, and L505 photolabeled PS1-NTF and this labeling was specific since excess amount of L458 blocked the labeling (Figure 3.2B, middle panel). Furthermore, the photolabeling profile of PS1-NTF revealed that JC8 labeled PS1-NTF with the strongest intensity followed by L646. GY4 and L505, on the other hand, were both weaker photoprobes for PS1-NTF (Figure 3.2B, middle panel).

SPP was photocrosslinked with the same set of photoprobes and the labeling was specific as excess L458 was able to block the photoinsertion of the probes (Figure 3.2B, top panel). Additionally we used $(Z\text{-}LL)_2$-ketone, a peptidomimetic SPP

inhibitor with an *in vitro* IC_{50} of 50 nM (Weihofen et al., 2000), to confirm that SPP is being specifically labeled and inhibited in our system (Figure 3.2C). As expected, excess $(Z\text{-}LL)_2$-ketone blocked the photolabeling of SPP completely (Figure 3.2C, top panel) but had little effect on the photolabeling of PS1-NTF (Figure 3.2C, bottom panel). Additionally, we showed that the photolabeling profile of SPPL2A, a close homologue of SPP that cleaves different substrates, is different from that of both γ-secretase and SPP. L646 and L505 labeled SPPL2A most efficiently, with the other photoprobes showing weaker labeling (Figure 3.2B, bottom panel).

These results indicate that the photolabeling profiles of PS1, SPP, and SPPL2A are different. Here we focus on the differences between PS1and SPP: Although JC8 labeled both PS1 and SPP with the strongest intensity, L646 was a much weaker photoprobe for SPP. Instead, L505 photolabeled SPP with similar efficiency to JC8. GY4 was a weaker photoprobe for both PS1 and SPP (Figure 3.2B). Comparison of the PS1 and SPP photolabeling profiles reveals that while two probes label the enzymes with similar efficiency (JC8 and GY4), the other two probes exhibit opposite labeling efficiencies (L646 and L505), suggesting that γ-secretase and SPP have similar architecture of the S1' and S1 sub-pockets, whereas the S2 and S3' sub-pockets are organized differently (Figure 3.2D). In conclusion, the overall structures of the PS1, SPP, and SPPL2A active sites are similar since the enzymes can be specifically labeled by all four active site-directed photoprobes, but the structure of the active site subsites differs among the enzymes, exemplified by the difference in labeling efficiency among photoprobes. How variation of these subsites contributes to the activity and specificity of γ-secretase, SPP, and SPPL2A remains to be investigated.

Figure 3.2. L458-based photoreactive probes specifically label PS1 and SPP. A. Structures of L458 and photoreactive probes JC8, L646, GY4, and L505. L458 side chain residues (P and P' sites) interact with corresponding sub-pockets of γ-secretase and SPP (S and S' sites). Photoreactive probes JC8, L646, GY4, and L505 have an L458 backbone (black), a biotin moiety (green), and a crosslinkable benzophenone (BP). Each probe has a BP incorporated into a different site on the L458 backbone. The location of the BP is illustrated by the color scheme. For example, JC8 has a BP at the P1' site, in place of the red benzene ring. JC8, L646, GY4, and L505 label S1', S2, S1, and S3' subsites of the enzymes, respectively. B. HeLa membranes were labeled with 20 nM of photoprobes JC8, L646, GY4, or L505 in the presence of 0.25% CHAPSO, and either with (+) or without (-) 2 μM L458. Samples were run on SDS-PAGE and analyzed by Western blot. Anti-SPP, PS1-NTF, or SPPL2A antibodies were used to detect SPP (top panel), PS1-NTF (middle panel), or SPPL2A (bottom panel). C. Same as B, except 2 μM $(Z\text{-}LL)_2$-ketone was used to block the labeling of SPP (top panel) and PS1-NTF (bottom panel). D. Active site-directed probes show subtle differences in the structures of PS1, SPP, and SPPL2A active sites. Ovals – the active site. Stars – the active site-directed probes. Smaller ovals, in which there is a closer interaction between enzyme active site and probe, represent tighter binding /higher efficiency of probe binding. Bigger ovals represent lower efficiency of probe binding.

Figure 3.2

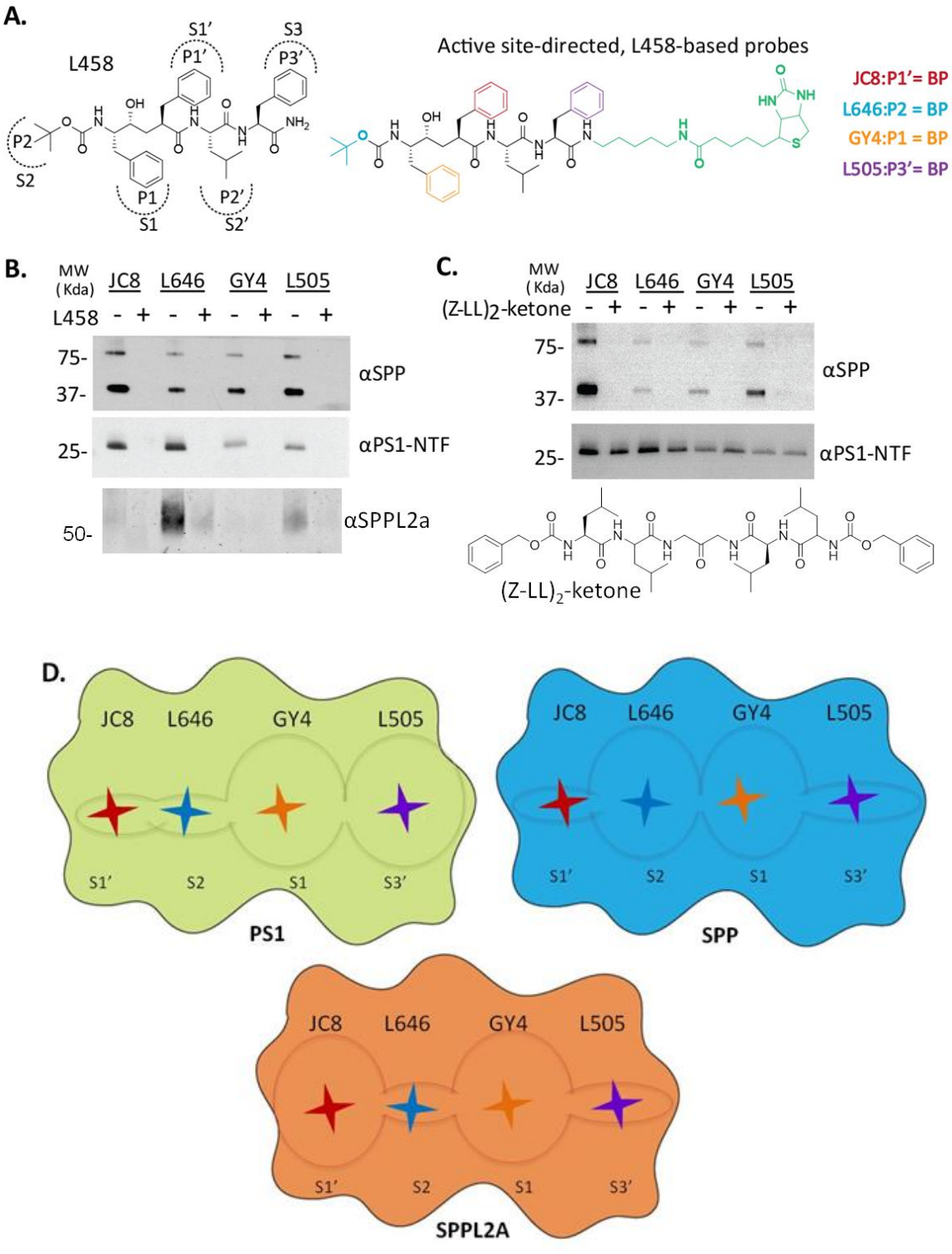
A.
L458
S1′
P1′
S3
P3′
P2
S2
P1
S1
P2′
S2′
Active site-directed, L458-based probes
JC8:P1′= BP
L646:P2 = BP
GY4:P1 = BP
L505:P3′= BP
B.
MW (Kda)
JC8
L646
GY4
L505
L458 - + - + - + - +
75-
37-
αSPP
25-
αPS1-NTF
50-
αSPPL2a
C.
MW (Kda)
JC8
L646
GY4
L505
(Z-LL)2-ketone - + - + - + - +
75-
37-
αSPP
25-
αPS1-NTF
(Z-LL)2-ketone
D.
JC8
L646
GY4
L505
S1′
S2
S1
S3′
PS1
SPP
SPPL2A

Active SPP exists predominantly as a homodimer

Initial characterization of SPP showed that endogenous SPP is a monomer (Weihofen et al., 2002;Weihofen et al., 2003). Further studies by Nyborg *et al.* demonstrated that SPP is a homodimer that is SDS-stable and partially heat-labile (Nyborg et al., 2004b;Nyborg et al., 2006). However, only the monomeric form of SPP was labeled with the active site-directed photoprobe III-63 (Sato et al., 2006;Sato et al., 2008). Additionally, endogenous n-Dodecyl β-D-maltoside (DDM)-solubilized human and drosophila SPP formed higher molecular weight complexes around 180-200kDa (Miyashita et al., 2011). We utilized a photolabeling approach to elucidate whether endogenous active SPP is a homodimer or monomer. We synthesized JC10, a photoprobe structurally similar to JC8 except with the addition of a disulfide bond in the biotin linker that can be eluted from the streptavidin matrix with the reducing agent TCEP (Figure 3.3A) (Chun et al., 2004). Our data showed that the majority of SPP was monomeric when heat was used to elute SPP from JC8 (Figure 3.3B, first panel), with some residual SPP dimer still detected. However, in the absence of heat, JC10 photolabeled SPP was predominantly a homodimer (Figure 3.3B, third panel). Similar to the SPP labeled with JC8 (Figure 3.2B, C and 3.3B), most of the SPP dimer was converted into the monomer when heat was applied (Figure 3.3B, fourth panel). This confirmed the finding that dimer SPP is heat-labile and provided further evidence that endogenous, active SPP exists as a homodimer. To detect predominantly SPP dimer we eluted proteins with Laemmli Sample Buffer + 2 mM biotin at 70° C. Under these conditions SPP does not dissociate into its monomeric form (Figure 3.3B, second panel). As a result, we show only SPP dimer in subsequent experiments.

Figure 3.3. Endogenous, active SPP is a homodimer. A. Structures of JC8, JC10, and schematic of experimental protocol. HeLa membrane was labeled either with JC8 or JC10, UV crosslinked and pulled-down with streptavidin beads. JC8-labeled sample can be eluted with heat and JC10 labeled sample can be eluted with TCEP. B. JC8 and JC10 were used to photolabel SPP. TCEP and/or different degrees of heat were used to elute photolabeled proteins

Figure 3.3

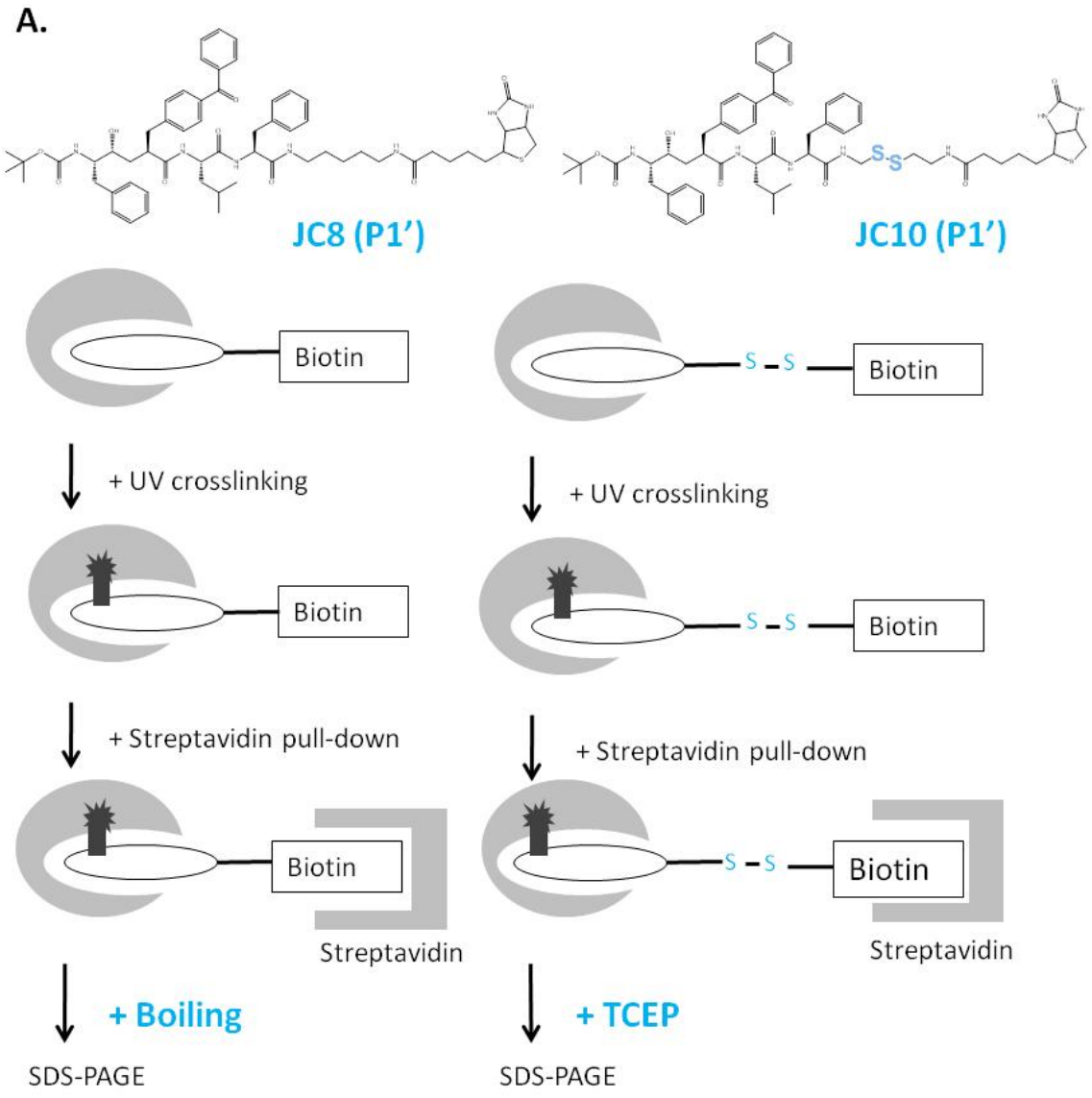
A.
JC8 (P1')
JC10 (P1')
Biotin
S – S
Biotin
+ UV crosslinking
+ UV crosslinking
Biotin
S – S
Biotin
+ Streptavidin pull-down
+ Streptavidin pull-down
Biotin
S – S
Biotin
Streptavidin
Streptavidin
+ Boiling
+ TCEP
SDS-PAGE
SDS-PAGE

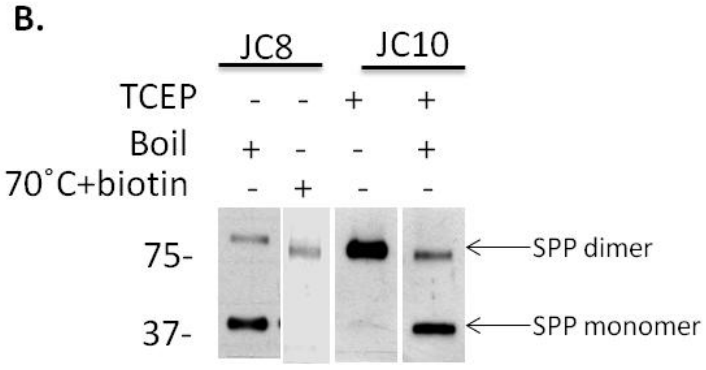
B.
JC8
JC10
TCEP - - + +
Boil + - - +
70˚C+biotin - + - -
75-
37-
SPP dimer
SPP monomer

GSIs and GSMs have opposite effects on the active site conformational changes of PS1 and SPP

We have previously used photoprobes to detect γ-secretase active site conformational changes induced by the binding of GSIs and GSMs (Shelton et al., 2009;Tian et al., 2010a;Crump et al., 2011). However, the effect of GSIs and GSMs on the active site conformation of SPP has not been reported.

We investigated the effects of four GSIs and two GSMs on the active site conformations of γ-secretase and SPP (Figure 3.4). GSIs inhibit production of Notch intracellular domain (NICD) and all Aβ species including Aβ40 and Aβ42 while GSMs have little impact on NICD production and selectively inhibit production of Aβ42 (Crump et al., 2013). BMS-708163, commonly known as avagacestat, was discordantly reported as both a Notch-sparing GSI (Gillman et al., 2010) and a nonselective GSI (Chavez-Gutierrez et al., 2012;Crump et al., 2012b), that completed phase II clinical trials but did not proceed any further. LY450139, also known as semagacestat, advanced into a Phase III clinical trial but was terminated prematurely due to side effects potentially stemming from Notch-associated toxicity (Doody et al., 2013). Compound X (cpd X) and GSI-34 are both GSIs (Placanica et al., 2010;Yang et al., 2010). E2012 is an imidazole-derived GSM which has been shown to bind SPP (Pozdnyakov et al., 2013), and GSM-616 is an acetic acid GSM that binds SPP (Crump et al., 2011).

We tested the effects of BMS-708163, LY450139, cpd X, and GSI-34 on the photolabeling of PS1 and SPP by active site-directed probes. The effect of these GSIs was assessed by comparison to vehicle control. As anticipated, these GSIs inhibited the photolabeling of PS1-NTF (Figure 3.4D). Surprisingly, they selectively enhanced the labeling of SPP (Figure 3.4C). These data suggest that the GSIs tested have

opposite effects on the active site conformations of SPP and γ-secretase. The increase in SPP labeling in the presence of GSIs may be due to a direct interaction between the GSI and SPP, leading to a change in SPP active site conformation that improves labeling with the active site-directed probe. Alternatively, the increase in labeling may be due to increased availability of the active site-directed probe as a result of a reduction in the number of active γ-secretase complexes available for binding. The latter hypothesis does not require direct binding between GSIs and SPP, and is based on the data that shows a reduction in PS1 labeling in the presence of GSIs (Figure 3.4B and D), which may suggest that the active site-directed probes that are not engaged in labeling PS1 are labeling SPP. While both hypotheses are feasible explanations for the increase in SPP labeling in the presence of GSIs, the data support the "direct labeling" hypothesis for the following reasons: First, in the presence of GSIs, SPP labeling is enhanced for some, but not all, active site-directed probes. If the increase in SPP labeling were a result of an increase in probe availability, all active site-directed probes would be expected to label SPP more robustly, but we do not observe this. Second, Fuwa *et al.* found that a compound E-based probe, which is identical to cpd X with the exception of a single hydroxyl group, specifically labels SPP, showing direct binding between this GSI and SPP (Fuwa et al., 2007). For these reasons it is likely that the GSIs studied here are directly binding SPP. We also tested the effects of E2012 and GSM-616 on the photolabeling of PS1 and SPP. Although these GSMs have been shown to modulate γ-secretase activity (Crump et al., 2011;Pozdnyakov et al., 2013), they had little effect on the active site labeling of PS1-NTF (with the exception of the S1 subsite for GSM-616), suggesting that these compounds affect γ-secretase activity without drastically altering the active site conformation (Figure 3.4D). More interestingly, these GSMs partially reduced the active site labeling of SPP by all photoprobes except L646 (Figure 3.4C), suggesting

that both of these structurally distinct GSMs affect the same sub-pockets of the SPP active site. Additionally, we and others have reported that GSM-1, which is a close homologue of GSM-616, and GSM E2012, directly bind SPP (Crump et al., 2011;Pozdnyakov et al., 2013).

The combined data show that while GSIs inhibit labeling of PS1 and have no effect on or enhance labeling of SPP, the opposite is true of GSMs, which inhibit labeling of SPP and have little to no effect on labeling of PS1. A clear exception is the pronounced increase in GY4 labeling of PS1 in the presence of GSM-616 (Figure 3.4D), which was previously reported (Crump et al., 2011). The trend, therefore, is that GSIs and GSMs have opposite effects on the photolabeling profiles of γ-secretase and SPP (Figure 3.5). The data suggest that not only GSMs, as previously reported, but also GSIs directly bind to SPP, potentially leading to the observed conformational change in its active site. Consequently, GSIs in clinical trials for cancer and GSMs developed for AD treatment may lead to undesirable effects associated with concomitant changes in SPP structure. This possibility is worth studying as SPP is essential in eukaryotes (Grigorenko et al., 2004;Casso et al., 2005;Krawitz et al., 2005) and a change in its activity and specificity may affect the therapeutic windows of GSIs and GSMs.

Figure 3.4. GSIs and GSMs have opposite effects on the photolabeling profiles of γ-secretase and SPP. A. Structures of E2012, GSM-616, BMS-708163, LY450139, cpd X and GSI-34. B. Photoprobes JC8, L646, GY4 and L505 were incubated with HeLa membrane in 0.25% CHAPSO in the presence of 25 uM GSMs E2012/616, (green) or 10 uM GSIs 708163/139/cpd X/GSI-34 (blue). Samples were run on SDS-PAGE and analyzed by western blot. Anti-SPP and PS1-NTF antibodies were used to detect SPP (top panel) and PS1-NTF (bottom panel). C. Densitometry quantification of SPP labeling. GSMs are graphed in green, GSIs are graphed in blue. D. Same as C, except PS1-NTF. ns $P > 0.05$; * $P \leq 0.05$; ** $P \leq 0.01$; *** $P \leq 0.001$

Figure 3.4

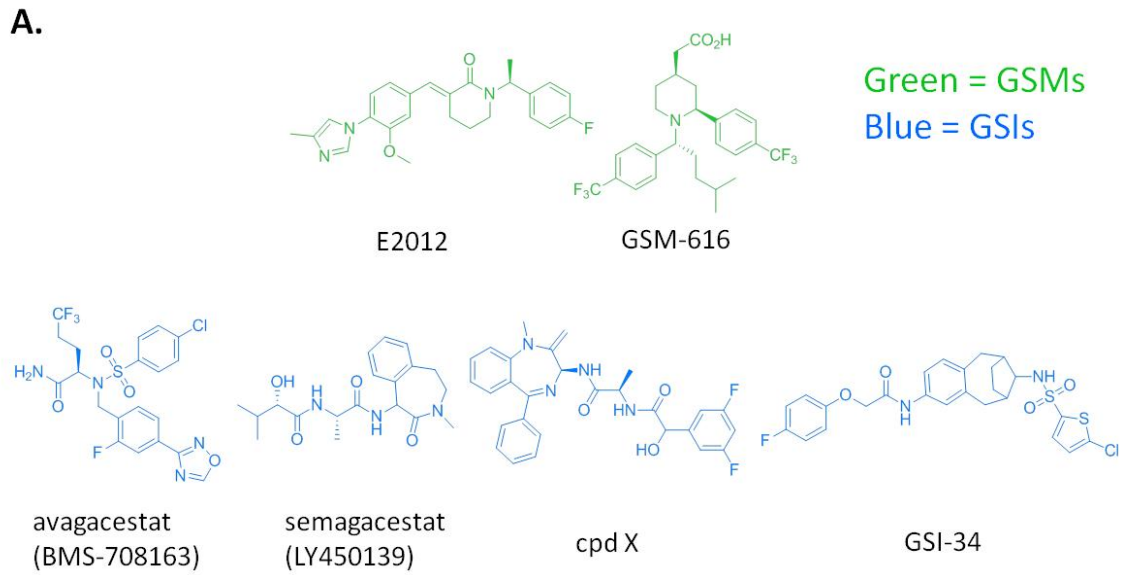
A.
Green = GSMs
Blue = GSIs
E2012
GSM-616
avagacestat
(BMS-708163)
semagacestat
(LY450139)
cpd X
GSI-34

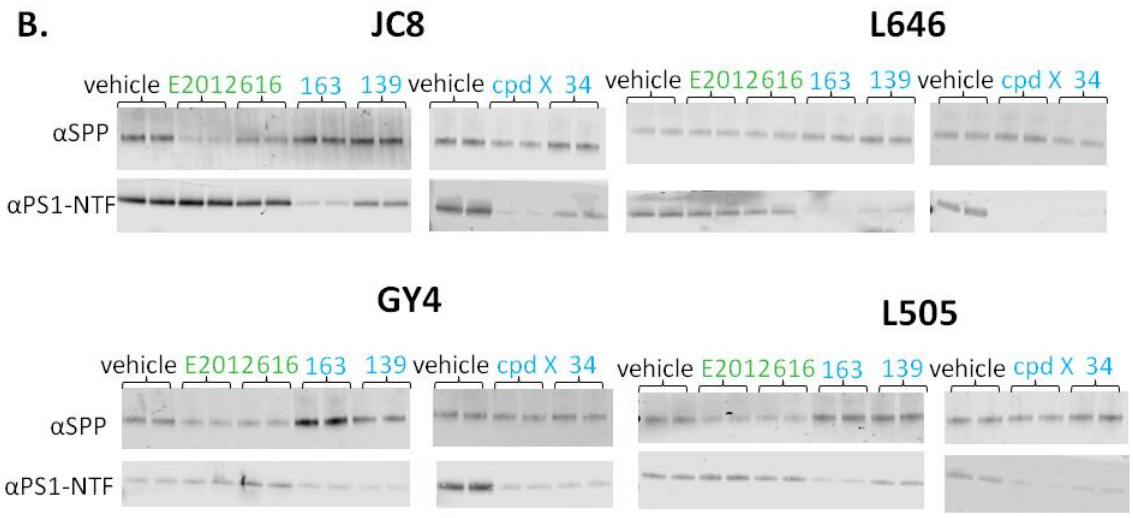
B.
JC8
L646
GY4
L505
vehicle E2012 616 163 139 vehicle cpd X 34
αSPP
αPS1-NTF

Figure 3.4 continued

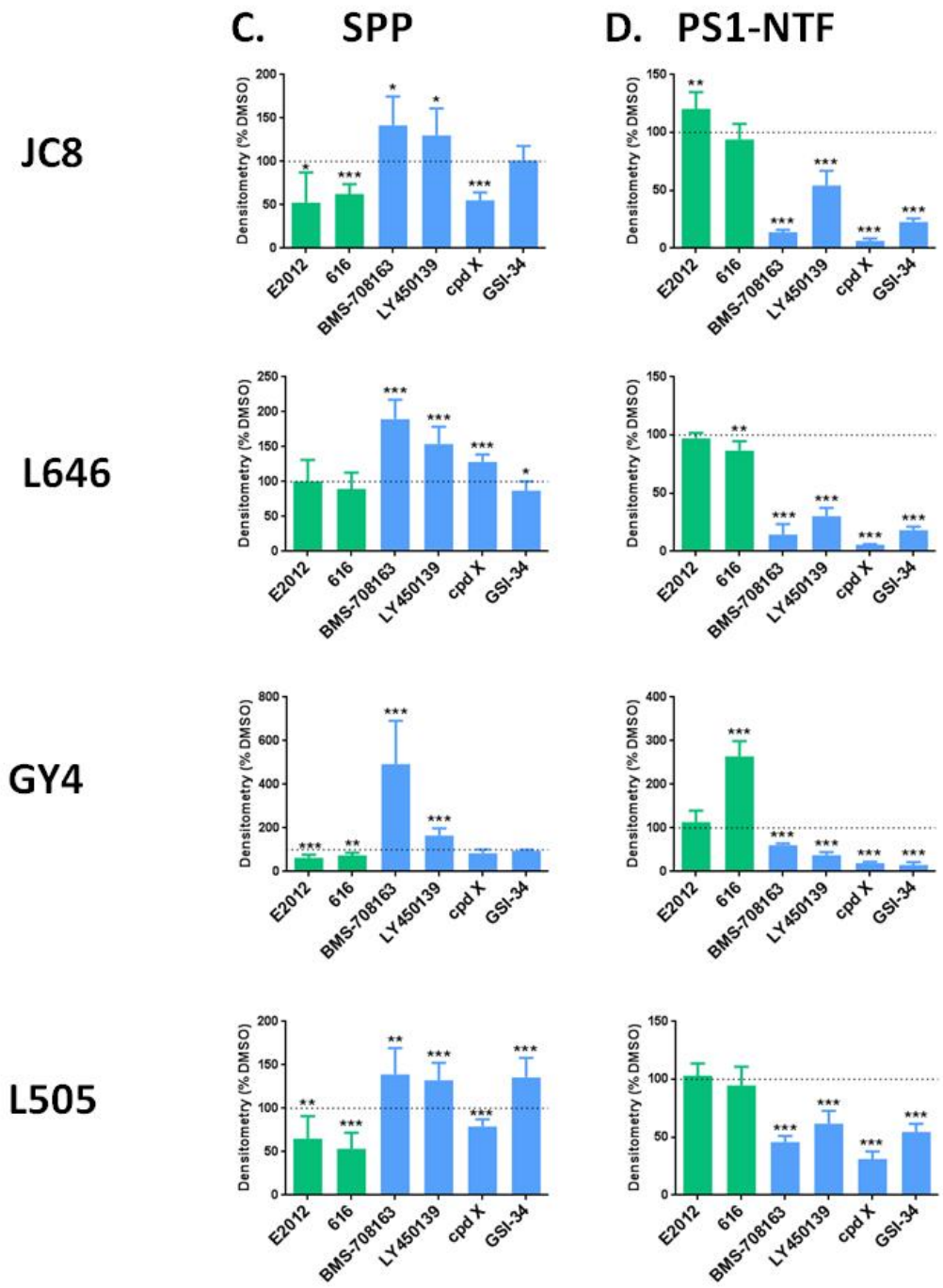

3.3 Conclusion and Discussion

Determining allosteric site-induced conformational changes in the active sites of enzymes for which atomic resolution is not available has been a big challenge. To address this, we developed and applied the photophore walking technique for probing the active sites of two such enzymes, γ-secretase and SPP. We found that while the S1' and S1 sub-pockets of both enzymes are similar, the S2 and S3' sub-pockets are structurally distinct. The strong overall similarity in the active sites of these two enzymes that cleave entirely different substrates may mean that the active site does not play an important role in determining substrate specificity. On the flipside, some substrate specificity may be conferred by the subtle differences in two of the four active site sub-pockets. It is possible that the conserved structure of the S1' and S1 subsites is a result of the importance of these subsites in catalysis. We were surprised to find that the active sites of γ-secretase and SPP are differently affected by allosteric GSIs and GSMs. Despite the strong structural homology of the active sites of these enzymes, GSIs had a diametrical impact on the conformations of the two enzyme active sites, as gauged by interaction with active site-directed probes (Figure 3.5). Although enzyme binding to active site-directed probes is not a direct proxy for activity, there is a high likelihood that if the active site is changing, so is enzyme activity/specificity. This has important ramifications for drug development, as changes in SPP activity may occur during GSI/GSM treatment.

Semagacestat and avagacestat were both terminated in late phase clinical trials due to toxicity. The precise cause of the toxicity remains unknown, but we and others believe it is probably "mechanism-based," meaning that the drugs' interaction with its γ-secretase target is what caused the Notch-associated non-melanoma skin cancer and GI toxicity. However, this does not rule out the possibility that off-target toxicities

compounded this problem. For most drug candidates, the identities of the off-target interacting proteins is not known, but GSIs and GSMs are the rare case in which SPP has been identified as a potential off-target binding partner. In 2002, a homology search on SPP revealed PS as an ortholog (Weihofen et al., 2002), and today we know that this very structural conservation may pose a threat to GSI/GSM development. Through the above experiments we have taken the first step to understanding how SPP is structurally impacted by GSIs and GSMs. If we are to bring these drugs to the clinic we must harness and augment the vast work that has been done in understanding their mechanism of action not only with respect to γ-secretase, but also with respect to other, albeit unintended, targets.

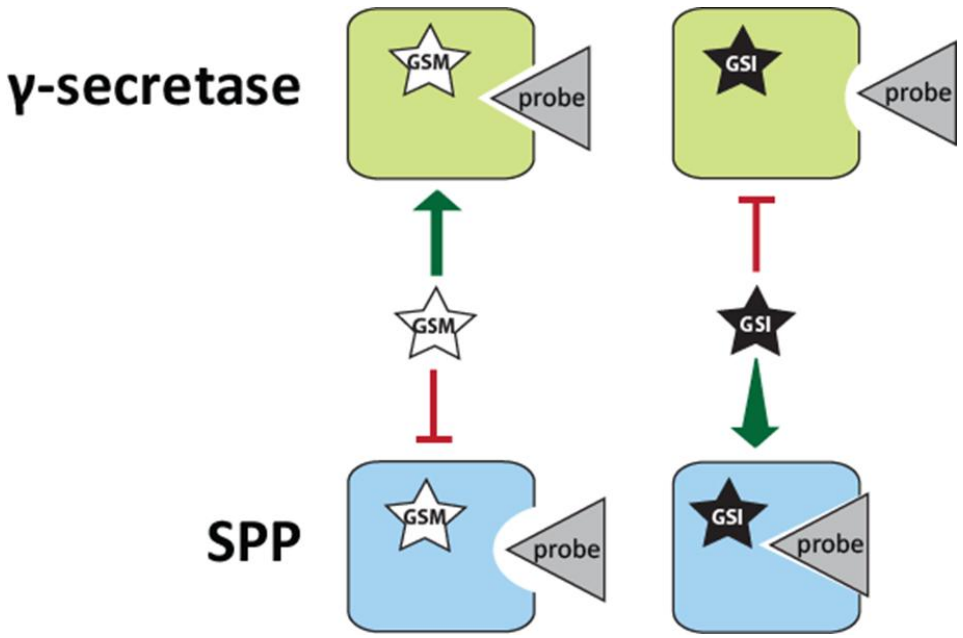

Figure 3.5. Model for the change in active site conformation of γ-secretase and SPP that occurs upon binding by GSIs and GSMs. We propose that the GSIs and GSMs studied here allosterically bind to γ-secretase and SPP, causing a conformational change in the active sites of the enzymes. Surprisingly, the induced conformational change is opposite for the two enzymes, as evidenced by their binding to active site-directed probes. Specifically, GSIs cause decreased binding between γ-secretase and probe while increasing binding between SPP and probe. GSMs cause little change in binding between γ-secretase and probe but reduce binding between SPP and probe. This suggests a model in which GSIs cause the active site of γ-secretase to assume a "closed" conformation, but have the reverse impact on the active site structure of SPP.

3.4 Methods

HeLa cell membrane preparation and chemicals

HeLa membrane fraction was isolated from HeLa-S3 cells (National Cell Culture Center) as previously described (Li et al., 2000b;Tian et al., 2010a). Synthesis of L458, cpd X, GSI-34, L646, GY4, JC8, L505, and $(Z\text{-}LL)_2$-ketone were described previously (Li et al., 2000b;Seiffert et al., 2000;Shearman et al., 2000;Weihofen et al., 2000;Chun et al., 2004;Yang et al., 2009). LY450139, BMS-708163, E2012, and GSM-616 were kindly provided by Dr. Douglas Johnson from Pfizer.

Peptide synthesis and anti-SPP antibody production

SPP peptide corresponding to the N-terminal of human SPP (MDSALSDPHNGSAEAC) was synthesized by Dr. Deming Chau with an automated solid phase peptide synthesizer (ProteinTech) using Fmoc chemistry. The purified peptide was conjugated to maleimide functionalized keyhole limpet hemocyanin (KLH) according to the manufacturer's instructions (Pierce). This antigen was used to immunize rabbits for polyclonal antibody produc tion (Covance). Serum was collected and tested for SPP detection using Western blot analysis.

Photolabeling of γ-secretase and SPP

Total HeLa cell membrane was pre-incubated in the presence of 0.25% CHAPSO with or without inhibitors at 37° C for 30 minutes (Li et al., 2000b;Crump et al., 2011;Chau et al., 2012;Crump et al., 2012b;Gertsik et al., 2014a). Then, 20 nM of photoactive probes was added to the mixture and incubated for an additional 1 hour at 37°C. The reaction mixtures were irradiated at 350 nm for 45 minutes and solubilized with RIPA buffer (50 mM Tris base, pH 8.0, 150 mM NaCl, 0.1% SDS, 1% NP-40, 0.5%

deoxycholate) for 1 hour. Photocrosslinked proteins in the soluble fraction were pulled-down with Streptavidin Plus UltraLink Resin (Pierce) overnight at 4° C. The resin was washed with RIPA buffer and proteins were eluted with Laemmli Sample Buffer (32.9 mM Tris-HCl, pH 6.8, 1% SDS, 13% (w/v) glycerol, 0.005% bromophenol blue) at 95° C (Figure 3.2 and 3.3), 25 mM TCEP in PBS (Figure 3.3), or 2 mM biotin in Laemmli Sample Buffer at 70° C (Figure 3.4). Eluted proteins were resolved on SDS-PAGE and transferred to PVDF (Millipore). PS1-NTF, PS1-CTF, SPP, and SPPL2A were detected with anti-PS1-NTF (gift from Dr. Min Xu), anti-PS1-CTF (Millipore), anti-SPP, or anti-SPPL2A epitope 8 (gift from Dr. Bernd Schroder) antibody.

CHAPTER 4

Mapping the binding site of BMS-708163, a γ-secretase inhibitor, using cleavable linker probes

4.1 Introduction

γ-Secretase's complexity, flexibility, and hydrophobicity have caused it to be refractory to crystallization, making high resolution drug-target studies particularly challenging. A recent 3.4 Å cryo EM structure (Bai et al., 2015b) of γ-secretase has begun to shed some light on the way in which the enzyme's structure may account for its highly regulated yet fairly promiscuous function (Gertsik et al., 2014b), but many questions about γ-secretase's active site and interaction with clinically relevant small molecules remain.

Avidin-based pull-down of biotin labeled proteins has been used widely to study interactions between proteins and small molecules. In particular, this tool, coupled with photoaffinity labeling, allowed for the identification of presenilin (PS) as the active subunit of γ-secretase (Li et al., 2000b), and for the identification of γ-secretase as the target of γ-secretase modulators (GSMs) (Crump et al., 2011). However, the affinity of the biotin-(strept)avidin interaction ($K_d \sim 10^{-15}$ M) (Green, 1990) means that harsh conditions, such as boiling (Li et al., 2000b), excess biotin (Gertsik et al., 2015), or on-bead trypsin digestion (Dieterich et al., 2007), are required for elution. The concomitant elution of non-specific proteins that occurs during such stringent procedures can be tolerated for some studies, for example when the identity of the protein of interest is known, but is suboptimal for others, especially if they include mass spectrometry. Cleavable linkers that require mild cleavage conditions may be the solution to avoiding protein contamination in the eluted sample. In addition to reducing contamination, mild elution of cleavable linkers accomplishes another

significant feat: it separates the reactive end of the molecule from the bulky, hydrophobic biotin group. This is particularly important for studying transmembrane proteins, like γ-secretase, which may become too hydrophobic for mass spectrometry detection when attached to biotin.

γ-Secretase inhibitors (GSIs), which are in clinical trials for cancer, pan-inhibit γ-secretase and prevent it from cleaving its substrates, including APP and Notch. GSMs, which are promising AD therapies, reduce levels of the amyloidogenic Aβ42 while maintaining total Aβ levels constant and without impeding Notch signaling. The interaction between γ-secretase and GSIs/GSMs has been explored in a variety of ways, including photoaffinity labeling (Li et al., 2000b;Seiffert et al., 2000;Kornilova et al., 2005;Fuwa et al., 2007;Shelton et al., 2009;Tian et al., 2010a;Crump et al., 2011;Crump et al., 2012a;Crump et al., 2012b;Gertsik et al., 2014a;Gertsik et al., 2015), fluorescence lifetime imaging (FLIM) (Lleo et al., 2004;Uemura et al., 2010), and surface cysteine accessibility method (SCAM) (Ohki et al., 2011). These studies provided insight into the mechanisms of GSIs/GSMs, but to our knowledge there have been no reports that mapped the precise GSI/GSM binding site on γ-secretase. Here we develop BMS-708163-based photoactive (Crump et al., 2012b), cleavable probes for the study of γ-secretase, provide a side-by-side comparison of their efficiency for photolabeling and eluting PS1-NTF, and identify a binding site of the GSI BMS-708163 (avagacestat) on PS1.

4.2 Results

BMS-708163-based probes are potent inhibitors of γ-secretase and target PS1-NTF

We designed four biotinylated BMS-708163-based probes with various cleavable linkers in order to expand the arsenal of tools with which to study γ-secretase (Figure

4.1A). BP-DDE can be cleaved with hydrazine (H_2N_2) (Yang and Verhelst, 2013), BP-vicinal diol can be cleaved by oxidation with sodium periodate ($NaIO_4$) (Yang et al., 2013), BP-azobenzene can be cleaved by reduction with sodium hydrosulfite ($Na_2S_2O_4$) (Blum et al., 2013), and BP-DADPS can be cleaved by formic acid (CH_2O_2) (Szychowski et al., 2010;Wang et al., 2015). We also included BP-biotin which does not have a cleavable linker and can be eluted with heat. We established that all five probes are potent γ-secretase inhibitors as they have IC_{50}s in the low nanomolar range, just like parent compound BMS-708163 (Figure 4.1B). However, the IC_{50}s of the probes varied slightly, with BP-vicinal diol being the most potent inhibitor of Aβ40 production (IC_{50} = 1.1 nM) and BP-DADPS being the least potent (IC_{50} = 8.0 nM). Clearly, the presence of different linkers affects IC_{50} in spite of the fact that the linker is significantly removed from the reactive end of the molecule.

Next we performed a side-by-side comparison of the efficiency of PS1-NTF photolabeling by all probes (Figure 4.1C). HeLa membrane was photolabeled with 20 nM of each probe in the presence of 0.25% CHAPSO, samples were pulled-down with streptavidin beads, eluted with 2 mM biotin in Laemmli sample buffer at 70˚ C for 10 minutes, resolved on SDS-PAGE, and probed for PS1-NTF. PS1-NTF was robustly and specifically labeled by all probes, with some variation in labeling efficiency evident among different probes. Comparing among the cleavable linker probes, BP-vicinal diol and BP-DDE label PS1-NTF most robustly while BP-azobenzene and BP-DADPS show weaker labeling. The photolabeling profile of the probes closely reflects the IC_{50}s: the two most potent probes (BP-DDE and BP-vicinal diol) label PS1-NTF with higher efficiency while the two least potent probes (BP-azobenzene and BP-DADPS) label PS1-NTF with lower efficiency. This finding is reassuring, as it suggests that the photolabeling efficiency of these probes is predominantly a function

of IC_{50} and less a function of the orientation of the benzophenone with respect to the protein.

We attempted to obtain equal labeling among all probes by correcting for IC_{50} (Figure 4.1D). The IC_{50} of each probe was multiplied by 50 (10X to saturate the γ-secretase binding sites and 5X to make up for the fact that we have a 5X higher concentration of HeLa membrane in the photolabeling reaction than we do in the activity assay) and HeLa membrane was labeled with this corrected concentration. Samples were pulled-down, eluted, and Western blotted as in Figure 4.1C. We were able to get closer to equal labeling by using these adjusted concentrations, although BP-azobenzene labeling was still lower than that of other probes.

Figure 4.1. A. Structures of parent compound BMS-708163 and probes BP-biotin, BP-DDE, BP-vicinal diol, BP-azobenzene, and BP-DADPS. B. *In vitro* inhibitory potency (IC_{50}) of BMS-7081635 and five BMS-708163-based probes. C. HeLa membrane was photolabeled with 20 nM BP-DDE, BP-vicinal diol, BP-azobenzene, BP-DADPS, or BP-biotin in the presence (+) or absence (-) of 1 μM BMS-708163. Samples were pulled-down with streptavidin beads, eluted with 2 mM biotin in Laemmli sample buffer at 70˚ C, run on SDS-PAGE, and analyzed by Western blot. D. HeLa membrane was photolabeled with 95 nM BP-DDE, 55 nM BP-vicinal diol, 140 nM BP-azobenzene, 400 nM BP-DADPS, or 165 nM BP-biotin. Samples were treated the same as in "1C." Densitometry quantification of PS1-NTF labeling (right panels for C and D).

Figure 4.1

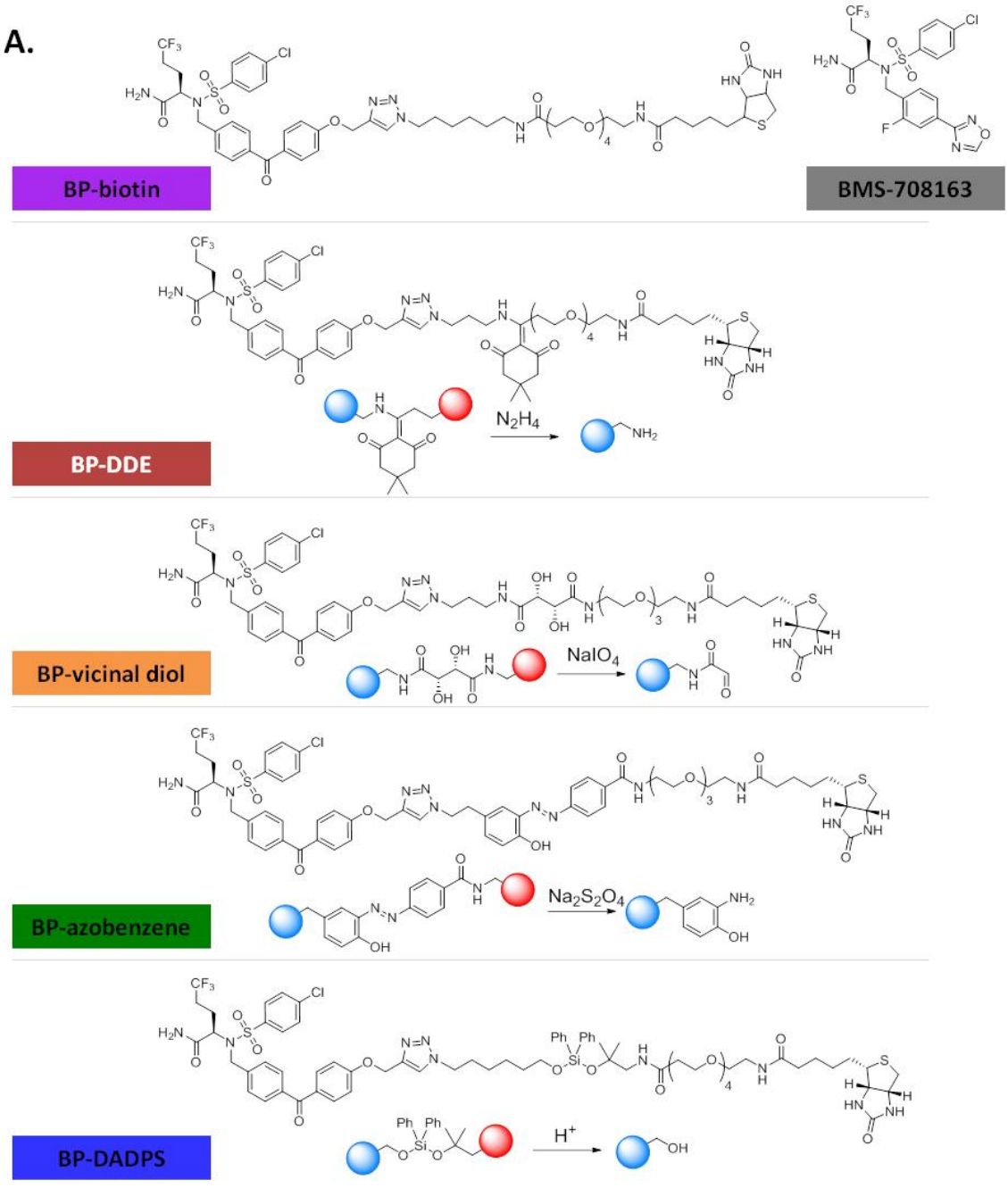
A.
BP-biotin
BMS-708163
BP-DDE
N_2H_4
BP-vicinal diol
$NaIO_4$
BP-azobenzene
$Na_2S_2O_4$
BP-DADPS
H^+

Figure 4.1 continued

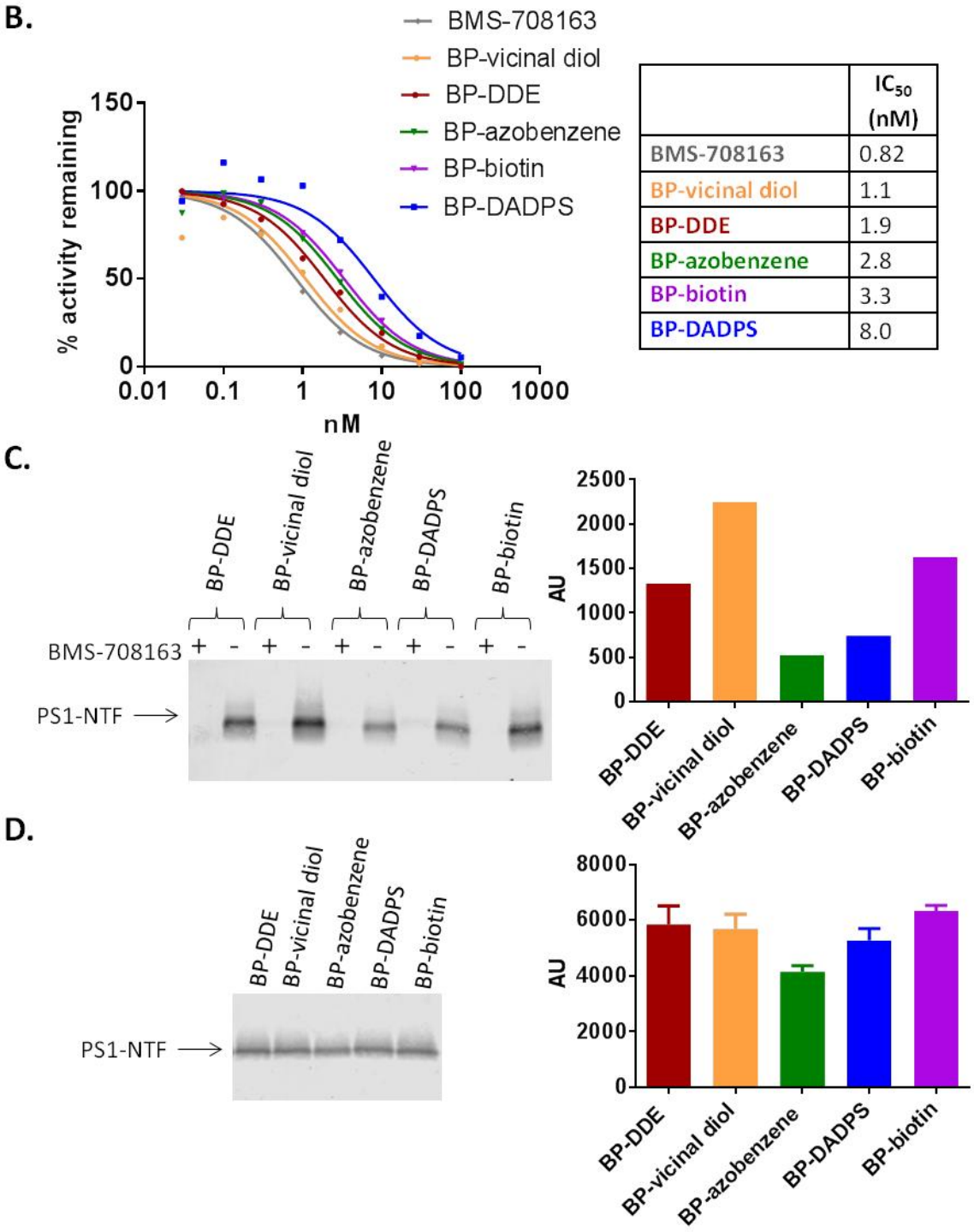

	IC_{50} (nM)
BMS-708163	0.82
BP-vicinal diol	1.1
BP-DDE	1.9
BP-azobenzene	2.8
BP-biotin	3.3
BP-DADPS	8.0

Comparison of PS1-NTF elution efficiency for all cleavable probes

We used these IC_{50}-adjusted concentrations to optimize elution conditions for all cleavable probes (Figure 4.2). While three of the four probes (BP-DDE, BP-vicinal diol, BP-azobenzene) photolabel and release PS1-NTF efficiently, BP-DADPS is not compatible with PS1-NTF due to instability of the protein in formic acid. Different concentrations of eluting reagent + SDS (0.05-1%) were tried for all probes. Only optimized conditions are shown (Figure 4.2). Briefly, we labeled 400 μg of HeLa membrane with IC_{50}-adjusted concentration of photoprobe, pulled-down with streptavidin beads, and eluted samples twice with cleavage-specific conditions. We then washed samples thoroughly with 0.1% SDS to remove eluted proteins and cleavage reagents and eluted a third time with 2 mM biotin in Laemmli sample buffer at 70˚ C for 10 minutes. Equivalent amounts of each elution was loaded onto SDS-PAGE and analyzed by Western blot, probing for PS1-NTF. Cleavage of BP-DDE with 2% hydrazine + 0.05% SDS resulted in exhaustive elution of PS1-NTF such that subsequent elution with 2 mM biotin in Laemmli sample buffer at 70˚ C for 10 minutes (elution 3) was not able to recover any additional protein (Figure 4.2A). In contrast, cleavage-specific elution of BP-vicinal diol, BP-azobenzene, and BP-DADPS all showed some elution of PS1-NTF, but PS1-NTF was also present in subsequent heat elution samples (Figure 4.2B-D). This illustrates that elution by cleavage-specific conditions is not complete for any probe tested except BP-DDE.

To directly compare cleavage/elution capacity of probes, we labeled HeLa membrane with IC_{50}-adjusted concentrations of photoprobes BP-DDE, BP-vicinal diol, and BP-azobenzene in triplicate and then eluted samples with *either* cleavage specific conditions *or* 2 mM biotin in Laemmli sample buffer at 70˚ C for 10 minutes (Figure 4.2E, bottom panel). We analyzed samples by Western blot and normalized cleavage-

specific bands to heat eluted bands. We then normalized that signal to BP-DDE, and graphed the results (Figure 4.2E, bottom panel). For a representative Western blot, see Figure 4.2E, top panel. BP-DDE is far superior to the other probes at capturing and eluting PS1-NTF: Specifically, the PS1-NTF signal of BP-DDE is ~4X higher than that of BP-vicinal diol and ~3X higher than that of BP-azobenzene.

Elution of BP-DDE bound PS1-NTF with hydrazine and SDS is 100% efficient

Interestingly, when HeLa membrane was photolabeled with BP-DDE, elution of PS1-NTF with hydrazine was 2X higher than elution of PS1-NTF with 2 mM biotin in Laemmli sample buffer at 70˚ C for 10 minutes (data not shown). This was surprising as we expected heat elution to always be stronger than elution with cleavage-specific reagents. At first we hypothesized that the reason hydrazine elution appears higher than heat elution is because hydrazine causes proteins to run/transfer/bind antibody differently than does sample buffer. To test this, we added hydrazine to samples eluted with sample buffer + heat and compared those samples to hydrazine eluted samples. Addition of hydrazine to heat eluted samples did not improve the PS1-NTF signal on Western blot (data not shown), suggesting that the presence of hydrazine was not causing any artifact leading to signal enhancement.

Alternatively, we hypothesized that the reason hydrazine elution is stronger than heat elution is because heat elution is not comprehensive and leaves some PS1-NTF either bound to the streptavidin beads or aggregated. We confirmed this hypothesis by eluting BP-DDE with various sample buffer + detergent + heat conditions and finding that the addition of Triton X-100 to sample buffer actually improves heat elution and brings its efficiency closer to that of hydrazine (Figure 4.2F). This reaffirms the finding that elution of BP-DDE labeled PS1-NTF with cleavage-specific conditions detailed here is ~100% efficient. Cleavage of BP-vicinal diol with sodium periodate is

2X less efficient at eluting PS1-NTF than is heat elution of the same probe, and cleavage of BP-azobenzene with sodium hydrosulfite is 4X less efficient at eluting PS1-NTF than is heat elution of the same probe. The combined data suggest either that BP-DDE, once bound to the enzyme, is more readily cleaved than the other probes or that PS1-NTF is more stable/soluble in hydrazine than in the other cleavage reagents.

BP-DADPS is a poor probe for PS1-NTF as PS1-NTF is unstable at low pH

Elution of BP-DADPS with 1 or 5% formic acid in the absence or presence of SDS did not show any PS1-NTF on the Western blot (Fig. 4.2D). We hypothesized that the low pH of the sample interfered with SDS-PAGE, so we neutralized all samples with Tris-OH (data not shown). However, even after samples had been brought back to neutral pH and run on SDS-PAGE, there was no PS1-NTF signal on the Western blot. Next, we hypothesized that PS1-NTF is unstable in extremely acidic conditions so we tried eluting proteins with 100 or 500 mM glycine HCl, pH=2 or 3 in the absence or presence of SDS (data not shown). However, these conditions were unable to cleave BP-DADPS and elute proteins. We noticed that adding sample buffer to sample in 5% formic acid yielded a nice PS1-NTF band, but transferring acidic sample from one tube to the other and then adding sample buffer yielded no band. This led us to believe that PS1-NTF may be aggregating and precipitating out of solution at low pH, but can be resolubilized with the addition of sample buffer. To test whether PS1-NTF can be stabilized at low pH, we eluted proteins with 1 or 5% formic acid with 0.1 mg/ml BSA (Figure 4.2D). The addition of BSA stabilized PS1-NTF so that it finally became visible on Western blot. Interestingly, PS1-NTF was only visible when SDS was absent. The reason for this is that SDS precipitates BSA under low pH. We tried adding BSA to other cleavage reagents, such as 2% hydrazine, in order to see whether BSA can stabilize PS1-NTF in the absence of SDS. However, we were unable to

detect PS1-NTF under these conditions. While BP-DADPS is not a viable probe for γ-secretase due to the low pH conditions required for protein elution, it may well work for other, more hydrophilic candidates (Szychowski et al., 2010).

Figure 4.2. A. PS1-NTF labeled with BP-DDE and eluted with hydrazine (N_2H_4). HeLa membrane was photolabeled with 95 nM BP-DDE and pulled-down with streptavidin beads. Samples A, B, and C were eluted two times with 2% hydrazine + varying amounts of SDS (elutions 1 and 2). They were then eluted a third time with 2 mM biotin in Laemmli sample buffer at 70˚ C for 10 minutes (elution 3). Sample D was eluted only with 2 mM biotin in Laemmli sample buffer at 70˚ C for 10 minutes. B. PS1-NTF labeled with BP-vicinal diol and eluted with sodium periodate ($NaIO_4$). HeLa membrane was photolabeled with 55 nM BP-vicinal diol and pulled-down with streptavidin beads. Samples A, B, C, and D were eluted two consecutive times with 10 or 20 mM sodium periodate +/- 0.5% SDS (elutions 1 and 2). They were then eluted a third time with 2 mM biotin in Laemmli sample buffer at 70˚ C for 10 minutes (elution 3). Sample E was eluted only with 2 mM biotin in Laemmli sample buffer at 70˚ C for 10 minutes. C. PS1-NTF labeled with BP-azobenzene and eluted with sodium hydrosulfite ($Na_2S_2O_4$). HeLa membrane was photolabeled with 140 nM BP-azobenzene and pulled-down with streptavidin beads. Samples A and B were eluted two consecutive times with 25 mM sodium hydrosulfite +/- 0.05% SDS (elutions 1 and 2). They were then eluted a third time with 2 mM biotin in Laemmli sample buffer at 70˚ C for 10 minutes (elution 3). Sample C was eluted only with 2 mM biotin in Laemmli sample buffer at 70˚ C for 10 minutes. D. PS1-NTF labeled with BP-DADPS and eluted with formic acid (CH_2O_2). HeLa membrane was photolabeled with 400 nM BP-DADPS and pulled-down with streptavidin beads. Samples A, B, C, and D were eluted once with 1% or 5% formic acid +/- 0.5% SDS, all in the presence of 0.1 mg/ml BSA (elution 1). They were then eluted a second time with 2 mM biotin in Laemmli sample buffer at 70˚ C for 10 minutes (elution 2). Sample E was eluted only with 2 mM biotin in Laemmli sample buffer at 70˚ C for 10 minutes. All samples were run on SDS-PAGE and analyzed by Western blot. E. HeLa membrane was photolabeled with 95 nM BP-DDE, 55 nM BP-vicinal diol, or 140 nM BP-azobenzene and pulled-down with streptavidin beads. Samples were eluted twice with 40 ul of 2% hydrazine + 0.05% SDS, 20 mM sodium periodate + 0.5% SDS, or 25 mM sodium hydrosulfite + 0.05% SDS. Elutions 1 and 2 were combined. Samples were then eluted with 80 ul of 2 mM biotin in Laemmli sample buffer at 70˚ C for 10 minutes (elution 3). Equivalent amounts of elutions 1 + 2 and elution 3 were loaded onto SDS-PAGE gel and analyzed by Western blot. F. HeLa membrane was photolabeled with 95 nM BP-DDE and pulled-down with streptavidin beads. Samples were eluted *either* with hydrazine *or* with heat: Sample A was eluted with 2% hydrazine + 0.05% SDS, samples B through F were eluted with various combinations of sample buffer, detergent, and heat.

Figure 4.2

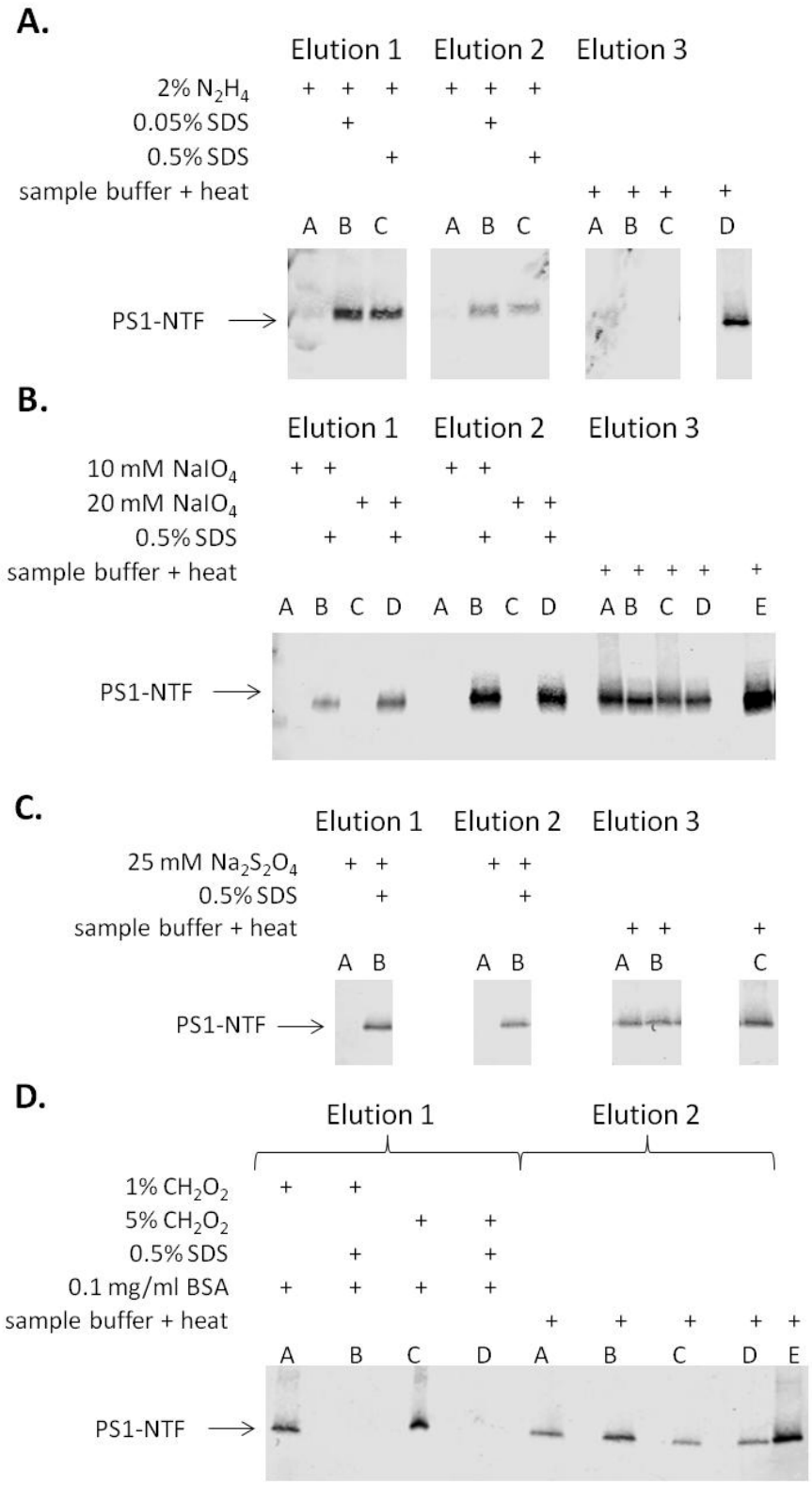
A.
Elution 1
Elution 2
Elution 3
2% N_2H_4
0.05% SDS
0.5% SDS
sample buffer + heat
A B C
A B C
A B C D
PS1-NTF
B.
Elution 1
Elution 2
Elution 3
10 mM $NaIO_4$
20 mM $NaIO_4$
0.5% SDS
sample buffer + heat
A B C D
A B C D
A B C D E
PS1-NTF
C.
Elution 1
Elution 2
Elution 3
25 mM $Na_2S_2O_4$
0.5% SDS
sample buffer + heat
A B
A B
A B
C
PS1-NTF
D.
Elution 1
Elution 2
1% CH_2O_2
5% CH_2O_2
0.5% SDS
0.1 mg/ml BSA
sample buffer + heat
A B C D
A B C D E
PS1-NTF

Figure 4.2 continued

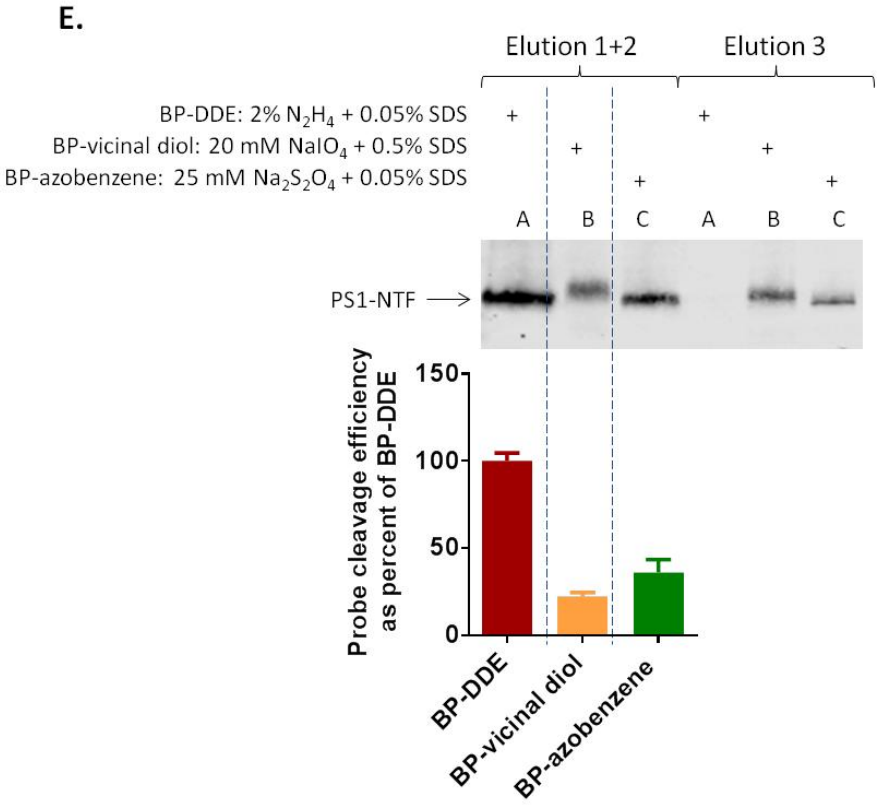

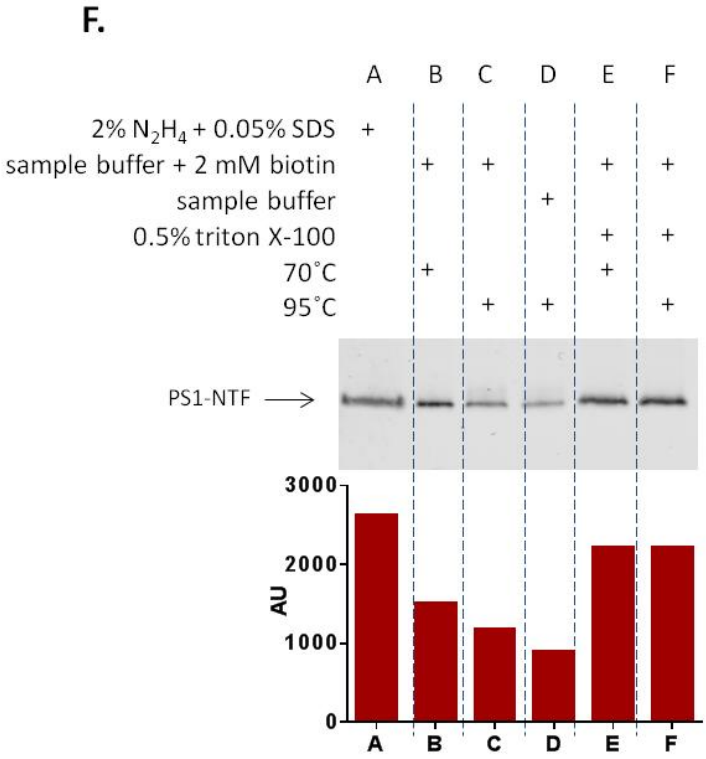

SDS is not required for probe cleavage but is required for solubility of PS1-NTF

The finding that PS1-NTF appeared on the Western blot when eluted with formic acid + BSA in the absence of SDS suggested that SDS is not required for cleavage but is required for protein stability. To test whether SDS is required for probe cleavage we performed a series of experiments in which proteins were eluted with cleavage-specific conditions in the presence or absence of SDS, beads were washed thoroughly with water, resuspended in sample buffer at room temperature, sample buffer was removed, and beads were eluted with 2 mM biotin in Laemmli sample buffer at 70˚ C for 10 minutes (Figure 4.3A-D). To our surprise, samples that were eluted with cleavage reagents in the absence of SDS showed a great deal of PS1-NTF in the subsequent sample buffer-resuspended fraction. On the contrary, proteins that were eluted with reagents containing SDS showed much less PS1-NTF in the subsequent sample buffer-resuspended fraction. This reveals that reagents lacking SDS are efficient at probe cleavage, but the hydrophobic PS1-NTF aggregates/sticks to the beads or tube and so does not get loaded onto the gel. With the addition of SDS, the reagents cleave the probe and the detergent forms a micelle that keeps PS1-NTF soluble. Therefore, the cleavage-specific reagents and detergent are both critical as they are performing entirely different but necessary functions during elution.

To show that SDS alone does not elute proteins, we eluted beads with 0.05 or 0.5% SDS, washed beads with water, resuspended beads in Laemmli sample buffer (~1% SDS final), removed sample buffer, and eluted beads with 2 mM biotin in Laemmli sample buffer at 70˚ C for 10 minutes (Figure 4.3C and D, lanes C). We found that 0.05 and 0.5% SDS alone do not elute proteins and Laemmli sample buffer elutes a very small fraction of protein. However, the amount of PS1-NTF eluted with sample

buffer is much lower than that eluted with cleavage reagents + SDS, suggesting that SDS alone does not elute proteins to any significant amount.

Figure 4.3. A. HeLa membrane was photolabeled with 95 nM BP-DDE and pulled-down with streptavidin beads. Samples A and B were eluted two times with 2% hydrazine + 0.05% SDS (elutions 1 and 2). Beads were then washed with water and briefly resuspended in Laemmli sample buffer (resuspension). Sample buffer was removed and samples A and B were eluted a third time with 2 mM biotin in Laemmli sample buffer at 70˚ C for 10 minutes (elution 3). Sample C was eluted only with 2 mM biotin in Laemmli sample buffer at 70˚ C for 10 minutes. B. HeLa membrane was photolabeled with 55 nM BP-vicinal diol and pulled-down with streptavidin beads. Samples A and B were eluted two consecutive times with 20 mM sodium periodate +/- 0.5% SDS (elutions 1 and 2). Beads were then washed with water and briefly resuspended in Laemmli sample buffer (resuspension). They were then eluted a third time with 2 mM biotin in Laemmli sample buffer at 70˚ C for 10 minutes (elution 3). Sample C was eluted only with 2 mM biotin in Laemmli sample buffer at 70˚ C for 10 minutes. C. HeLa membrane was photolabeled with 140 nM BP-azobenzene and pulled-down with streptavidin beads. Samples A and B were eluted two consecutive times with 25 mM sodium hydrosulfite +/- 0.05% SDS (elutions 1 and 2). Sample C was eluted two consecutive times with 0.05% SDS. Beads were then washed with water and briefly resuspended in Laemmli sample buffer (resuspension). They were then eluted a third time with 2 mM biotin in Laemmli sample buffer at 70˚ C for 10 minutes (elution 3). D. HeLa membrane was photolabeled with 400 nM BP-DADPS and pulled-down with streptavidin beads. Samples A and B were eluted two consecutive times with 5% formic acid +/- 0.5% SDS (elutions 1 and 2). Sample C was eluted two consecutive times with 0.05% SDS. Beads were then washed with water and briefly resuspended in Laemmli sample buffer (resuspension). They were then eluted a third time with 2 mM biotin in Laemmli sample buffer at 70˚ C for 10 minutes (elution 3). All samples were run on SDS-PAGE and analyzed by Western blot.

Figure 4.3

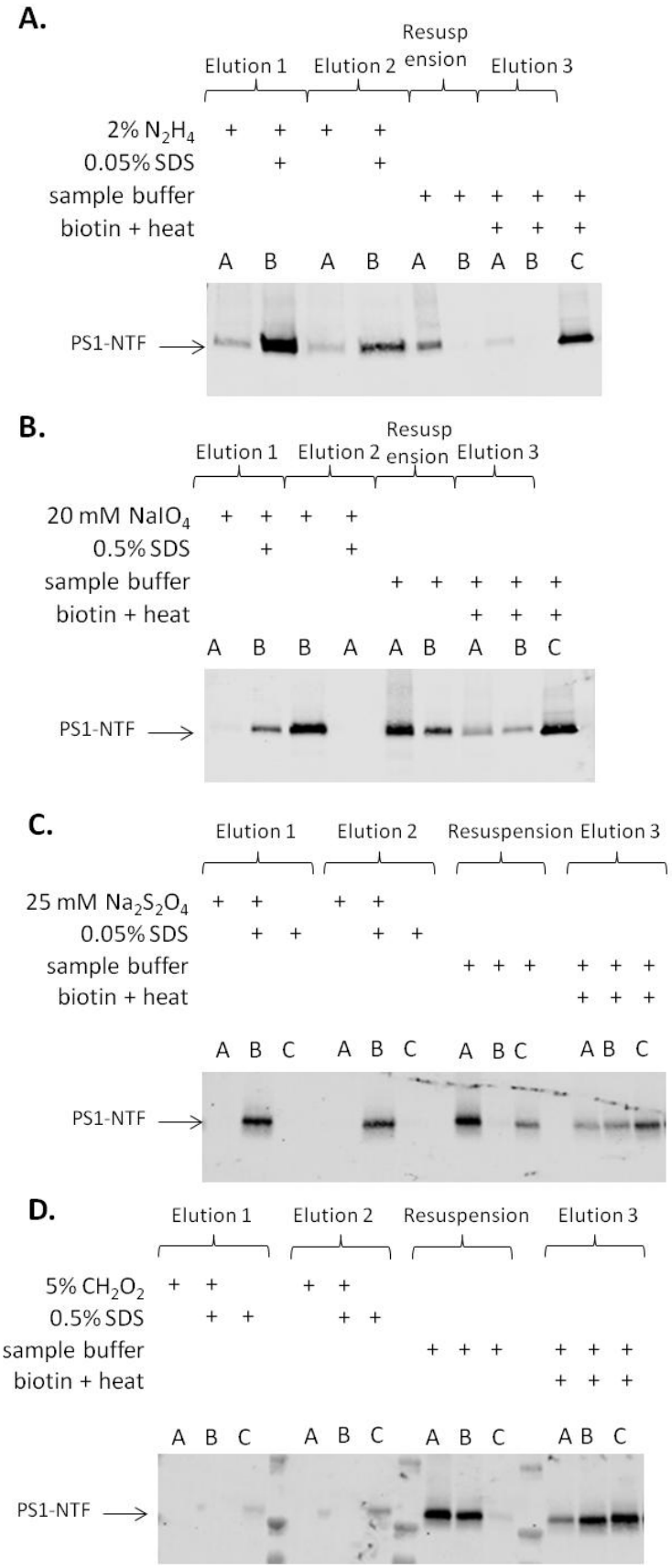
A.
Elution 1
Elution 2
Resusp ension
Elution 3
2% N_2H_4
0.05% SDS
sample buffer
biotin + heat
A B A B A B A B C
PS1-NTF
B.
Elution 1
Elution 2
Resusp ension
Elution 3
20 mM $NaIO_4$
0.5% SDS
sample buffer
biotin + heat
A B B A A B A B C
PS1-NTF
C.
Elution 1
Elution 2
Resuspension
Elution 3
25 mM $Na_2S_2O_4$
0.05% SDS
sample buffer
biotin + heat
A B C A B C A B C A B C
PS1-NTF
D.
Elution 1
Elution 2
Resuspension
Elution 3
5% CH_2O_2
0.5% SDS
sample buffer
biotin + heat
A B C A B C A B C A B C
PS1-NTF

BP-DDE large-scale photolabeling of PS1-NTF for LCMS analysis

As a result of BP-DDE's superiority at both labeling (Figure 4.1C, D) and eluting (Figure 4.2E) PS1-NTF, we used it in large scale photolabeling experiments in order to identify its binding site on PS1. First we established the optimal concentration of BP-DDE with which to label ANPP (HEK293 cells that overexpresses all four subunits of γ-secretase) membrane; the desirable concentration is one that saturates the γ-secretase sites without giving a high background signal, as established by blocking with BMS-708163. We determined that 100 nM of BP-DDE achieved high signal and low background, and increasing the concentration to 300 nM increased the noise but did not appreciably change the signal (data not shown). Briefly, 6 mg of ANPP membrane was photolabeled each with 100 nM BP-DDE with (+) or without (-) 10 μM parent compound BMS-708163. Samples were pulled-down with streptavidin beads, eluted with 2% hydrazine + 0.05% SDS, and concentrated. The resulting labeling of PS1-NTF is both specific and abundant as can be seen when 1 μl of 60 μl concentrated sample was loaded on SDS-PAGE and Western blotted for PS1-NTF (Figure 4.4A).

BP-TAMRA labels PS1-NTF and other potential protein targets

We wondered whether BMS-708163 has protein targets other than PS-NTF. We designed BP-TAMRA, a BMS-708163-based probe that is conjugated to TAMRA for fluorescence (Figure 4.4B). BP-TAMRA appears to have targets other than PS-NTF, as photolabeling of HeLa membrane followed by in-gel fluorescence shows additional protein bands (Figure 4.4C). However, none of these bands, with the exception of PS-NTF, can be marked as being specific, as they are not visibly competed by excess BMS-708163. When HeLa membrane was photolabeled by BP-TAMRA, followed by streptavidin pull-down and in-gel fluorescence, only the PS-NTF band was visible

(Figure 4.4D). This suggests that the other bands seen in Figure 4.4C may be non-specific or may be γ-secretase interacting partners that are stripped off during the stringent wash conditions used for streptavidin pull-down.

To identify BMS-708163 interacting proteins, we performed proteomic analysis on the large-scale labeling sample shown in Figure 4.4A. Samples with or without BMS-708163 competitor were digested in solution either by LysC or trypsin. Over 500 proteins were detected in both competed (+BMS-708163) and uncompeted (-BMS-708163) samples, but the presence of the competitor compound significantly decreased the capture of PS1, PS2, and Nct (Figure 4.4E). This result established that photoaffinity labeling of γ -secretase depended on specific binding of the probe to one of its subunits, the identity of which is PS and likely not Nct. The presence of the Nct hit can mean either that BP-DDE binds Nct directly or that Nct comes along for the ride as it is a PS interacting partner. Based on the finding that increased stringency of bead washing can dissociate Nct and other γ-secretase subunits from the BP-biotin-PS complex, we conclude that BP-DDE is stabilizing the γ-secretase complex and causing Nct to associate tighter with PS. Additional proteins significantly affected by the presence of competitor included epoxide hydrolase 1, a promiscuous target of benzophenone affinity labels, and lanosterol 14-α demethylase. Whether these proteins are being targeted by BP-DDE or are γ-secretase interacting partners remains to be investigated.

Figure 4.4. A. 6 mg of ANPP membrane was photolabeled each with 100 nM BP-DDE in the presence (+) or absence (-) of 10 μM BMS-708163. Samples were pulled-down, eluted with hydrazine + SDS, concentrated, and small quantity was used to detect PS1-NTF on Western blot. Input = 5 μg ANPP membrane B. Structure of BP-TAMRA C. Left: 400 μg of HeLa membrane was photolabeled each with 20 nM BP-TAMRA in the presence (+) or absence (-) of 1 μM BMS-708163. Samples were visualized by in-gel fluorescence Right: Coomassie blue stain of same gel D. 400 μg of HeLa membrane was photolabeled each with 20 nM BP-TAMRA in the presence (+) or absence (-) of 1 μM BMS-708163. Samples were pulled-down with streptavidin beads and visualized by in-gel fluorescence. E. Top: Effect of competitor compound BMS-708163 on the affinity capture of proteins from HeLa cell membrane preparation. Each point corresponds to one protein. Displacement of a protein to the right of the main population indicates that its capture was subject to competition by BMS-708163. Bottom: Top-scoring proteins (by Mascot protein score) from photoaffinity labeling/capture of HeLa cell membranes in absence and presence of competitor compound BMS-708163 (nd, not detected).

Figure 4.4

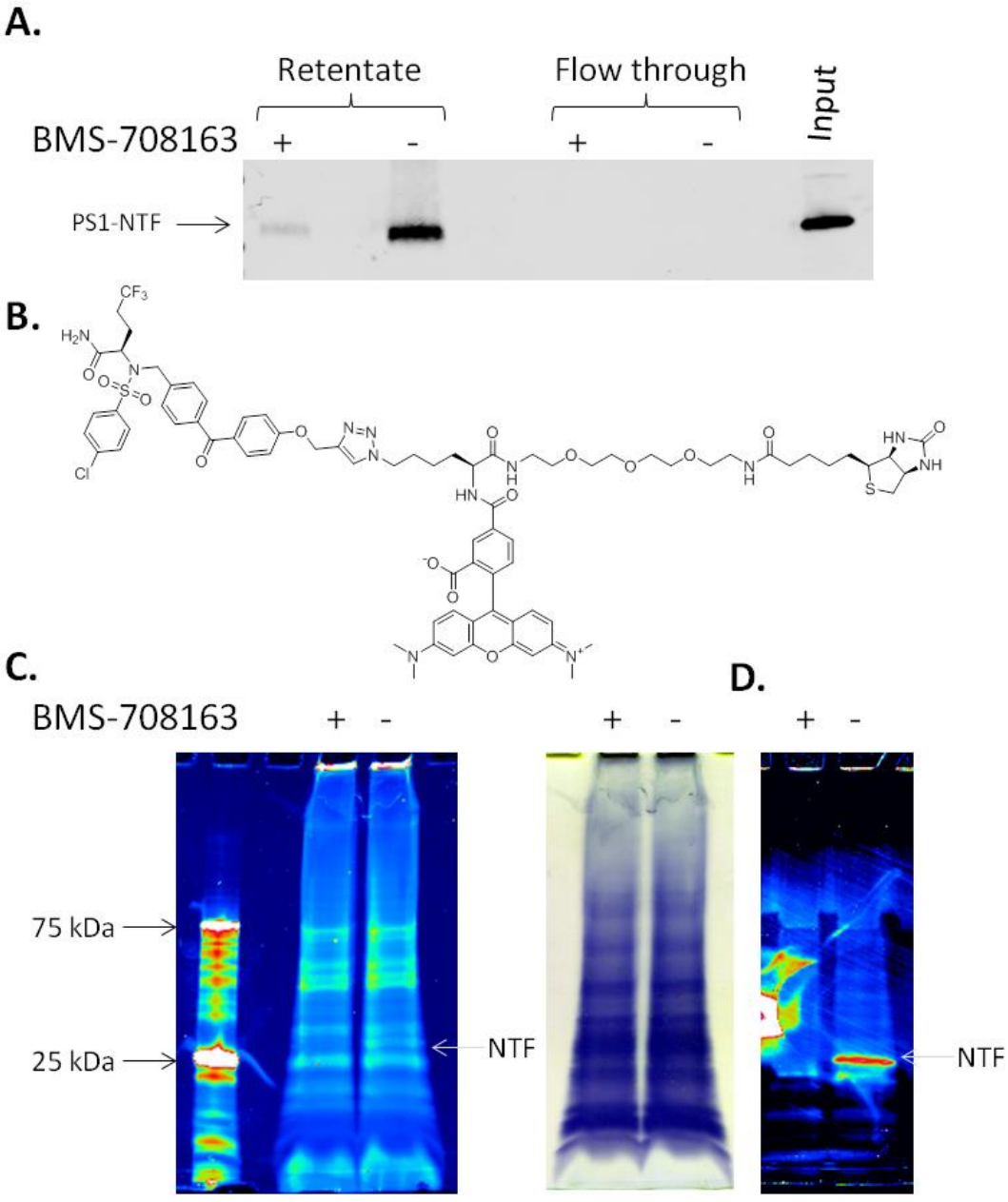
A.
Retentate
Flow through
Input
BMS-708163
+
-
+
-
PS1-NTF
B.
C.
D.
BMS-708163
+
-
+
-
+
-
75 kDa
25 kDa
NTF
NTF

Figure 4.4 continued

E.

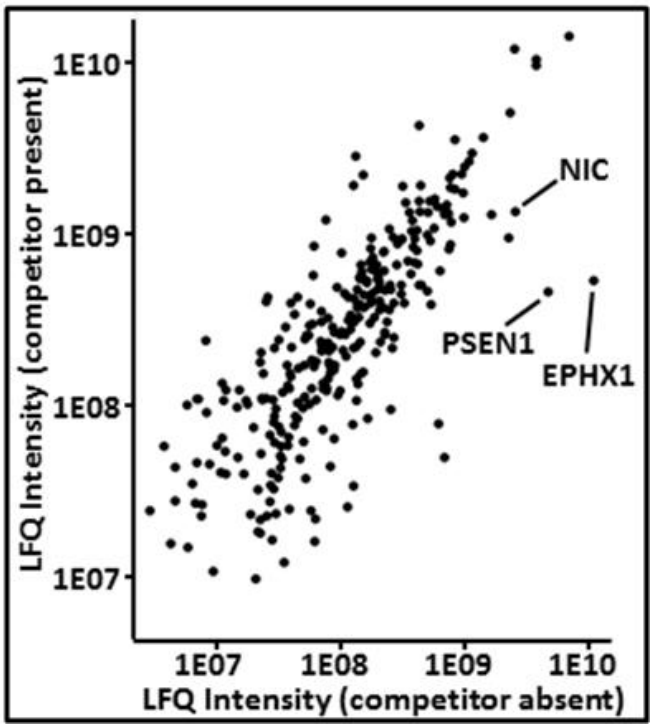

Protein	Rank uncompeted	Rank competed
Streptavidin – *S. avidinii*	1	1
Lysyl endopeptidase – *A. lyticus*	2	2
ATP synthase subunit beta, mitochondrial	3	3
ATP synthase subunit alpha, mitochondrial	4	4
Keratin, type II cytoskeletal	5	10
Trifunctional enzyme subunit alpha	6	5
Keratin, type I cytoskeletal 9	7	9
Trypsin - *Sus scrofa*	8	7
Keratin, type I cytoskeletal 10	9	8
Epoxide hydrolase 1	10	108
Keratin, type II cytoskeletal 2	11	10
Presenilin-1	12	134
60S ribosomal protein L7	13	20
Nicastrin	14	27
Prohibitin-2	15	11
Presenilin-2	35	nd

BP-DDE binds PS1-NTF in its endoproteolytic loop between TMDs 6 and 7

We next re-searched the data using a small database containing the sequences of the four recognized γ-secretase subunits together with the sequences of the highest-scoring contaminant proteins already recognized in the sample. This search strategy carried an increased risk of false-positive identifications of photolabeled peptides, but also reduced the risk of missing a genuine modified peptide because of low scoring caused by untypical fragmentation in the MS/MS spectrum. In a search that permitted BP-DDE modification of Leu, Val, Ile, Met, or Ala and specified semitryptic cleavage (i.e. at least one end of any peptide identified must result from a tryptic cleavage), a plausible hit was reported for peptide 279-291 of PS1 modified by BP-DDE at Leu282. This peptide has the sequence NETLFPALIYSST, with the N-terminus resulting from a tryptic cleavage following Arg278. The nontryptic C-terminus of Thr291 is reported in UniProtKB (accession P49768) as an alternative C-terminus of the PS-NTF, consistent with it having existed in the protein before tryptic digestion.

The mass spectrum and high-energy collisional dissociation spectrum of the detected product defined its identity. $[M+2H]^{2+}$ obsd. had m/z = 1074.460; the theoretical value for peptide 279-291 modified by BP-DDE is m/z = 1074.462 (mass discrepancy 1.9 ppm). Simulation of the spectrum based on the product's proposed elementary analysis closely matched the experiment (Figure 4.5A). In the tandem mass spectrum (Figure 4.5B), the site of modification was confined to Leu282, the fourth residue in the tridecapeptide, by detection of b_2, b_3, y_8, and y_9 ions lacking any modification by BP-DDE. Dehydrated b_5, b_7, b_8, and b_9 ions bearing the modification were also fully consistent with modification having occurred at Leu282. However, the data did not include information indicating which atom in Leu282 provided the attachment site for BP-DDE. There is reason to believe that the α-carbon of Leu282 is the attachment

atom, as it is the most stable radical species. However, this does not exclude the carbons of the amino acid side-chain as potential targets for the benzophenone.

Figure 4.5. A. Top: Peak cluster identified as $[M+2H]^{2+}$ of peptide 279-291 modified with hydrazine-cleaved residue of BP-DDE. Bottom: For comparison, simulated spectrum of proposed product, based on theoretical elementary composition of $C_{98}H_{134}ClF_3N_{20}O_{27}S$ plus two adduct protons. B. Tandem mass spectrum of modified peptide 279-291 with peak identities assigned according to the structure shown in the Inset. Modification is shown as occurring at the alpha-carbon of Leu282, but the site of attachment with Leu282 is not known with certainty. C. Close-up view of the transmembrane region of γ-secretase in complex with DAPT (Bai et al., 2015a). DAPT not shown. Yellow – Pen2, cyan – PS, green – Nct, orange – Aph1. Leucine 282 (shown in magenta) is facing the inside of the horseshoe.

Figure 4.5

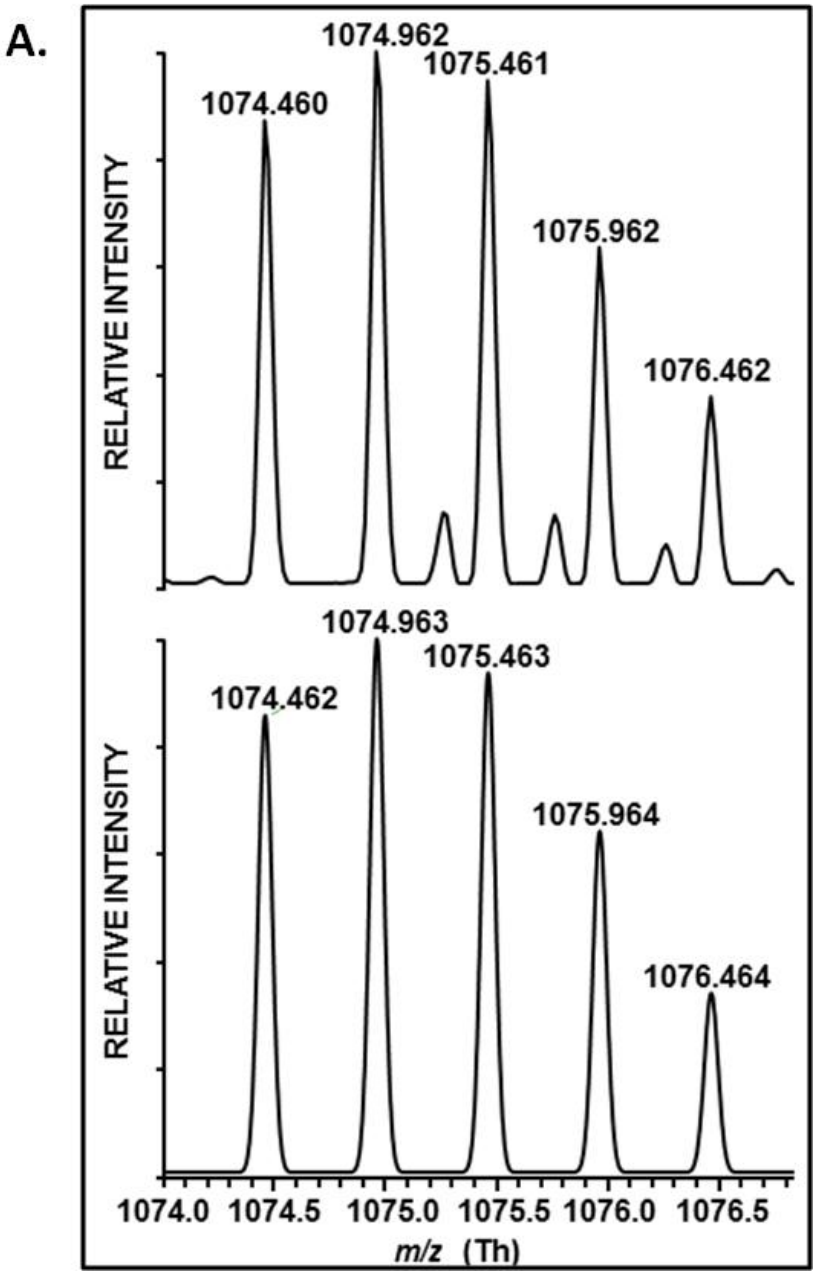
A.
1074.962
1075.461
1074.460
1075.962
1076.462
RELATIVE INTENSITY
1074.963
1075.463
1074.462
1075.964
1076.464
RELATIVE INTENSITY
1074.0 1074.5 1075.0 1075.5 1076.0 1076.5
m/z (Th)

Figure 4.5 continued

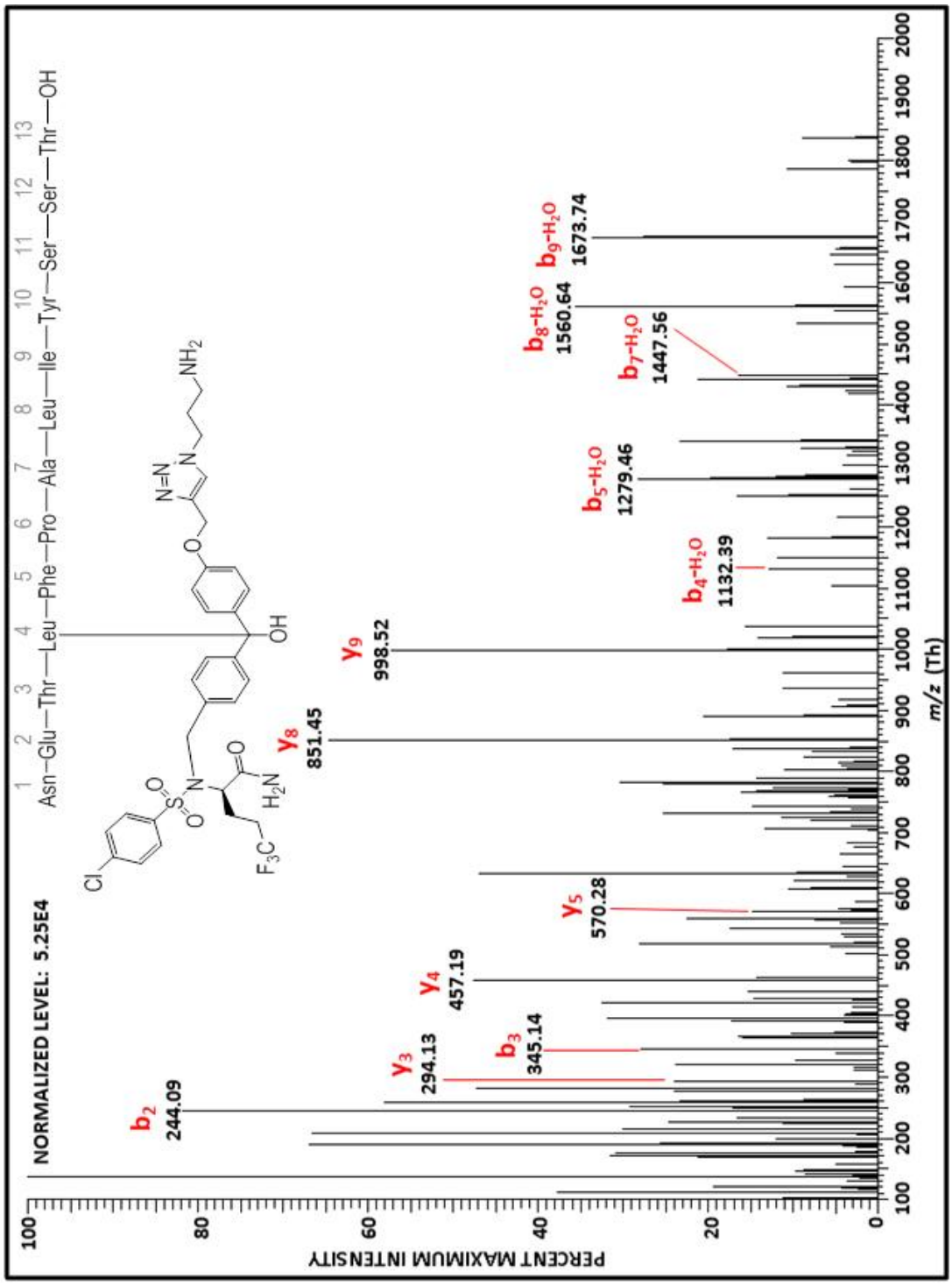

Figure 4.5 continued

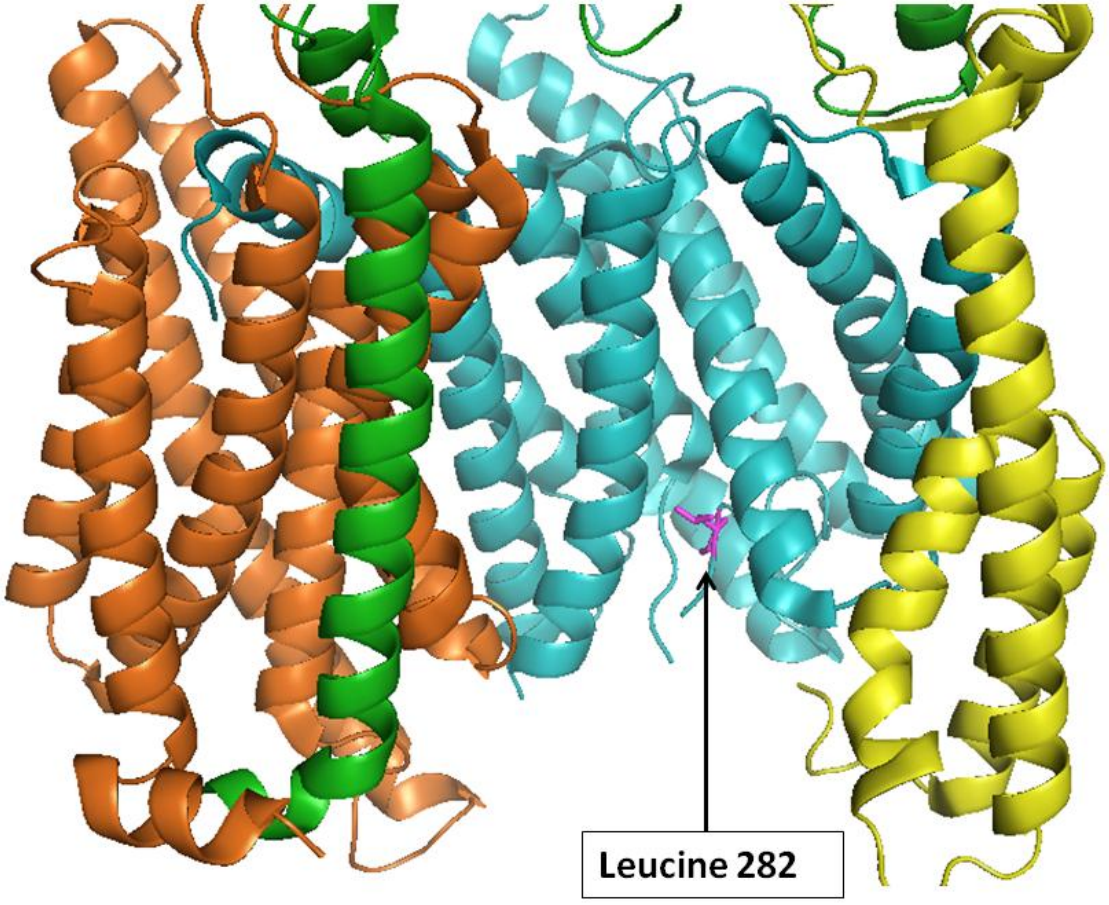

Structure adapted from PDB accession #5FN2; Bai et al., Elife 2015

Endoproteolysis of PS is required for BMS-708163 binding

While we knew that BMS-708163 binds the endoproteolytic loop of PS, we did not know whether this binding required a loose fragment end, as in PS1-NTF, or a complete, uncleaved loop, as in PS-FL. To test whether BP-DDE labels PS1-FL, we photolabeled ANP24 (Hek293 cells that overexpress all three components of γ-secretase except Pen2, resulting in an overabundance of PS-FL) membrane with various concentrations (20 nM – 500 nM) of BP-DDE in the presence or absence of 10 μM BMS-708163. Samples were pulled-down with streptavidin beads, eluted with hydrazine, run on SDS-PAGE, and Western blotted for PS1-NTF. While we did see some labeling at the molecular weight that corresponds to PS1-FL, this labeling was not competed in the presence of BMS-708163, suggesting it is not specific (data not shown). This illustrated that BP-DDE binds PS1-NTF, but not PS1-FL.

In order to eliminate the possibility that BMS-708163 is inhibiting endoproteolysis, we treated HeLa, SH-SY5Y, and SK-N-SH cells with 10 μM CBAP, BMS-708163, GSI-877 (a BMS-708163-based probe with a benzophenone and alkyne for azide-alkyne cycloaddition), L458, and DMSO control for 4 to 7 days, lysed cells, ran lysate on SDS-PAGE, and Western blotted for PS1-NTF. We did not treat cells with BP-DDE because the bulky biotin group would likely make the compound cell-impermeable. CBAP, a compound that potently inhibits endoproteolysis, accumulated PS1-FL, but neither BMS-708163 nor GSI-877 were able to do the same (data not shown). This reveals that BMS-708163 and BMS-708163-based probes do not inhibit endoproteolysis. For more information on CBAP, see Chapter 2.

The binding sites of BP-DDE and DAPT overlap

According to a recent high resolution cryo-EM structure, DAPT binds close to the active site of γ-secretase (Bai et al., 2015a). However, this finding is based largely on molecular modeling in areas of high flexibility that lack resolution, meaning the docking of DAPT may be imprecise. In order to gain greater insight into the binding of BMS-708163 on γ-secretase, we performed cross-labeling studies in which we looked for competition between BP-DDE and excess DAPT. When 1 μM DAPT and 20 nM BP-DDE were incubated with HeLa membrane, photolabeling of PS1-NTF was strongly inhibited. However, up to 100 μM DAPT was unable to block photolabeling of PS1-NTF by the active site-directed probe, JC8. This finding can be explained by one of the following: 1. DAPT binds the hydrophobic stretch of the cytoplasmic loop of PS, close to Leucine 282, which was found to be the BP-DDE modified residue or 2. The binding of DAPT near the active site allosterically changes the conformation of the loop region in such a way that it no longer interacts with BP-DDE. While possible, explanation 2 seems unlikely, as the loop between TMDs 6 and 7 has been shown to modulate the active site, but the reverse has not been found. Additionally, DAPT is unlikely to bind the active site as it does not interfere with labeling of the active site-directed probe, JC8. In all likelihood, and contrary to previous findings, DAPT shares a binding site with BP-DDE, which is in an allosteric region on the cytoplasmic side of the enzyme.

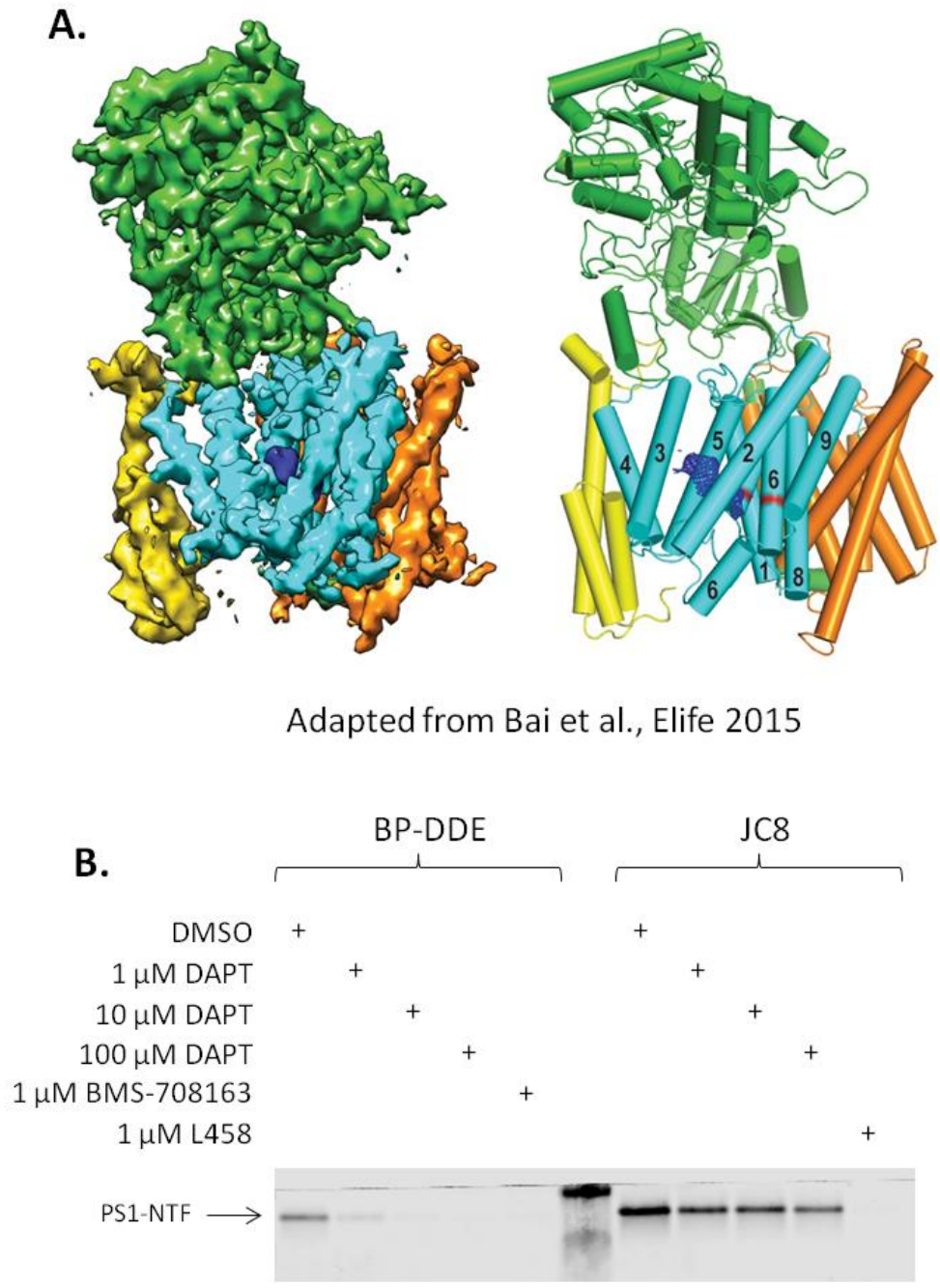

Figure 4.6. A. Cryo-EM structure of γ-secretase in complex with DAPT (Bai et al., 2015a). Left: The reconstructed density for the entire complex. Density attributed to DAPT is shown in deep purple. Right: Schematic representation of the atomic model. TMs of PS1 are numbered. B. HeLa membrane was photolabeled with 20 nM of either BP-DDE or JC8 in the presence (+) of various concentrations of DAPT. This was compared to DMSO lanes. Parent compounds BMS-708163 or L458 were added at 1 μM to completely block photolabeling. Lane in the middle is the protein ladder.

4.3 Conclusion and Discussion

In this work we developed four cleavable linker probes for the study of γ-secretase and compared them side-by-side, revealing their potency and cleavage efficiency. Each probe, with the exception of BP-DADPS, can be used in future studies to explore γ-secretase-small molecule interactions. However, the most efficient probe in our studies was BP-DDE: the high efficiency of BP-DDE-labeled PS1-NTF elution improved protein yield significantly over both heat eluted probes (BP-biotin) and probes with other cleavable linkers (BP-vicinal diol, BP-azobenzene, BP-DADPS). Given this advantage, we used BP-DDE to map the binding site of BMS-708163 on γ-secretase.

We were able to localize BP-DDE binding to amino acids 279-291 of PS1. Furthermore, we identified Leu282 as the probe-modified residue. This probe-modified region is adjacent to amino acids 291-292, which is one of the endoproteolytic sites of γ-secretase. In the process of endoproteolysis, PS-FL is converted into PS-NTF/CTF, an event necessary for activation of wild type γ-secretase. The 291-292 region is one of several potential cut sites, but a M292D mutation abolishes all endoproteolytic cleavage (Steiner et al., 1999b), confirming that this region is required for endoproteolysis. The M292D mutation mimics an FAD mutation, PS1ΔE9, in which the entire endoproteolysis site is deleted (amino acids 290-319), resulting in an active, endoproteolysis deficient γ-secretase (Thinakaran et al., 1996). The existence of these mutations suggests that the endoproteolytic loop is highly functional and may play an inhibitory role. While it was conceivable that BMS-708163 was exerting its inhibitory activity by inhibiting endoproteolysis, this turned out to not be the case, as BMS-708163 has no effect on autocatalytic cleavage of PS-FL and does not appear to bind PS-FL. It is possible, then, that BMS-708163 is inhibiting γ-secretase by mimicking the role of the inhibitory loop region of PS-FL.

A 3.4 Å cryo-EM reconstruction of γ-secretase gave tremendous insight into the enzyme's structure, but some regions of this 20 pass transmembrane protein were missing in the model due to their disordered nature (Bai et al., 2015b). One of these missing regions was the hydrophilic and disordered surface loop between TMDs 6 and 7 (amino acids 262-378), which houses the sites of endoproteolysis. When the structure was solved again with DAPT (a GSI) binding, some of these missing regions were resolved, so that the structure now reached amino acid 288 (Bai et al., 2015a). However, 289-377 remain unresolved. We propose that by solving the γ-secretase structure bound to BMS-708163, we can begin to stabilize these flexible regions in order to resolve them.

BMS-708163 (avagacestat), an arylsulfonamide GSI, made it to human trials but was terminated in phase 2 due to high gastrointestinal toxicity, nonmelanoma skin cancer, and a worsening in cognition (Coric et al., 2012). While the compound was initially reported to be Notch-sparing (Gillman et al., 2010), later research showed that it had very little selectivity for APP over Notch (Chavez-Gutierrez et al., 2012;Crump et al., 2012b). As a result, some of the observed toxicities were likely due to the compound's inhibition of Notch signaling. A better understanding of the compound's effect on γ-secretase activity and its interaction with γ-secretase could have prevented the failed trials. In this work we have extended our understanding of BMS-708163 through structural insights into its target engagement. Specifically, we identified the binding site of BP-DDE, a probe form of BMS-708163, on PS. To our knowledge, this is the first time that the binding site of a GSI/GSM has been mapped at atomic resolution.

4.4 Methods

Photolabeling for Western blot

400 μg of HeLa membrane was pre-incubated with indicated concentrations of blocking compound (BMS-708163), where applicable, in the presence of 0.25% CHAPSO in 1 ml of PBS in a 24 well plate at 37˚ C for 20 minutes with gentle shaking. Indicated concentration of probe (BP-DDE, BP-vicinal diol, BP-azobenzene, BP-DADPS, or BP-biotin) was added and incubation was continued for 1 more hour. Samples were UV irradiated at 350 nm for 45 minutes on ice block, solubilized with 1X RIPA for an hour, spun down at 15,700 x*g* for 10 min to pellet insoluble matter, and supernatants were pulled-down with 25 μl Streptavidin Plus UltraLink Resin. The streptavidin beads were washed 3X with RIPA, 2X with PBS, and 1X with cleavage specific buffer (BP-DDE – PBS; BP-vicinal diol – 100 mM sodium phosphate buffer pH 7.4; BP-azobenzene – 250 mM ammonium bicarbonate; BP-DADPS – PBS; BP-biotin – PBS). Proteins were eluted with cleavage-specific conditions and/or with 2 mM biotin in Laemmli Sample Buffer at 70˚ C for 10 minutes. Cleavage-specific conditions: Proteins were eluted 2 consecutive times, 30 minutes each, at 25˚ C with 40 μl of cleavage specific reagents. Beads were then washed 3X each with 1 ml of 0.1% SDS and eluted a third time with 2 mM biotin in Laemmli Sample Buffer at 70˚ C for 10 minutes. One sample was usually reserved for elution only with 2 mM biotin in Laemmli Sample Buffer at 70˚ C for 10 minutes. Where noted, proteins were washed 3X with 1 ml water (no SDS) between elutions 2 and 3. Laemmli Sample Buffer was added to samples and proteins were separated on SDS-PAGE. The desired proteins were detected via Western blot.

Photolabeling for LCMS

6 mg of ANPP8 membrane protein was photolabeled each with 100 nM BP-DDE either with or without 10 uM BMS-708163. Photolabeling was performed identical to the above except with the addition of PI and PMSF and without CHAPSO. After UV irradiation samples were ultracentrifuged at 100,000 x*g*, supernatants were discarded, and pellets were resuspended in 500 µl RIPA buffer using TissuLyser. Samples were spun down at 15,700 x*g* for 10 min to pellet insoluble matter. 3 500 µl samples were combined and pulled-down with 30 µl streptavidin beads. Beads were washed 3X with RIPA and 3X with PBS. Beads were then eluted 2X with 40 µl of 2% hydrazine + 0.05% SDS and washed 2X with 40 µl of water and these elutions and washes were combined and frozen. When all samples had been eluted (over the course of 1 week), they were all combined and concentrated on 10 kDa Amicon Ultra Centricon. Samples were concentrated ~24X, from 1440 µl down to 60 µl. Samples were sent to Pfizer and analyzed by LCMS.

Photolabeling and blocking with DAPT

400 µg of HeLa membrane was pre-incubated with indicated concentrations of blocking compound (BMS-708163, L458, or DAPT) in 1 ml of PBS in a 24 well plate at 37˚ C for 20 minutes with gentle shaking. 20 nM probe (BP-DDE or JC8) was added and incubation was continued for 1 more hour. Samples were UV irradiated at 350 nm for 45 minutes on ice block and ultracentrifuged at 100,000 x*g*, supernatants were discarded, and pellets were resuspended in 500 µl RIPA buffer using TissuLyser. Samples were spun down at 15,700 x*g* for 10 min to pellet insoluble matter, supernatants were pulled-down and eluted with 2 mM biotin in Laemmli Sample Buffer at 70˚ C for 10 minutes as usual.

LCMS

60 µl of each concentrated sample was treated with 60 µl of water and 480 µl of acetone, and incubated at -20° C overnight. The samples were then centrifuged at 4° C for 5 min at 15,000 x*g*, supernatants were discarded, and the residues were dried in a centrifugal evaporator. They were next redissolved in 40 µl of 8 M urea containing 5 mM dithiothreitol and incubated at 60^{o} C for 1 h, after which they were allowed to cool to room temperature, treated with iodoacetamide to a final concentration of 10 mM, and then incubated for 1 h at room temperature. The samples were then treated with 40 µl of 0.05 M NH_4HCO_3 containing 0.2 µg of LysC (Wako) and incubated overnight at 37° C, after which they were treated with 160 µl of 0.05 M NH_4HCO_3 containing 0.2 µg of trypsin (Promega sequencing grade), and incubated for 4 h at 37^{o}C. Following this, each sample was acidified to pH < 3 by addition of trifluoroacetic acid, and subjected to solid-phase extraction of peptides using StageTips (Rappsilber et al., 2007). The resulting samples were dried in the centrifugal evaporator, redissolved in 40 µl of 0.1% trifluoroacetic acid, and 7.5 µl portions were analyzed by liquid-chromatography/mass spectrometry using a Waters nanoAcquity system operating at 250 nl/min and a Q Exactive mass spectrometer (ThermoFisher Scientific). General proteomic searches were conducted using Proteome Discoverer 2.0 (ThermoFisher Scientific) connected to the Mascot search engine (licensed from Matrix Science, Boston, MA) and targeting the UniProtHuman database supplemented with sequences of common protein contaminants (keratins, porcine trypsin, etc.). More specific searches for products of photolabeling were conducted against a custom-built small database containing the sequences of human γ-secretase subunits together with the sequences of known abundant contaminants and with conjugation of BP-DDE to selected amino acids allowed in the Mascot search as a variable modification.

Theoretical peptide masses and MS/MS fragmentations were calculated using GPMAW v. 9.5 (Lighthouse data, Odense, Denmark) and ChemBioDraw Ultra v. 13.0 (Perkin-Elmer).

4.5 Acknowledgments

I'd like to thank Kieran F. Geoghegan, Pfizer, for performing the LCMS and writing the LCMS methods and findings. I also thank Christopher W. am Ende, Pfizer, for synthesis of the cleavable linker probes. Special thanks to Douglas S. Johnson, Pfizer, for collaborating on this project with us. Thank you to David B. Iaea, Weill Cornell Medical, for insights on all parts of this project, and especially on the 3D structural data.

CHAPTER 5

Thesis Implications

γ-Secretase's role in AD has positioned it in the spotlight for drug development. However, after years of diligent research and in spite of a strong genetic understanding of disease causes, there is still no FDA approved treatment for this age-related epidemic. Some have taken this dichotomy to mean that Aβ plaques are not the driving force of disease progression, reasoning that if we are not able to cure AD by inhibiting γ-secretase and reducing plaques, then maybe plaques are a consequence of disease and not its cause. Genetic evidence, however, tells an entirely different story. The presence of fully-penetrant, autosomal dominant FAD mutations in γ-secretase that increase the Aβ42:Aβ40 ratio, and even more convincingly, the presence of mutations in γ-secretase that decrease the Aβ42:Aβ40 ratio and protect from disease, are overt alerts of Aβ's causative role in disease pathogenesis (Jonsson et al., 2012). The inability to treat/cure AD to date has likely been a result of inaccurate patient recruitment (many patients had a form of dementia other than AD), non-optimal drug dosages (patients were dosed intermittently instead of regularly), poorly understood drug toxicities, and less-than-ideal compound selection (non-selective GSIs were used, which caused mechanism-based toxicity). Many of these problems are now being addressed in the community and by our lab: Positron emission tomography (PET) brain scans can be used to ensure that we are enlisting the right patients in clinical trials, as doing AD trials on patients that do not, and never will, present with Aβ plaques is a sure way to destroy what could have been a good drug. Drug dosages remain a complex issue, but we have learned a great deal about drug administration from the clinical trials of BMS-708163 and LY450139. Off-target effects, while unavoidable, must be further studied if we are to make safe therapies. In this work we

explored the impact of GSIs/GSMs on SPP, a widely expressed enzyme that is required in eukaryotes and whose activity may be affected by drugs that target γ-secretase (Gertsik et al., 2015). A thorough understanding of SPP-mediated pathways altered by drug treatment is vital for further GSI/GSM development. Finally, compound selection is a critical step in early stage drug development that requires more robust and a wider range of γ-secretase activity assays in order to attain accurate profiling of compound effects. Our lab has developed such assays and employed them to show that BMS-708163, which was initially reported as a Notch-sparing GSI (Gillman et al., 2010), was actually a nonselective GSI (Chavez-Gutierrez et al., 2012;Crump et al., 2012b). Had this information come to light before clinical trials, I suspect it would have saved both patients and pharmaceutical companies from unnecessary suffering and spending. Furthermore, in this work we have mapped the binding site of BMS-708163 on γ-secretase, providing high resolution information for the way in which this compound interacts with its target. Such atomic resolution structure-function information can pave the way for rational drug design of GSIs/GSMs.

In addition to providing valuable information for development of GSIs/GSMs as therapeutics, the work performed here has made important contributions to the study of complex transmembrane proteins for which high resolution structural information may not be available. First, we have shown that photoreactive transition state active site-directed probes can sense subtle changes in active site architecture of their target proteins. These probes are able to distinguish between PS1 and SPP, two proteins with very similar active sites. Furthermore, we showed that allosteric GSIs/GSMs have an impact on the active site conformations of PS1 and SPP, illustrating that structurally distinct compounds with different protein binding sites can engender active site

changes that are detectable with L458-based probes. Whether the structural changes observed here lead to alterations in activity of SPP remains to be determined. An increase in active site-directed probe labeling of enzyme does not necessarily translate to an increase in enzymatic activity, so we must be cautious in interpreting the photoaffinity results. We further used active site-directed probes to determine that SPP is a dimer in its active form. While both monomeric and dimeric forms of SPP have been found by various groups, it was unclear which of these forms was active and whether one or the other was an artifact of protein preparation. Our findings not only support the assertion that SPP is a dimer, but also illustrate an additional utility of L458-based probes – that is, their ability to be eluted with mild cleavage-specific conditions (in this case we used a disulfide linker, which was cleaved with a reducing agent) that minimize the perturbation to the proteins quaternary structure.

We expanded on the ability of cleavable linker probes to label and elute target proteins under desirable conditions. Specifically, we made four different cleavable linker probe variants of BMS-708163 with the intention of identifying the binding site of BMS-708163 on γ-secretase. We hypothesized that the acid-cleavable probe would work best, as its utility had been shown before and its elution with formic acid was compatible with LCMS (Szychowski et al., 2010). However, we were surprised to find that PS1 is unstable in acidic conditions, indicating that acid-cleavable probes are sub-optimal for the study of γ-secretase. Through the synthesis of various linkers and the optimization of PS1 elution, we generated a set of tools for the study of γ-secretase and made important conclusions about the stability of the enzyme in various conditions. Importantly, we found that PS1 is highly stable in 2% hydrazine + 0.05% SDS. The high yield of PS1-NTF obtained from this cleavage condition can be widely useful for the study of γ-secretase. Moreover, we were successful in localizing the

binding site of BMS-708163 on γ-secretase, marking an important milestone in the study of GSI/GSM-γ-secretase interaction. Our lab had previously shown that structurally distinct GSIs/GSMs bind to different regions of PS1 (Crump et al., 2013), but the precise location of this binding was unknown. In this work we have circumvented the inherent difficulty of crystallizing a multipass transmembrane enzyme by using a combination of novel chemical biology and proteomics approaches to localize the binding site of BMS-708163 on γ-secretase. We have shown for the first time that it is possible to identify the amino acid residue to which these compounds bind. Our findings contribute not only to a better understanding of the structure and function of γ-secretase in order to elucidate disease mechanism and develop effective AD therapy, but also raise the bar for what is possible in the high resolution study of complex transmembrane proteins.

Chapter 6

Materials and Methods

6.1 Materials

HeLa cell pellet (mid-log) for membrane preparation was purchased from Biovest. ANPP8 (HEK293 cells that overexpress PS1, Aph1, Nct, and Pen2) and ANP24 cells (HEK293 cells that overexpress PS1, Aph1, and Nct) were a gift from Dr. Sangram Sisodia and were grown in-house for membrane preparation and in-cell labeling. Biotin-PEG_2-azide for azide-alkyne cycloaddition was purchased from ChemPep. Streptavidin Plus UltraLink Resin was purchased from Pierce. TAMRA azide was synthesized by Pfizer and provided as a gift. Protease Inhibitor cocktail was made in house from powders purchased from Sigma Aldrich, and used at final concentrations as follows: 1 mM benzamidine, 2.9 μM leupeptin, 5 μM antipain, 100 μM EDTA, and 100 μM phenylmethanesulfonyl fluoride (PMSF). Typhoon Trio Variable Mode Imager (GE Healthcare) was used for in-gel fluorescence scans. Western blots were developed either with film or scanned with Odyssey CLx from LI-COR. Small scale membrane samples for photolabeling experiments were resuspended with TissueLyser.

Primary antibodies for Western blot: anti-Aph1a 28-3600 was purchased from Invitrogen. Anti-PS1-CTF loop MAB 5232 was purchased from Millipore. Anti-Pen2 18189 rabbit polyclonal was purchased from Abcam. Anti-PS1-NTF was provided by Dr. Min-Tain Lai (Merck Research Laboratories). Anti-SPP was made by Dr. Deming Chau in our lab by immunizing rabbits with a peptide epitode from the N-terminal region of SPP. Anti-NCT was similarly made in-house by immunizing rabbits with a NCT peptide. Secondary antibodies for Western blots scanned on Odyssey were purchased from LI-COR: IRDye 800 CW goat anti-rabbit and IRDye 680 RD goat anti-mouse.

AlphaLISA detection reagents such as streptavidin coated donor beads, anti-mouse acceptor beads and protein A coated acceptor beads for γ-secretase activity assay were purchased from PerkinElmer. 10-G3, which is an Aβ42 cleavage-specific antibody, was a gift from Dr. Douglas Johnson at Pfizer. G2-10, which is an Aβ40 cleavage-specific antibody, was a gift from Merck Research Laboratories. SM320, the Notch1 intracellular domain (NICD)-specific antibody, was generated by Dr. Deming Chau (Chau et al., 2012). Recombinant protein substrates Sb4 and N1-Sb1 were cloned from the cDNA of APP and Notch1, respectively (Tian et al., 2010a;Chau et al., 2012). These substrates are overexpressed with a biotin on one end for alphaLISA detection and a thrombin-cleavable MBP tag on the other, to allow for purification and optional removal. Proteins were purified with an amylose column and the AKTA Prime FPLC technology (GE Healthcare). AlphaLISA signal was detected with an EnVision multilabel plate reader (PerkinElmer).

6.2 γ-Secretase activity assay

In vitro activity assay has been described before (Tian et al., 2010a;Chau et al., 2012). A γ-secretase source, specifically 80 μg/ml of HeLa membrane, was incubated with its APP (Sb4) or Notch1 (N1-Sb1) substrate in the presence of 0.25% CHAPSO at 37˚C for 4 hours in the presence or absence of inhibitors or modulators. The amount of cleavage product generated was detected with a solution of cleavage specific antibody (G2-10 for Aβ40, 10-G3 for Aβ42, or SM320 for NICD) and alphaLISA protein A (Aβ42 and NICD) or alphaLISA anti-mouse acceptor beads (Aβ40) plus streptavidin coated donor beads from PerkinElmer. The reaction and detection mixtures were combined 1:1 (20 μl + 20 μl) in a 384 well plate, incubated overnight, and read the next morning with EnVision multilabel plate reader.

6.3 Photoaffinity labeling with active site-directed probes

Photoaffinity labeling was performed as previously described (Placanica et al., 2009a;Shelton et al., 2009). In a 24 well plate 400 µg HeLa membrane was incubated with 20 nM active site-directed probe (JC8, L646, GY4, or L505) and some concentration of blocking compound (GSI/GSM) in the presence of 0.25% CHAPSO. The total volume of each sample was 1 ml, made up with PBS. The concentration of DMSO in each reaction did not exceed 2.5% v/v. Plate was gently shaken at 37˚C for one hour. Next the plate was UV irradiated at 350 nm for 45 minutes on an ice block. Subsequently, samples were transferred to an Eppendorf tube and RIPA (50 mM Tris base, pH 8.0, 150 mM NaCl, 0.1% SDS, 1% NP-40, 0.5% deoxycholate) solubilized, rotating at room temperature for 1 hour. Samples were spun down at 15,700 x*g* for 10 minutes to pellet insoluble matter. The supernatants were transferred to a dolphin-nosed tube with 20 µl Streptavidin Plus UltraLink Resin and biotinylated proteins were pulled-down with rotation at 4˚ C overnight. The next day, samples were spun down at 100 x*g* and supernatant was removed. The streptavidin slurry pellet was washed 3X with RIPA and once with PBS. Proteins were eluted with Laemmli sample buffer + 2 mM biotin at 70˚ C for 10 minutes and separated on SDS-PAGE. The desired proteins were detected via Western blot. JC8 (Chun et al., 2004), GY4 (Yang et al., 2009), and L646 and L505 (Li et al., 2000b) were described previously.

JC8, L646, GY4, and L505 are highly potent (IC_{50} ~ 1 nM) biotinylated photoaffinity probes based on L-685,458 (L458), a transition state active site-directed γ-secretase inhibitor with a hydroxyethylene dipeptide isostere (Figure 6.1A). These probes differ from one another in the location of the benzophenone, where the benzophenone was placed into various positions around the L458 backbone. Amino acids (termed “P”) on the N-terminal side of the scissile bond are numbered and amino acids on the C-

terminal of the scissile bond are named with a number followed by a “prime” symbol (Schechter and Berger, 1967). By moving the benzophenone to different P sites, we created probes that can target various sub-sites of the enzyme active site. This technique is known as “photophore walking” (Shelton et al., 2009;Chau et al., 2012). Because crosslinking of the probe to the enzyme depends on the distance and orientation of the benzophenone to the contact residues, each probe has a different efficiency of insertion. Upon perturbation to the enzyme structure, this efficiency may change. Changes in efficiency of insertion reveal changes in the enzyme active site. Allosteric GSIs/GSMs may bind PS far from its active site, but nevertheless this binding may cause changes in the structure of the active site itself (Figure 6.1B). These changes are detectable with active site-directed probes described here. Depending on the structural perturbation, all of the probes may change in insertion efficiency, or only one may change. Importantly, addition of excess competitor, which is the parent compound (in this example, L458) without the benzophenone and biotin, should inhibit labeling entirely. This technique has been used to study changes in the enzyme active site architecture in the presence of GSIs, GSMs, and FAD mutations (Shelton et al., 2009;Tian et al., 2010a;Crump et al., 2011;Chau et al., 2012;Crump et al., 2012b;Gertsik et al., 2015).

Figure 6.1. A. Structures of biotinylated probes JC8, L646, GY4, L505, and parent compound L458. B. Active site-directed probe, with crosslinkable benzophenones (orange sun) in one of four possible positions, labels the active site (light blue) of γ-secretase at either the S1, S2, S1', or S3' subsites. The addition of a GSI or GSM (black star) changes the active site conformation of the enzyme, leading to a change in the interaction between the probe and its contact residues. C. Biotinylated, photoreactive, active site-directed probes are used to label the active sites of enzyme targets. Biotinylated proteins are pulled-down with streptavidin beads and visualized on a Western blot.

Figure 6.1

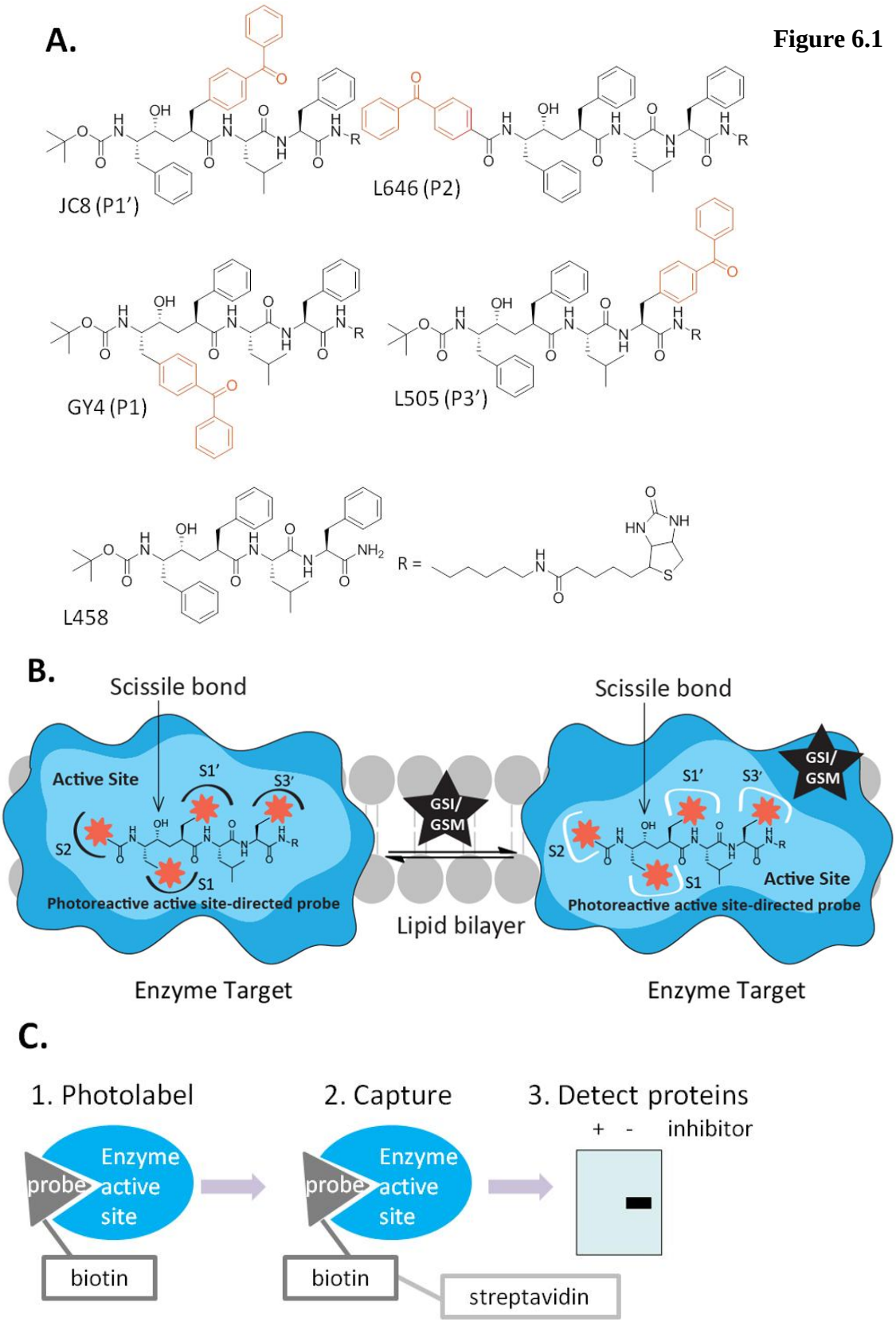
A.
JC8 (P1')
L646 (P2)
GY4 (P1)
L505 (P3')
L458
R =
B.
Scissile bond
Active Site
S1'
S3'
S2
S1
Photoreactive active site-directed probe
GSI/
GSM
Lipid bilayer
Scissile bond
GSI/
GSM
S1'
S3'
S2
S1
Active Site
Photoreactive active site-directed probe
Enzyme Target
Enzyme Target
C.
1. Photolabel
2. Capture
3. Detect proteins
+ - inhibitor
Enzyme
probe
active
site
biotin
Enzyme
probe
active
site
biotin
streptavidin

6.4 Photoaffinity labeling with azide-alkyne cycloaddition (Figure 6.2)

Probes with a benzophenone moiety for crosslinking and an alkyne moiety for conjugation to biotin for pull-down were incubated with 600 µg HeLa membrane and indicated concentration of GSI/GSM in a 24 well plate in 0.5 or 1 ml total volume, made up with PBS, shaking at 37˚ C for one hour. Next samples were UV irradiated at 350 nm for 45 minutes on an ice block. Samples were ultracentrifuged at 100,000 x*g* to pellet the membrane fraction, supernatant was discarded and the pellet was resuspended in 200 µl PBS with the TissueLyser. Probe-labeled proteins were conjugated to biotin via copper catalyzed azide-alkyne cycloaddition (CuAAC): samples were rotated for 1 hour at room temperature with 1 mM $CuSO_4$, 1 mM TCEP, 0.1 mM TBTA, 100 µM biotin-azide, 5% t-butanol, and 1% DMSO in PBS. Samples were ultracentrifuged at 100,000 x*g*, supernatant was discarded and pellet was resuspended in 500 µl RIPA buffer using TissuLyser. Samples were spun down at 15,700 x*g* for 10 minutes to pellet insoluble matter. The supernatants were transferred to a dolphin-nosed tube with 20 µl Streptavidin Plus UltraLink Resin and biotinylated proteins were pulled-down with rotation at 4˚ C overnight. The next day, samples were spun down at 100 x*g* and supernatant was removed. The streptavidin slurry pellet was washed 3X with RIPA and once with tris buffered saline, 0.1% tween-20. Proteins were eluted with 40 µl of 2 mM biotin in Laemmli sample buffer at 70˚ C for 10 minutes and 20 µl of eluate was loaded and separated on SDS-PAGE. Proteins were transferred to PVDF membrane and probed with appropriate antibodies.

6.5 Photoaffinity labeling with in-gel fluorescence (Figure 6.2)

Probes with a benzophenone moiety for crosslinking and an alkyne moiety for conjugation to tetramethyl rhodamine (TAMRA) were incubated with 400 µg HeLa membrane and indicated concentration of GSI/GSM in a 24 well plate in 1 ml total

volume, made up with PBS, shaking at 37˚ C for one hour. Next samples were UV irradiated at 350 nm for 45 minutes on an ice block. Samples were ultracentrifuged at 100,000 x*g* to pellet the membrane fraction, supernatant was discarded and the pellet was resuspended in 200 µl PBS. Probe-labeled proteins were conjugated to TAMRA via CuAAC: samples were rotated for 1 hour in the dark at room temperature with 1 mM $CuSO_4$, 1 mM TCEP, 0.1 mM TBTA, 60 µM TAMRA-azide, 5% t-butanol, and 1% DMSO in PBS. Proteins were precipitated with cold acetone (80% acetone, 20% sample) at -20˚ C for 30 minutes. Samples were spun down at 15,700 x*g* for 10 minutes to precipitate proteins and the pellet was washed once with 1 ml cold acetone. Acetone was removed, pellet was dried for 10 minutes and resuspended in Laemmli sample buffer without dye. Proteins were separated on SDS-PAGE, gel was washed and fixed with 20% methanol, and gel was scanned on Typhoon Trio Variable Mode Imager. The gel was then stained with Coomassie blue to ensure equal protein was loaded in all lanes.

Probes that already had a TAMRA group directly attached did not require CuAAC. Following ultracentrifugation, these samples were resuspended in 250 µl 1% SDS in PBS and acetone precipitated. The rest was the same as above.

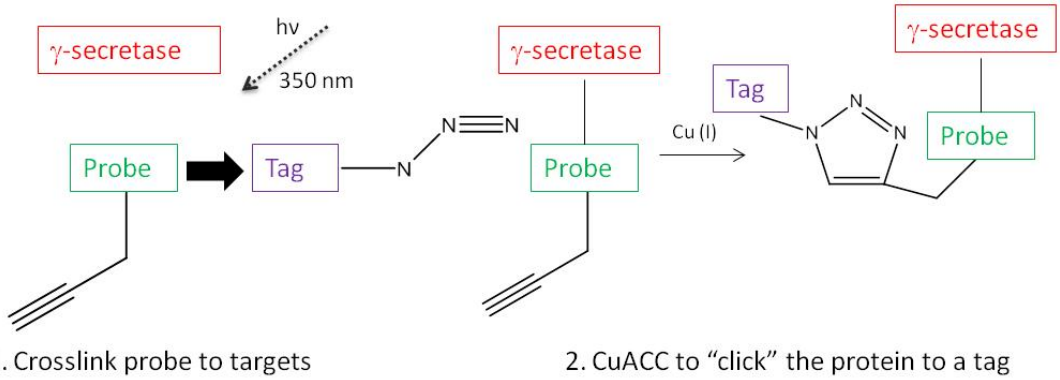

Figure 6.2. Photoreactive probe with an alkyne is incubated with an enzyme source and covalently labels γ-secretase. Azide conjugated to a tag, such as a biotin or fluorophore, is "clicked" to the alkyne. The tag is used for protein isolation or visualization.

CHAPTER 7

References

Ahn, K., Shelton, C.C., Tian, Y., Zhang, X., Gilchrist, M.L., Sisodia, S.S., and Li, Y.-M. (2010). Activation and intrinsic γ-secretase activity of presenilin 1. *Proc Natl Acad Sci U S A* 107**,** 21435-21440.

Alzforum (2015). Semagacestat Failure Analysis: Should γ-Secretase Remain a Target? *http://www.alzforum.org/news/research-news/semagacestat-failure-analysis-should-g-secretase-remain-target*.

Alzheimer's Association (2015). 2015 Alzheimer's disease facts and figures. *Alzheimers Dement* 11**,** 332-384.

Bai, X.C., Rajendra, E., Yang, G., Shi, Y., and Scheres, S.H. (2015a). Sampling the conformational space of the catalytic subunit of human gamma-secretase. *Elife* 4.

Bai, X.C., Yan, C., Yang, G., Lu, P., Ma, D., Sun, L., Zhou, R., Scheres, S.H., and Shi, Y. (2015b). An atomic structure of human gamma-secretase. *Nature* 525**,** 212-217.

Bammens, L., Chavez-Gutierrez, L., Tolia, A., Zwijsen, A., and De Strooper, B. (2011). Functional and topological analysis of Pen-2, the fourth subunit of the gamma-secretase complex. *J Biol Chem* 286**,** 12271-12282.

Barrett, P.J., Sanders, C.R., Kaufman, S.A., Michelsen, K., and Jordan, J.B. (2011). NSAID-based gamma-secretase modulators do not bind to the amyloid-beta polypeptide. *Biochemistry* 50**,** 10328-10342.

Beel, A.J., and Sanders, C.R. (2008). Substrate specificity of gamma-secretase and other intramembrane proteases. *Cell Mol Life Sci* 65**,** 1311-1334.

Beher, D., Clarke, E.E., Wrigley, J.D., Martin, A.C., Nadin, A., Churcher, I., and Shearman, M.S. (2004). Selected non-steroidal anti-inflammatory drugs and their derivatives target gamma-secretase at a novel site. Evidence for an allosteric mechanism. *J Biol Chem* 279**,** 43419-43426.

Beher, D., Fricker, M., Nadin, A., Clarke, E.E., Wrigley, J.D., Li, Y.M., Culvenor, J.G., Masters, C.L., Harrison, T., and Shearman, M.S. (2003). In vitro characterization of the presenilin-dependent gamma-secretase complex using a novel affinity ligand. *Biochemistry* 42**,** 8133-8142.

Beher, D., Wrigley, J.D., Nadin, A., Evin, G., Masters, C.L., Harrison, T., Castro, J.L., and Shearman, M.S. (2001). Pharmacological knock-down of the presenilin

1 heterodimer by a novel gamma -secretase inhibitor: implications for presenilin biology. *J Biol Chem* 276**,** 45394-45402.

Berlau, D.J., Corrada, M.M., Head, E., and Kawas, C.H. (2009). APOE epsilon2 is associated with intact cognition but increased Alzheimer pathology in the oldest old. *Neurology* 72**,** 829-834.

Biogen (2015). Biogen Idec Presents Positive Interim Results from Phase 1B Study of Investigational Alzheimer's Disease Treatment Aducanumab (BIIB037) at 2015 AD/PD™ Conference. *http://media.biogen.com/press-release/corporate/biogen-idec-presents-positive-interim-results-phase-1b-study-investigational*.

Blum, G., Bothwell, I.R., Islam, K., and Luo, M. (2013). Profiling protein methylation with cofactor analog containing terminal alkyne functionality. *Curr Protoc Chem Biol* 5**,** 67-88.

Borgegard, T., Jureus, A., Olsson, F., Rosqvist, S., Sabirsh, A., Rotticci, D., Paulsen, K., Klintenberg, R., Yan, H., Waldman, M., Stromberg, K., Nord, J., Johansson, J., Regner, A., Parpal, S., Malinowsky, D., Radesater, A.C., Li, T., Singh, R., Eriksson, H., and Lundkvist, J. (2012). First and second generation gamma-secretase modulators (GSMs) modulate amyloid-beta (Abeta) peptide production through different mechanisms. *J Biol Chem* 287**,** 11810-11819.

Botev, A., Munter, L.M., Wenzel, R., Richter, L., Althoff, V., Ismer, J., Gerling, U., Weise, C., Koksch, B., Hildebrand, P.W., Bittl, R., and Multhaup, G. (2011). The amyloid precursor protein C-terminal fragment C100 occurs in monomeric and dimeric stable conformations and binds gamma-secretase modulators. *Biochemistry* 50**,** 828-835.

Brown, M.S., Ye, J., Rawson, R.B., and Goldstein, J.L. (2000). Regulated intramembrane proteolysis: a control mechanism conserved from bacteria to humans. *Cell* 100**,** 391-398.

Brunkan, A.L., Martinez, M., Walker, E.S., and Goate, A.M. (2005a). Presenilin endoproteolysis is an intramolecular cleavage. *Mol Cell Neurosci* 29**,** 65-73.

Brunkan, A.L., Martinez, M., Wang, J., Walker, E.S., Beher, D., Shearman, M.S., and Goate, A.M. (2005b). Two domains within the first putative transmembrane domain of presenilin 1 differentially influence presenilinase and gamma-secretase activity. *J Neurochem* 94**,** 1315-1328.

Cai, D., Netzer, W.J., Zhong, M., Lin, Y., Du, G., Frohman, M., Foster, D.A., Sisodia, S.S., Xu, H., Gorelick, F.S., and Greengard, P. (2006). Presenilin-1 uses phospholipase D1 as a negative regulator of beta-amyloid formation. *Proc Natl Acad Sci U S A* 103**,** 1941-1946.

Campbell, W.A., Iskandar, M.K., Reed, M.L., and Xia, W. (2002). Endoproteolysis of presenilin in vitro: inhibition by gamma-secretase inhibitors. *Biochemistry* 41**,** 3372-3379.

Campbell, W.A., Reed, M.L., Strahle, J., Wolfe, M.S., and Xia, W. (2003). Presenilin endoproteolysis mediated by an aspartyl protease activity pharmacologically distinct from gamma-secretase. *J Neurochem* 85**,** 1563-1574.

Capell, A., Kaether, C., Edbauer, D., Shirotani, K., Merkl, S., Steiner, H., and Haass, C. (2003). Nicastrin interacts with gamma-secretase complex components via the N-terminal part of its transmembrane domain. *J Biol Chem* 278**,** 52519-52523.

Casso, D.J., Tanda, S., Biehs, B., Martoglio, B., and Kornberg, T.B. (2005). Drosophila signal peptide peptidase is an essential protease for larval development. *Genetics* 170**,** 139-148.

Chau, D.M., Crump, C.J., Villa, J.C., Scheinberg, D.A., and Li, Y.M. (2012). Familial Alzheimer Disease Presenilin-1 Mutations Alter the Active Site Conformation of gamma-secretase. *J Biol Chem* 287**,** 17288-17296.

Chau, D.M., Shum, D., Radu, C., Bhinder, B., Gin, D., Gilchrist, M.L., Djaballah, H., and Li, Y.M. (2013). A novel high throughput 1536-well Notch1 gamma - secretase AlphaLISA assay. *Comb Chem High Throughput Screen* 16**,** 415-424.

Chavez-Gutierrez, L., Bammens, L., Benilova, I., Vandersteen, A., Benurwar, M., Borgers, M., Lismont, S., Zhou, L., Van Cleynenbreugel, S., Esselmann, H., Wiltfang, J., Serneels, L., Karran, E., Gijsen, H., Schymkowitz, J., Rousseau, F., Broersen, K., and De Strooper, B. (2012). The mechanism of gamma-Secretase dysfunction in familial Alzheimer disease. *EMBO J* 31**,** 2261-2274.

Chavez-Gutierrez, L., Tolia, A., Maes, E., Li, T., Wong, P.C., and De Strooper, B. (2008). Glu(332) in the Nicastrin ectodomain is essential for gamma-secretase complex maturation but not for its activity. *J Biol Chem* 283**,** 20096-20105.

Chen, F., Hasegawa, H., Schmitt-Ulms, G., Kawarai, T., Bohm, C., Katayama, T., Gu, Y., Sanjo, N., Glista, M., Rogaeva, E., Wakutani, Y., Pardossi-Piquard, R., Ruan, X., Tandon, A., Checler, F., Marambaud, P., Hansen, K., Westaway, D., St George-Hyslop, P., and Fraser, P. (2006). TMP21 is a presenilin complex component that modulates gamma-secretase but not epsilon-secretase activity. *Nature* 440**,** 1208-1212.

Chu, J., Lauretti, E., Craige, C.P., and Pratico, D. (2014). Pharmacological modulation of GSAP reduces amyloid-beta levels and tau phosphorylation in a mouse model of Alzheimer's disease with plaques and tangles. *J Alzheimers Dis* 41**,** 729-737.

Chun, J., Yin, Y.I., Yang, G., Tarassishin, L., and Li, Y.M. (2004). Stereoselective Synthesis of Photoreactive Peptidomimetic gamma-Secretase Inhibitors. *J Org Chem* 69**,** 7344-7347.

Clarke, E.E., Churcher, I., Ellis, S., Wrigley, J.D., Lewis, H.D., Harrison, T., Shearman, M.S., and Beher, D. (2006). Intra- or intercomplex binding to the gamma-secretase enzyme. A model to differentiate inhibitor classes. *J Biol Chem* 281**,** 31279-31289.

Corder, E.H., Saunders, A.M., Strittmatter, W.J., Schmechel, D.E., Gaskell, P.C., Small, G.W., Roses, A.D., Haines, J.L., and Pericak-Vance, M.A. (1993). Gene dose of apolipoprotein E type 4 allele and the risk of Alzheimer's disease in late onset families. *Science* 261**,** 921-923.

Coric, V., Van Dyck, C.H., Salloway, S., Andreasen, N., Brody, M., Richter, R.W., Soininen, H., Thein, S., Shiovitz, T., Pilcher, G., Colby, S., Rollin, L., Dockens, R., Pachai, C., Portelius, E., Andreasson, U., Blennow, K., Soares, H., Albright, C., Feldman, H.H., and Berman, R.M. (2012). Safety and tolerability of the gamma-secretase inhibitor avagacestat in a phase 2 study of mild to moderate Alzheimer disease. *Arch Neurol* 69**,** 1430-1440.

Crump, C.J., Am Ende, C.W., Ballard, T.E., Pozdnyakov, N., Pettersson, M., Chau, D.M., Bales, K.R., Li, Y.M., and Johnson, D.S. (2012a). Development of clickable active site-directed photoaffinity probes for gamma-secretase. *Bioorg Med Chem Lett* 22**,** 2997-3000

Crump, C.J., Castro, S.V., Wang, F., Pozdnyakov, N., Ballard, T.E., Sisodia, S.S., Bales, K.R., Johnson, D.S., and Li, Y.M. (2012b). BMS-708,163 Targets Presenilin and Lacks Notch-Sparing Activity. *Biochemistry* 51**,** 7209-7211.

Crump, C.J., Fish, B.A., Castro, S.V., Chau, D.M., Gertsik, N., Ahn, K., Stiff, C., Pozdnyakov, N., Bales, K.R., Johnson, D.S., and Li, Y.M. (2011). Piperidine acetic acid based gamma-secretase modulators directly bind to Presenilin-1. *ACS Chem Neurosci* 2**,** 705-710.

Crump, C.J., Johnson, D.S., and Li, Y.M. (2013). Development and mechanism of gamma-secretase modulators for Alzheimer's disease. *Biochemistry* 52**,** 3197-3216.

Cruts, M., Theuns, J., and Van Broeckhoven, C. (2012). Locus-specific mutation databases for neurodegenerative brain diseases. *Hum Mutat* 33**,** 1340-1344.

Cupers, P., Orlans, I., Craessaerts, K., Annaert, W., and De Strooper, B. (2001). The amyloid precursor protein (APP)-cytoplasmic fragment generated by gamma-secretase is rapidly degraded but distributes partially in a nuclear fraction of neurones in culture. *J Neurochem* 78**,** 1168-1178.

De Strooper, B. (2003). Aph-1, Pen-2, and Nicastrin with Presenilin generate an active gamma-Secretase complex. *Neuron* 38**,** 9-12.

De Strooper, B. (2014). Lessons from a failed gamma-secretase Alzheimer trial. *Cell* 159**,** 721-726.

De Strooper, B., Annaert, W., Cupers, P., Saftig, P., Craessaerts, K., Mumm, J.S., Schroeter, E.H., Schrijvers, V., Wolfe, M.S., Ray, W.J., Goate, A., and Kopan, R. (1999). A presenilin-1-dependent gamma-secretase-like protease mediates release of Notch intracellular domain. *Nature* 398**,** 518-522.

De Strooper, B., and Chavez Gutierrez, L. (2015). Learning by failing: ideas and concepts to tackle gamma-secretases in Alzheimer's disease and beyond. *Annu Rev Pharmacol Toxicol* 55**,** 419-437.

De Strooper, B., Saftig, P., Craessaerts, K., Vanderstichele, H., Guhde, G., Annaert, W., Von Figura, K., and Van Leuven, F. (1998). Deficiency of presenilin-1 inhibits the normal cleavage of amyloid precursor protein. *Nature* 391**,** 387-390.

Deng, Y., Tarassishin, L., Kallhoff, V., Peethumnongsin, E., Wu, L., Li, Y.M., and Zheng, H. (2006). Deletion of presenilin 1 hydrophilic loop sequence leads to impaired gamma-secretase activity and exacerbated amyloid pathology. *J Neurosci* 26**,** 3845-3854.

Dieterich, D.C., Lee, J.J., Link, A.J., Graumann, J., Tirrell, D.A., and Schuman, E.M. (2007). Labeling, detection and identification of newly synthesized proteomes with bioorthogonal non-canonical amino-acid tagging. *Nat Protoc* 2**,** 532-540.

Doody, R.S., Raman, R., Farlow, M., Iwatsubo, T., Vellas, B., Joffe, S., Kieburtz, K., He, F., Sun, X., Thomas, R.G., Aisen, P.S., Alzheimer's Disease Cooperative Study Steering, C., Siemers, E., Sethuraman, G., Mohs, R., and Semagacestat Study, G. (2013). A phase 3 trial of semagacestat for treatment of Alzheimer's disease. *N Engl J Med* 369**,** 341-350.

Dovey, H.F., John, V., Anderson, J.P., Chen, L.Z., De Saint Andrieu, P., Fang, L.Y., Freedman, S.B., Folmer, B., Goldbach, E., Holsztynska, E.J., Hu, K.L., Johnson-Wood, K.L., Kennedy, S.L., Kholodenko, D., Knops, J.E., Latimer, L.H., Lee, M., Liao, Z., Lieberburg, I.M., Motter, R.N., Mutter, L.C., Nietz, J., Quinn, K.P., Sacchi, K.L., Seubert, P.A., Shopp, G.M., Thorsett, E.D., Tung, J.S., Wu, J., Yang, S., Yin, C.T., Schenk, D.B., May, P.C., Altstiel, L.D., Bender, M.H., Boggs, L.N., Britton, T.C., Clemens, J.C., Czilli, D.L., Dieckman-Mcginty, D.K., Droste, J.J., Fuson, K.S., Gitter, B.D., Hyslop, P.A., Johnstone, E.M., Li, W.Y., Little, S.P., Mabry, T.E., Miller, F.D., and Audia, J.E. (2001). Functional gamma-secretase inhibitors reduce beta-amyloid peptide levels in brain. *J Neurochem* 76**,** 173-181.

Dries, D.R., Shah, S., Han, Y.H., Yu, C., Yu, S., Shearman, M.S., and Yu, G. (2009). Glu-333 of nicastrin directly participates in gamma-secretase activity. *J Biol Chem* 284**,** 29714-29724.

Ebke, A., Luebbers, T., Fukumori, A., Shirotani, K., Haass, C., Baumann, K., and Steiner, H. (2011). Novel gamma-secretase enzyme modulators directly target presenilin protein. *J Biol Chem* 286**,** 37181-37186.

Edbauer, D., Willem, M., Lammich, S., Steiner, H., and Haass, C. (2002). Insulin-degrading enzyme rapidly removes the beta-amyloid precursor protein intracellular domain (AICD). *J Biol Chem* 277**,** 13389-13393.

Edbauer, D., Winkler, E., Regula, J.T., Pesold, B., Steiner, H., and Haass, C. (2003). Reconstitution of gamma-secretase activity. *Nat Cell Biol* 5**,** 486-488.

Esler, W.P., Kimberly, W.T., Ostaszewski, B.L., Diehl, T.S., Moore, C.L., Tsai, J.Y., Rahmati, T., Xia, W., Selkoe, D.J., and Wolfe, M.S. (2000). Transition-state analogue inhibitors of gamma-secretase bind directly to presenilin-1. *Nat Cell Biol* 2**,** 428-434.

Fluhrer, R., Steiner, H., and Haass, C. (2009). Intramembrane proteolysis by signal peptide peptidases: a comparative discussion of GXGD-type aspartyl proteases. *J Biol Chem* 284**,** 13975-13979.

Francis, R., Mcgrath, G., Zhang, J., Ruddy, D.A., Sym, M., Apfeld, J., Nicoll, M., Maxwell, M., Hai, B., Ellis, M.C., Parks, A.L., Xu, W., Li, J., Gurney, M., Myers, R.L., Himes, C.S., Hiebsch, R., Ruble, C., Nye, J.S., and Curtis, D. (2002). aph-1 and pen-2 are required for Notch pathway signaling, gamma-secretase cleavage of betaAPP, and presenilin protein accumulation. *Dev Cell* 3**,** 85-97.

Freeman, M. (2008). Rhomboid proteases and their biological functions. *Annu Rev Genet* 42**,** 191-210.

Friedmann, E., Lemberg, M.K., Weihofen, A., Dev, K.K., Dengler, U., Rovelli, G., and Martoglio, B. (2004). Consensus analysis of signal peptide peptidase and homologous human aspartic proteases reveals opposite topology of catalytic domains compared with presenilins. *J Biol Chem* 279**,** 50790-50798.

Frykman, S., Teranishi, Y., Hur, J.Y., Sandebring, A., Yamamoto, N.G., Ancarcrona, M., Nishimura, T., Winblad, B., Bogdanovic, N., Schedin-Weiss, S., Kihara, T., and Tjernberg, L.O. (2012). Identification of two novel synaptic gamma-secretase associated proteins that affect amyloid beta-peptide levels without altering Notch processing. *Neurochem Int* 61**,** 108-118.

Fuwa, H., Takahashi, Y., Konno, Y., Watanabe, N., Miyashita, H., Sasaki, M., Natsugari, H., Kan, T., Fukuyama, T., Tomita, T., and Iwatsubo, T. (2007). Divergent synthesis of multifunctional molecular probes to elucidate the enzyme specificity of dipeptidic gamma-secretase inhibitors. *ACS Chem Biol* 2**,** 408-418.

Gertsik, N., Ballard, T.E., Am Ende, C.W., Johnson, D.S., and Li, Y.M. (2014a). Development of CBAP-BPyne, a probe for gamma-secretase and presenilinase. *Medchemcomm* 5**,** 338-341.

Gertsik, N., Chau, D.M., and Li, Y.M. (2015). gamma-Secretase Inhibitors and Modulators Induce Distinct Conformational Changes in the Active Sites of gamma-Secretase and Signal Peptide Peptidase. *ACS Chem Biol* 10**,** 1925-1931.

Gertsik, N., Chiu, D., and Li, Y.M. (2014b). Complex regulation of gamma-secretase: from obligatory to modulatory subunits. *Front Aging Neurosci* 6**,** 342.

Gillman, K.W., Starrett, J.E., Parker, M.F., Xie, K., Bronson, J.J., Marcin, L.R., Mcelhone, K.E., Bergstrom, C.P., Mate, R.A., Williams, R., Meredith, J.E., Burton, C.R., Barten, D.M., Toyn, J.H., Roberts, S.B., Lentz, K.A., Houston, J.G., Zaczek, R., Albright, C.F., Decicco, C.P., Macor, J.E., and Olson, R.E. (2010). Discovery and Evaluation of BMS-708163, a Potent, Selective and Orally Bioavailable γ-Secretase Inhibitor. *ACS Medicinal Chemistry Letters* 1**,** 120-124.

Glenner, G.G., and Wong, C.W. (1984a). Alzheimer's disease and Down's syndrome: sharing of a unique cerebrovascular amyloid fibril protein. *Biochem Biophys Res Commun* 122**,** 1131-1135.

Glenner, G.G., and Wong, C.W. (1984b). Alzheimer's disease: initial report of the purification and characterization of a novel cerebrovascular amyloid protein. *Biochem Biophys Res Commun* 120**,** 885-890.

Goate, A., Chartier-Harlin, M.C., Mullan, M., Brown, J., Crawford, F., Fidani, L., Giuffra, L., Haynes, A., Irving, N., James, L., and Et Al. (1991). Segregation of a missense mutation in the amyloid precursor protein gene with familial Alzheimer's disease. *Nature* 349**,** 704-706.

Godbolt, A.K., Beck, J.A., Collinge, J., Garrard, P., Warren, J.D., Fox, N.C., and Rossor, M.N. (2004). A presenilin 1 R278I mutation presenting with language impairment. *Neurology* 63**,** 1702-1704.

Golde, T.E., Koo, E.H., Felsenstein, K.M., Osborne, B.A., and Miele, L. (2013). gamma-Secretase inhibitors and modulators. *Biochim Biophys Acta* 1828**,** 2898-2907.

Goutte, C., Tsunozaki, M., Hale, V.A., and Priess, J.R. (2002). APH-1 is a multipass membrane protein essential for the Notch signaling pathway in Caenorhabditis elegans embryos. *Proc Natl Acad Sci U S A* 99**,** 775-779.

Green, N.M. (1990). Avidin and streptavidin. *Methods Enzymol* 184**,** 51-67.

Green, R.C., Schneider, L.S., Amato, D.A., Beelen, A.P., Wilcock, G., Swabb, E.A., Zavitz, K.H., and Tarenflurbil Phase 3 Study, G. (2009). Effect of tarenflurbil on cognitive decline and activities of daily living in patients with mild Alzheimer disease: a randomized controlled trial. *JAMA* 302**,** 2557-2564.

Grigorenko, A.P., Moliaka, Y.K., Soto, M.C., Mello, C.C., and Rogaev, E.I. (2004). The Caenorhabditis elegans IMPAS gene, imp-2, is essential for development and is functionally distinct from related presenilins. *Proc Natl Acad Sci U S A* 101**,** 14955-14960.

Grundke-Iqbal, I., Iqbal, K., Quinlan, M., Tung, Y.C., Zaidi, M.S., and Wisniewski, H.M. (1986). Microtubule-associated protein tau. A component of Alzheimer paired helical filaments. *J Biol Chem* 261**,** 6084-6089.

Gu, Y., Sanjo, N., Chen, F., Hasegawa, H., Petit, A., Ruan, X., Li, W., Shier, C., Kawarai, T., Schmitt-Ulms, G., Westaway, D., St George-Hyslop, P., and Fraser, P.E. (2004). The presenilin proteins are components of multiple membrane-bound complexes that have different biological activities. *J Biol Chem* 279**,** 31329-31336.

Haapasalo, A., and Kovacs, D.M. (2011). The many substrates of presenilin/gamma-secretase. *J Alzheimers Dis* 25**,** 3-28.

Hardy, J., and Allsop, D. (1991). Amyloid deposition as the central event in the aetiology of Alzheimer's disease. *Trends Pharmacol Sci* 12**,** 383-388.

Hayashi, I., Takatori, S., Urano, Y., Miyake, Y., Takagi, J., Sakata-Yanagimoto, M., Iwanari, H., Osawa, S., Morohashi, Y., Li, T., Wong, P.C., Chiba, S., Kodama, T., Hamakubo, T., Tomita, T., and Iwatsubo, T. (2011). Neutralization of the gamma-secretase activity by monoclonal antibody against extracellular domain of nicastrin. *Oncogene*.

He, G., Luo, W., Li, P., Remmers, C., Netzer, W.J., Hendrick, J., Bettayeb, K., Flajolet, M., Gorelick, F., Wennogle, L.P., and Greengard, P. (2010). Gamma-secretase activating protein is a therapeutic target for Alzheimer's disease. *Nature* 467**,** 95-98.

Herreman, A., Hartmann, D., Annaert, W., Saftig, P., Craessaerts, K., Serneels, L., Umans, L., Schrijvers, V., Checler, F., Vanderstichele, H., Baekelandt, V., Dressel, R., Cupers, P., Huylebroeck, D., Zwijsen, A., Van Leuven, F., and De Strooper, B. (1999). Presenilin 2 deficiency causes a mild pulmonary phenotype and no changes in amyloid precursor protein processing but enhances the embryonic lethal phenotype of presenilin 1 deficiency. *Proc Natl Acad Sci U S A* 96**,** 11872-11877.

Holmes, O., Paturi, S., Ye, W., Wolfe, M.S., and Selkoe, D.J. (2012). Effects of membrane lipids on the activity and processivity of purified gamma-secretase. *Biochemistry* 51**,** 3565-3575.

Holtzman, D.M., Bales, K.R., Tenkova, T., Fagan, A.M., Parsadanian, M., Sartorius, L.J., Mackey, B., Olney, J., Mckeel, D., Wozniak, D., and Paul, S.M. (2000). Apolipoprotein E isoform-dependent amyloid deposition and neuritic degeneration in a mouse model of Alzheimer's disease. *Proc Natl Acad Sci U S A* 97**,** 2892-2897.

Hopkins, C.R. (2012). ACS chemical neuroscience molecule spotlight on Begacestat (GSI-953). *ACS Chem Neurosci* 3**,** 3-4.

Hur, J.Y., Gertsik, N., Johnson, D.S., and Li, Y.M. (2016). "Gamma-Secretase Inhibitors: from Chemical Probes to Drug Development " in *Developing Therapeutics for Alzheimer's Disease: Progress and Challenges,* ed. M.S. Wolfe. Academic Press, 63-76.

Hur, J.Y., Teranishi, Y., Kihara, T., Yamamoto, N.G., Inoue, M., Hosia, W., Hashimoto, M., Winblad, B., Frykman, S., and Tjernberg, L.O. (2012). Identification of novel gamma-secretase-associated proteins in detergent-resistant membranes from brain. *J Biol Chem* 287**,** 11991-12005.

Hussain, I., Fabregue, J., Anderes, L., Ousson, S., Borlat, F., Eligert, V., Berger, S., Dimitrov, M., Alattia, J.R., Fraering, P.C., and Beher, D. (2013). The role of gamma-secretase activating protein (GSAP) and imatinib in the regulation

of gamma-secretase activity and amyloid-beta generation. *J Biol Chem* 288**,** 2521-2531.

Iben, L.G., Olson, R.E., Balanda, L.A., Jayachandra, S., Robertson, B.J., Hay, V., Corradi, J., Prasad, C.V., Zaczek, R., Albright, C.F., and Toyn, J.H. (2007). Signal peptide peptidase and gamma-secretase share equivalent inhibitor binding pharmacology. *J Biol Chem* 282**,** 36829-36836.

Iwatsubo, T., Odaka, A., Suzuki, N., Mizusawa, H., Nukina, N., and Ihara, Y. (1994). Visualization of A beta 42(43) and A beta 40 in senile plaques with end-specific A beta monoclonals: evidence that an initially deposited species is A beta 42(43). *Neuron* 13**,** 45-53.

Jan, A., Gokce, O., Luthi-Carter, R., and Lashuel, H.A. (2008). The ratio of monomeric to aggregated forms of Abeta40 and Abeta42 is an important determinant of amyloid-beta aggregation, fibrillogenesis, and toxicity. *J Biol Chem* 283**,** 28176-28189.

Jonsson, T., Atwal, J.K., Steinberg, S., Snaedal, J., Jonsson, P.V., Bjornsson, S., Stefansson, H., Sulem, P., Gudbjartsson, D., Maloney, J., Hoyte, K., Gustafson, A., Liu, Y., Lu, Y., Bhangale, T., Graham, R.R., Huttenlocher, J., Bjornsdottir, G., Andreassen, O.A., Jonsson, E.G., Palotie, A., Behrens, T.W., Magnusson, O.T., Kong, A., Thorsteinsdottir, U., Watts, R.J., and Stefansson, K. (2012). A mutation in APP protects against Alzheimer's disease and age-related cognitive decline. *Nature* 488**,** 96-99.

Josien, H. (2002). Recent advances in the development of gamma-secretase inhibitors. *Curr Opin Drug Discov Devel* 5**,** 513-525.

Jumpertz, T., Rennhack, A., Ness, J., Baches, S., Pietrzik, C.U., Bulic, B., and Weggen, S. (2012). Presenilin Is the Molecular Target of Acidic gamma-Secretase Modulators in Living Cells. *PLoS ONE* 7**,** e30484.

Kim, J., Basak, J.M., and Holtzman, D.M. (2009). The role of apolipoprotein E in Alzheimer's disease. *Neuron* 63**,** 287-303.

Kim, J., Onstead, L., Randle, S., Price, R., Smithson, L., Zwizinski, C., Dickson, D.W., Golde, T., and Mcgowan, E. (2007). Abeta40 inhibits amyloid deposition in vivo. *J Neurosci* 27**,** 627-633.

Kim, S.H., Ikeuchi, T., Yu, C., and Sisodia, S.S. (2003). Regulated hyperaccumulation of presenilin-1 and the "gamma-secretase" complex. Evidence for differential intramembranous processing of transmembrane subatrates. *J Biol Chem* 278**,** 33992-34002.

Kimberly, W.T., Lavoie, M.J., Ostaszewski, B.L., Ye, W., Wolfe, M.S., and Selkoe, D.J. (2003). Gamma-secretase is a membrane protein complex comprised of presenilin, nicastrin, Aph-1, and Pen-2. *Proc Natl Acad Sci U S A* 100**,** 6382-6387.

Kopan, R., and Ilagan, M.X. (2004). Gamma-secretase: proteasome of the membrane? *Nat Rev Mol Cell Biol* 5**,** 499-504.

Kopan, R., and Ilagan, M.X. (2009). The canonical Notch signaling pathway: unfolding the activation mechanism. *Cell* 137**,** 216-233.

Kornilova, A.Y., Bihel, F., Das, C., and Wolfe, M.S. (2005). The initial substrate-binding site of gamma-secretase is located on presenilin near the active site. *Proc Natl Acad Sci U S A* 102**,** 3230-3235.

Krawitz, P., Haffner, C., Fluhrer, R., Steiner, H., Schmid, B., and Haass, C. (2005). Differential localization and identification of a critical aspartate suggest non-redundant proteolytic functions of the presenilin homologues SPPL2b and SPPL3. *J Biol Chem* 280**,** 39515-39523.

Kreft, A., Harrison, B., Aschmies, S., Atchison, K., Casebier, D., Cole, D.C., Diamantidis, G., Ellingboe, J., Hauze, D., Hu, Y., Huryn, D., Jin, M., Kubrak, D., Lu, P., Lundquist, J., Mann, C., Martone, R., Moore, W., Oganesian, A., Porte, A., Riddell, D.R., Sonnenberg-Reines, J., Stock, J.R., Sun, S.C., Wagner, E., Woller, K., Xu, Z., Zhou, H., and Steven Jacobsen, J. (2008). Discovery of a novel series of Notch-sparing gamma-secretase inhibitors. *Bioorg Med Chem Lett* 18**,** 4232-4236.

Kukar, T.L., Ladd, T.B., Bann, M.A., Fraering, P.C., Narlawar, R., Maharvi, G.M., Healy, B., Chapman, R., Welzel, A.T., Price, R.W., Moore, B., Rangachari, V., Cusack, B., Eriksen, J., Jansen-West, K., Verbeeck, C., Yager, D., Eckman, C., Ye, W., Sagi, S., Cottrell, B.A., Torpey, J., Rosenberry, T.L., Fauq, A., Wolfe, M.S., Schmidt, B., Walsh, D.M., Koo, E.H., and Golde, T.E. (2008). Substrate-targeting gamma-secretase modulators. *Nature* 453**,** 925-929.

Kumar-Singh, S., Theuns, J., Van Broeck, B., Pirici, D., Vennekens, K., Corsmit, E., Cruts, M., Dermaut, B., Wang, R., and Van Broeckhoven, C. (2006). Mean age-of-onset of familial alzheimer disease caused by presenilin mutations correlates with both increased Abeta42 and decreased Abeta40. *Hum Mutat* 27**,** 686-695.

Kuperstein, I., Broersen, K., Benilova, I., Rozenski, J., Jonckheere, W., Debulpaep, M., Vandersteen, A., Segers-Nolten, I., Van Der Werf, K., Subramaniam, V., Braeken, D., Callewaert, G., Bartic, C., D'hooge, R., Martins, I.C., Rousseau, F., Schymkowitz, J., and De Strooper, B. (2010). Neurotoxicity of Alzheimer's

disease Abeta peptides is induced by small changes in the Abeta42 to Abeta40 ratio. *EMBO J* 29**,** 3408-3420.

Lai, M.T., Chen, E., Crouthamel, M.C., Dimuzio-Mower, J., Xu, M., Huang, Q., Price, E., Register, R.B., Shi, X.P., Donoviel, D.B., Bernstein, A., Hazuda, D., Gardell, S.J., and Li, Y.M. (2003). Presenilin-1 and Presenilin-2 Exhibit Distinct yet Overlapping {gamma}-Secretase Activities. *J Biol Chem* 278**,** 22475-22481.

Lammich, S., Kojro, E., Postina, R., Gilbert, S., Pfeiffer, R., Jasionowski, M., Haass, C., and Fahrenholz, F. (1999). Constitutive and regulated alpha-secretase cleavage of Alzheimer's amyloid precursor protein by a disintegrin metalloprotease. *Proc Natl Acad Sci U S A* 96**,** 3922-3927.

Lammich, S., Okochi, M., Takeda, M., Kaether, C., Capell, A., Zimmer, A.K., Edbauer, D., Walter, J., Steiner, H., and Haass, C. (2002). Presenilin-dependent intramembrane proteolysis of CD44 leads to the liberation of its intracellular domain and the secretion of an Abeta-like peptide. *J Biol Chem* 277**,** 44754-44759.

Lanz, T.A., Himes, C.S., Pallante, G., Adams, L., Yamazaki, S., Amore, B., and Merchant, K.M. (2003). The gamma-secretase inhibitor N-[N-(3,5-difluorophenacetyl)-L-alanyl]-S-phenylglycine t-butyl ester reduces A beta levels in vivo in plasma and cerebrospinal fluid in young (plaque-free) and aged (plaque-bearing) Tg2576 mice. *J Pharmacol Exp Ther* 305**,** 864-871.

Laudon, H., Hansson, E.M., Melen, K., Bergman, A., Farmery, M.R., Winblad, B., Lendahl, U., Von Heijne, G., and Naslund, J. (2005). A nine-transmembrane domain topology for presenilin 1. *J Biol Chem* 280**,** 35352-35360.

Laudon, H., Karlstrom, H., Mathews, P.M., Farmery, M.R., Gandy, S.E., Lundkvist, J., Lendahl, U., and Naslund, J. (2004). Functional domains in presenilin 1: the Tyr-288 residue controls gamma-secretase activity and endoproteolysis. *J Biol Chem* 279**,** 23925-23932.

Lavoie, M.J., Fraering, P.C., Ostaszewski, B.L., Ye, W., Kimberly, W.T., Wolfe, M.S., and Selkoe, D.J. (2003). Assembly of the gamma-secretase complex involves early formation of an intermediate subcomplex of Aph-1 and nicastrin. *J Biol Chem* 278**,** 37213-37222.

Lee, J., Song, L., Terracina, G., Bara, T., Josien, H., Asberom, T., Sasikumar, T.K., Burnett, D.A., Clader, J., Parker, E.M., and Zhang, L. (2011). Identification of presenilin 1-selective gamma-secretase inhibitors with reconstituted gamma-secretase complexes. *Biochemistry* 50**,** 4973-4980.

Lee, S.F., Shah, S., Yu, C., Wigley, W.C., Li, H., Lim, M., Pedersen, K., Han, W., Thomas, P., Lundkvist, J., Hao, Y.H., and Yu, G. (2004). A conserved GXXXG motif in

APH-1 is critical for assembly and activity of the gamma-secretase complex. *J Biol Chem* 279**,** 4144-4152.

Lemberg, M.K., Bland, F.A., Weihofen, A., Braud, V.M., and Martoglio, B. (2001). Intramembrane proteolysis of signal peptides: an essential step in the generation of HLA-E epitopes. *J Immunol* 167**,** 6441-6446.

Lessard, C.B., Wagner, S.L., and Koo, E.H. (2010). And four equals one: presenilin takes the gamma-secretase role by itself. *Proc Natl Acad Sci U S A* 107**,** 21236-21237.

Levitan, D., Lee, J., Song, L., Manning, R., Wong, G., Parker, E., and Zhang, L. (2001). PS1 N- and C-terminal fragments form a complex that functions in APP processing and Notch signaling. *Proc Natl Acad Sci U S A* 98**,** 12186-12190.

Levy Lahad, E., Wasco, W., Poorkaj, P., Romano, D.M., Oshima, J., Pettingell, W.H., Yu, C.E., Jondro, P.D., Schmidt, S.D., Wang, K., and Et Al. (1995). Candidate gene for the chromosome 1 familial Alzheimer's disease locus. *Science* 269**,** 973-977.

Li, T., Li, Y.M., Ahn, K., Price, D.L., Sisodia, S.S., and Wong, P.C. (2011). Increased Expression of PS1 Is Sufficient to Elevate the Level and Activity of gamma-Secretase In Vivo. *PLoS One* 6**,** e28179.

Li, Y.M., Lai, M.T., Xu, M., Huang, Q., Dimuzio-Mower, J., Sardana, M.K., Shi, X.P., Yin, K.C., Shafer, J.A., and Gardell, S.J. (2000a). Presenilin 1 is linked with gamma-secretase activity in the detergent solubilized state. *Proc Natl Acad Sci U S A* 97**,** 6138-6143.

Li, Y.M., Xu, M., Lai, M.T., Huang, Q., Castro, J.L., Dimuzio-Mower, J., Harrison, T., Lellis, C., Nadin, A., Neduvelil, J.G., Register, R.B., Sardana, M.K., Shearman, M.S., Smith, A.L., Shi, X.P., Yin, K.C., Shafer, J.A., and Gardell, S.J. (2000b). Photoactivated gamma-secretase inhibitors directed to the active site covalently label presenilin 1. *Nature* 405**,** 689-694.

Liu, X., Zhao, X., Zeng, X., Bossers, K., Swaab, D.F., Zhao, J., and Pei, G. (2013). beta-Arrestin1 regulates gamma-secretase complex assembly and modulates amyloid-beta pathology. *Cell Res* 23**,** 351-365.

Lleo, A. (2008). Activity of gamma-secretase on substrates other than APP. *Curr Top Med Chem* 8**,** 9-16.

Lleo, A., Berezovska, O., Herl, L., Raju, S., Deng, A., Bacskai, B.J., Frosch, M.P., Irizarry, M., and Hyman, B.T. (2004). Nonsteroidal anti-inflammatory drugs lower Abeta42 and change presenilin 1 conformation. *Nat Med* 10**,** 1065-1066.

Lu, P., Bai, X.C., Ma, D., Xie, T., Yan, C., Sun, L., Yang, G., Zhao, Y., Zhou, R., Scheres, S.H., and Shi, Y. (2014). Three-dimensional structure of human gamma-secretase. *Nature* 512**,** 166-170.

Martone, R.L., Zhou, H., Atchison, K., Comery, T., Xu, J.Z., Huang, X., Gong, X., Jin, M., Kreft, A., Harrison, B., Mayer, S.C., Aschmies, S., Gonzales, C., Zaleska, M.M., Riddell, D.R., Wagner, E., Lu, P., Sun, S.C., Sonnenberg-Reines, J., Oganesian, A., Adkins, K., Leach, M.W., Clarke, D.W., Huryn, D., Abou-Gharbia, M., Magolda, R., Bard, J., Frick, G., Raje, S., Forlow, S.B., Balliet, C., Burczynski, M.E., Reinhart, P.H., Wan, H.I., Pangalos, M.N., and Jacobsen, J.S. (2009). Begacestat (GSI-953): a novel, selective thiophene sulfonamide inhibitor of amyloid precursor protein gamma-secretase for the treatment of Alzheimer's disease. *J Pharmacol Exp Ther* 331**,** 598-608.

Mayer, S.C., Kreft, A.F., Harrison, B., Abou-Gharbia, M., Antane, M., Aschmies, S., Atchison, K., Chlenov, M., Cole, D.C., Comery, T., Diamantidis, G., Ellingboe, J., Fan, K., Galante, R., Gonzales, C., Ho, D.M., Hoke, M.E., Hu, Y., Huryn, D., Jain, U., Jin, M., Kremer, K., Kubrak, D., Lin, M., Lu, P., Magolda, R., Martone, R., Moore, W., Oganesian, A., Pangalos, M.N., Porte, A., Reinhart, P., Resnick, L., Riddell, D.R., Sonnenberg-Reines, J., Stock, J.R., Sun, S.C., Wagner, E., Wang, T., Woller, K., Xu, Z., Zaleska, M.M., Zeldis, J., Zhang, M., Zhou, H., and Jacobsen, J.S. (2008). Discovery of begacestat, a Notch-1-sparing gamma-secretase inhibitor for the treatment of Alzheimer's disease. *J Med Chem* 51**,** 7348-7351.

Mclauchlan, J., Lemberg, M.K., Hope, G., and Martoglio, B. (2002). Intramembrane proteolysis promotes trafficking of hepatitis C virus core protein to lipid droplets. *EMBO J* 21**,** 3980-3988.

Mercken, M., Takahashi, H., Honda, T., Sato, K., Murayama, M., Nakazato, Y., Noguchi, K., Imahori, K., and Takashima, A. (1996). Characterization of human presenilin 1 using N-terminal specific monoclonal antibodies: Evidence that Alzheimer mutations affect proteolytic processing. *FEBS Lett* 389**,** 297-303.

Mitani, Y., Yarimizu, J., Saita, K., Uchino, H., Akashiba, H., Shitaka, Y., Ni, K., and Matsuoka, N. (2012). Differential effects between gamma-secretase inhibitors and modulators on cognitive function in amyloid precursor protein-transgenic and nontransgenic mice. *J Neurosci* 32**,** 2037-2050.

Miyashita, H., Maruyama, Y., Isshiki, H., Osawa, S., Ogura, T., Mio, K., Sato, C., Tomita, T., and Iwatsubo, T. (2011). Three-dimensional structure of the signal peptide peptidase. *J Biol Chem* 286**,** 26188-26197.

Morris, M., Maeda, S., Vossel, K., and Mucke, L. (2011). The many faces of tau. *Neuron* 70**,** 410-426.

Murayama, O., Murayama, M., Honda, T., Sun, X., Nihonmatsu, N., and Takashima, A. (1999). Twenty-nine missense mutations linked with familial Alzheimer's disease alter the processing of presenilin 1. *Prog Neuropsychopharmacol Biol Psychiatry* 23**,** 905-913.

Murray, M.M., Bernstein, S.L., Nyugen, V., Condron, M.M., Teplow, D.B., and Bowers, M.T. (2009). Amyloid beta protein: Abeta40 inhibits Abeta42 oligomerization. *J Am Chem Soc* 131**,** 6316-6317.

Nagy, C., Schuck, E., Ishibashi, A., Nakatani, Y., Rege, B., and Logovinsky, V. (2010). E2012, a novel gamma-secretase modulator, decreases plasma amyloid-beta (Aβ) levels in humans. *Alzheimers Dement , .* 6 (Suppl)**,** S574.

Nakaya, Y., Yamane, T., Shiraishi, H., Wang, H.Q., Matsubara, E., Sato, T., Dolios, G., Wang, R., De Strooper, B., Shoji, M., Komano, H., Yanagisawa, K., Ihara, Y., Fraser, P., St George-Hyslop, P., and Nishimura, M. (2005). Random mutagenesis of presenilin-1 identifies novel mutants exclusively generating long amyloid beta-peptides. *J Biol Chem* 280**,** 19070-19077.

Nam, S.H., Seo, S.J., Goo, J.S., Kim, J.E., Choi, S.I., Lee, H.R., Hwang, I.S., Jee, S.W., Lee, S.H., Bae, C.J., Park, J.Y., Kim, H.S., Shim, S.B., and Hwang, D.Y. (2011). Pen-2 overexpression induces Abeta-42 production, memory defect, motor activity enhancement and feeding behavior dysfunction in NSE/Pen-2 transgenic mice. *Int J Mol Med*.

Nicolas, M., Wolfer, A., Raj, K., Kummer, J.A., Mill, P., Van Noort, M., Hui, C.C., Clevers, H., Dotto, G.P., and Radtke, F. (2003). Notch1 functions as a tumor suppressor in mouse skin. *Nat Genet* 33**,** 416-421.

Niphakis, M.J., and Cravatt, B.F. (2014). Enzyme inhibitor discovery by activity-based protein profiling. *Annu Rev Biochem* 83**,** 341-377.

Nukina, N., and Ihara, Y. (1986). One of the antigenic determinants of paired helical filaments is related to tau protein. *J Biochem* 99**,** 1541-1544.

Nyborg, A.C., Herl, L., Berezovska, O., Thomas, A.V., Ladd, T.B., Jansen, K., Hyman, B.T., and Golde, T.E. (2006). Signal peptide peptidase (SPP) dimer formation as assessed by fluorescence lifetime imaging microscopy (FLIM) in intact cells. *Mol Neurodegener* 1**,** 16.

Nyborg, A.C., Jansen, K., Ladd, T.B., Fauq, A., and Golde, T.E. (2004a). A signal peptide peptidase (SPP) reporter activity assay based on the cleavage of type II membrane protein substrates provides further evidence for an inverted orientation of the SPP active site relative to presenilin. *J Biol Chem* 279**,** 43148-43156.

Nyborg, A.C., Kornilova, A.Y., Jansen, K., Ladd, T.B., Wolfe, M.S., and Golde, T.E. (2004b). Signal peptide peptidase forms a homodimer that is labeled by an active site-directed gamma-secretase inhibitor. *J Biol Chem* 279**,** 15153-15160.

Ohki, Y., Higo, T., Uemura, K., Shimada, N., Osawa, S., Berezovska, O., Yokoshima, S., Fukuyama, T., Tomita, T., and Iwatsubo, T. (2011). Phenylpiperidine-type gamma-secretase modulators target the transmembrane domain 1 of presenilin 1. *EMBO J* 30**,** 4815-4824.

Okochi, M., Steiner, H., Fukumori, A., Tanii, H., Tomita, T., Tanaka, T., Iwatsubo, T., Kudo, T., Takeda, M., and Haass, C. (2002). Presenilins mediate a dual intramembranous gamma-secretase cleavage of Notch-1. *Embo J* 21**,** 5408-5416.

Pamren, A., Wanngren, J., Tjernberg, L.O., Winblad, B., Bhat, R., Naslund, J., and Karlstrom, H. (2011). Mutations in Nicastrin Protein Differentially Affect Amyloid {beta}-Peptide Production and Notch Protein Processing. *J Biol Chem* 286**,** 31153-31158.

Placanica, L., Chien, J.W., and Li, Y.M. (2010). Characterization of an atypical gamma-secretase complex from hematopoietic origin. *Biochemistry* 49**,** 2796-2804.

Placanica, L., Tarassishin, L., Yang, G., Peethumnongsin, E., Kim, S.H., Zheng, H., Sisodia, S.S., and Li, Y.M. (2009a). Pen2 and Presenilin-1 Modulate the Dynamic Equilibrium of Presenilin-1 and Presenilin-2 {gamma}-Secretase Complexes. *J Biol Chem* 284**,** 2967-2977.

Placanica, L., Zhu, L., and Li, Y.M. (2009b). Gender- and age-dependent gamma-secretase activity in mouse brain and its implication in sporadic Alzheimer disease. *PLoS ONE* 4**,** e5088.

Podlisny, M.B., Citron, M., Amarante, P., Sherrington, R., Xia, W., Zhang, J., Diehl, T., Levesque, G., Fraser, P., Haass, C., Koo, E.H., Seubert, P., St George-Hyslop, P., Teplow, D.B., and Selkoe, D.J. (1997). Presenilin proteins undergo heterogeneous endoproteolysis between Thr291 and Ala299 and occur as stable N- and C-terminal fragments in normal and Alzheimer brain tissue. *Neurobiol Dis* 3**,** 325-337.

Portelius, E., Van Broeck, B., Andreasson, U., Gustavsson, M.K., Mercken, M., Zetterberg, H., Borghys, H., and Blennow, K. (2010). Acute effect on the Abeta isoform pattern in CSF in response to gamma-secretase modulator and inhibitor treatment in dogs. *J Alzheimers Dis* 21**,** 1005-1012.

Postina, R., Schroeder, A., Dewachter, I., Bohl, J., Schmitt, U., Kojro, E., Prinzen, C., Endres, K., Hiemke, C., Blessing, M., Flamez, P., Dequenne, A., Godaux, E., Van Leuven, F., and Fahrenholz, F. (2004). A disintegrin-metalloproteinase prevents amyloid plaque formation and hippocampal defects in an Alzheimer disease mouse model. *J Clin Invest* 113**,** 1456-1464.

Pozdnyakov, N., Murrey, H.E., Crump, C.J., Pettersson, M., Ballard, T.E., Am Ende, C.W., Ahn, K., Li, Y.M., Bales, K.R., and Johnson, D.S. (2013). gamma-Secretase modulator (GSM) photoaffinity probes reveal distinct allosteric binding sites on presenilin. *J Biol Chem* 288**,** 9710-9720.

Rappsilber, J., Mann, M., and Ishihama, Y. (2007). Protocol for micro-purification, enrichment, pre-fractionation and storage of peptides for proteomics using StageTips. *Nat Protoc* 2**,** 1896-1906.

Ratovitski, T., Slunt, H.H., Thinakaran, G., Price, D.L., Sisodia, S.S., and Borchelt, D.R. (1997). Endoproteolytic processing and stabilization of wild-type and mutant presenilin. *J Biol Chem* 272**,** 24536-24541.

Rawson, R.B., Zelenski, N.G., Nijhawan, D., Ye, J., Sakai, J., Hasan, M.T., Chang, T.Y., Brown, M.S., and Goldstein, J.L. (1997). Complementation cloning of S2P, a gene encoding a putative metalloprotease required for intramembrane cleavage of SREBPs. *Mol Cell* 1**,** 47-57.

Rostovtsev, V.V., Green, L.G., Fokin, V.V., and Sharpless, K.B. (2002). A stepwise huisgen cycloaddition process: copper(I)-catalyzed regioselective "ligation" of azides and terminal alkynes. *Angew Chem Int Ed Engl* 41**,** 2596-2599.

Sato, T., Ananda, K., Cheng, C.I., Suh, E.J., Narayanan, S., and Wolfe, M.S. (2008). Distinct pharmacological effects of inhibitors of signal peptide peptidase and gamma-secretase. *J Biol Chem* 283**,** 33287-33295.

Sato, T., Diehl, T.S., Narayanan, S., Funamoto, S., Ihara, Y., De Strooper, B., Steiner, H., Haass, C., and Wolfe, M.S. (2007). Active gamma-secretase complexes contain only one of each component. *J Biol Chem* 282**,** 33985-33993.

Sato, T., Nyborg, A.C., Iwata, N., Diehl, T.S., Saido, T.C., Golde, T.E., and Wolfe, M.S. (2006). Signal peptide peptidase: biochemical properties and modulation by nonsteroidal antiinflammatory drugs. *Biochemistry* 45**,** 8649-8656.

Schechter, I., and Berger, A. (1967). On the size of the active site in proteases. I. Papain. *Biochem Biophys Res Commun* 27**,** 157-162.

Scheuner, D., Eckman, C., Jensen, M., Song, X., Citron, M., Suzuki, N., Bird, T.D., Hardy, J., Hutton, M., Kukull, W., Larson, E., Levy-Lahad, E., Viitanen, M.,

Peskind, E., Poorkaj, P., Schellenberg, G., Tanzi, R., Wasco, W., Lannfelt, L., Selkoe, D., and Younkin, S. (1996). Secreted amyloid beta-protein similar to that in the senile plaques of Alzheimer's disease is increased in vivo by the presenilin 1 and 2 and APP mutations linked to familial Alzheimer's disease. *Nat Med* 2**,** 864-870.

Schroeter, E.H., Kisslinger, J.A., and Kopan, R. (1998). Notch-1 signalling requires ligand-induced proteolytic release of intracellular domain. *Nature* 393**,** 382-386.

Seiffert, D., Bradley, J.D., Rominger, C.M., Rominger, D.H., Yang, F., Meredith, J.E., Jr., Wang, Q., Roach, A.H., Thompson, L.A., Spitz, S.M., Higaki, J.N., Prakash, S.R., Combs, A.P., Copeland, R.A., Arneric, S.P., Hartig, P.R., Robertson, D.W., Cordell, B., Stern, A.M., Olson, R.E., and Zaczek, R. (2000). Presenilin-1 and -2 are molecular targets for gamma-secretase inhibitors. *J Biol Chem* 275**,** 34086-34091.

Selkoe, D.J. (2002). Alzheimer's disease is a synaptic failure. *Science* 298**,** 789-791.

Selkoe, D.J., and Wolfe, M.S. (2007). Presenilin: running with scissors in the membrane. *Cell* 131**,** 215-221.

Serneels, L., Van Biervliet, J., Craessaerts, K., Dejaegere, T., Horre, K., Van Houtvin, T., Esselmann, H., Paul, S., Schafer, M.K., Berezovska, O., Hyman, B.T., Sprangers, B., Sciot, R., Moons, L., Jucker, M., Yang, Z., May, P.C., Karran, E., Wiltfang, J., D'hooge, R., and De Strooper, B. (2009). gamma-Secretase heterogeneity in the Aph1 subunit: relevance for Alzheimer's disease. *Science* 324**,** 639-642.

Shah, S., Lee, S.F., Tabuchi, K., Hao, Y.H., Yu, C., Laplant, Q., Ball, H., Dann, C.E., 3rd, Sudhof, T., and Yu, G. (2005). Nicastrin functions as a gamma-secretase-substrate receptor. *Cell* 122**,** 435-447.

Shearman, M.S., Beher, D., Clarke, E.E., Lewis, H.D., Harrison, T., Hunt, P., Nadin, A., Smith, A.L., Stevenson, G., and Castro, J.L. (2000). L-685,458, an aspartyl protease transition state mimic, is a potent inhibitor of amyloid beta-protein precursor gamma-secretase activity. *Biochemistry* 39**,** 8698-8704.

Shelton, C.C., Zhu, L., Chau, D., Yang, L., Wang, R., Djaballah, H., Zheng, H., and Li, Y.M. (2009). Modulation of gamma-secretase specificity using small molecule allosteric inhibitors. *Proc Natl Acad Sci U S A* 106**,** 20228-20233.

Shen, J., Bronson, R.T., Chen, D.F., Xia, W., Selkoe, D.J., and Tonegawa, S. (1997). Skeletal and CNS defects in Presenilin-1-deficient mice. *Cell* 89**,** 629-639.

Sherrington, R., Rogaev, E.I., Liang, Y., Rogaeva, E.A., Levesque, G., Ikeda, M., Chi, H., Lin, C., Li, G., Holman, K., and Et Al. (1995). Cloning of a gene bearing missense mutations in early-onset familial Alzheimer's disease. *Nature* 375**,** 754-760.

Shirotani, K., Edbauer, D., Prokop, S., Haass, C., and Steiner, H. (2004). Identification of Distinct {gamma}-Secretase Complexes with Different APH-1 Variants. *J Biol Chem* 279**,** 41340-41345.

Skovronsky, D.M., Moore, D.B., Milla, M.E., Doms, R.W., and Lee, V.M. (2000). Protein kinase C-dependent alpha-secretase competes with beta-secretase for cleavage of amyloid-beta precursor protein in the trans-golgi network. *J Biol Chem* 275**,** 2568-2575.

Steiner, H., Duff, K., Capell, A., Romig, H., Grim, M.G., Lincoln, S., Hardy, J., Yu, X., Picciano, M., Fechteler, K., Citron, M., Kopan, R., Pesold, B., Keck, S., Baader, M., Tomita, T., Iwatsubo, T., Baumeister, R., and Haass, C. (1999a). A loss of function mutation of presenilin-2 interferes with amyloid beta-peptide production and notch signaling. *J Biol Chem* 274**,** 28669-28673.

Steiner, H., Kostka, M., Romig, H., Basset, G., Pesold, B., Hardy, J., Capell, A., Meyn, L., Grim, M.L., Baumeister, R., Fechteler, K., and Haass, C. (2000). Glycine 384 is required for presenilin-1 function and is conserved in bacterial polytopic aspartyl proteases. *Nat Cell Biol* 2**,** 848-851.

Steiner, H., Romig, H., Pesold, B., Philipp, U., Baader, M., Citron, M., Loetscher, H., Jacobsen, H., and Haass, C. (1999b). Amyloidogenic function of the Alzheimer's disease-associated presenilin 1 in the absence of endoproteolysis. *Biochemistry* 38**,** 14600-14605.

Struhl, G., and Adachi, A. (1998). Nuclear access and action of notch in vivo. *Cell* 93**,** 649-660.

Szychowski, J., Mahdavi, A., Hodas, J.J., Bagert, J.D., Ngo, J.T., Landgraf, P., Dieterich, D.C., Schuman, E.M., and Tirrell, D.A. (2010). Cleavable biotin probes for labeling of biomolecules via azide-alkyne cycloaddition. *J Am Chem Soc* 132**,** 18351-18360.

Takahashi, Y., Hayashi, I., Tominari, Y., Rikimaru, K., Morohashi, Y., Kan, T., Natsugari, H., Fukuyama, T., Tomita, T., and Iwatsubo, T. (2003). Sulindac sulfide is a noncompetitive gamma-secretase inhibitor that preferentially reduces Abeta 42 generation. *J Biol Chem* 278**,** 18664-18670.

Takasugi, N., Tomita, T., Hayashi, I., Tsuruoka, M., Niimura, M., Takahashi, Y., Thinakaran, G., and Iwatsubo, T. (2003). The role of presenilin cofactors in the gamma-secretase complex. *Nature* 422**,** 438-441.

Tarassishin, L., Yin, Y.I., Bassit, B., and Li, Y.M. (2004). Processing of Notch and amyloid precursor protein by gamma-secretase is spatially distinct. *Proc Natl Acad Sci U S A* 101**,** 17050-17055.

Teranishi, Y., Hur, J.Y., Gu, G.J., Kihara, T., Ishikawa, T., Nishimura, T., Winblad, B., Behbahani, H., Kamali-Moghaddam, M., Frykman, S., and Tjernberg, L.O. (2012). Erlin-2 is associated with active gamma-secretase in brain and affects amyloid beta-peptide production. *Biochem Biophys Res Commun* 424**,** 476-481.

Teranishi, Y., Hur, J.Y., Welander, H., Franberg, J., Aoki, M., Winblad, B., Frykman, S., and Tjernberg, L.O. (2010). Affinity pulldown of gamma-secretase and associated proteins from human and rat brain. *J Cell Mol Med* 14**,** 2675-2686.

Thathiah, A., Horre, K., Snellinx, A., Vandewyer, E., Huang, Y., Ciesielska, M., De Kloe, G., Munck, S., and De Strooper, B. (2013). beta-arrestin 2 regulates Abeta generation and gamma-secretase activity in Alzheimer's disease. *Nat Med* 19**,** 43-49.

Thathiah, A., Spittaels, K., Hoffmann, M., Staes, M., Cohen, A., Horre, K., Vanbrabant, M., Coun, F., Baekelandt, V., Delacourte, A., Fischer, D.F., Pollet, D., De Strooper, B., and Merchiers, P. (2009). The orphan G protein-coupled receptor 3 modulates amyloid-beta peptide generation in neurons. *Science* 323**,** 946-951.

Thinakaran, G., Borchelt, D.R., Lee, M.K., Slunt, H.H., Spitzer, L., Kim, G., Ratovitsky, T., Davenport, F., Nordstedt, C., Seeger, M., Hardy, J., Levey, A.I., Gandy, S.E., Jenkins, N.A., Copeland, N.G., Price, D.L., and Sisodia, S.S. (1996). Endoproteolysis of presenilin 1 and accumulation of processed derivatives in vivo. *Neuron* 17**,** 181-190.

Thinakaran, G., Harris, C.L., Ratovitski, T., Davenport, F., Slunt, H.H., Price, D.L., Borchelt, D.R., and Sisodia, S.S. (1997). Evidence that levels of presenilins (PS1 and PS2) are coordinately regulated by competition for limiting cellular factors. *J Biol Chem* 272**,** 28415-28422.

Tian, Y., Bassit, B., Chau, D., and Li, Y.M. (2010a). An APP inhibitory domain containing the Flemish mutation residue modulates gamma-secretase activity for Abeta production. *Nat Struct Mol Biol* 17**,** 151-158.

Tian, Y., Crump, C.J., and Li, Y.M. (2010b). Dual role of {alpha}-Secretase Cleavage in the regulation of {gamma}-secretase activity for amyloid production. *J Biol Chem*.

Tornoe, C.W., Christensen, C., and Meldal, M. (2002). Peptidotriazoles on solid phase: [1,2,3]-triazoles by regiospecific copper(i)-catalyzed 1,3-dipolar cycloadditions of terminal alkynes to azides. *J Org Chem* 67**,** 3057-3064.

Uemura, K., Farner, K.C., Hashimoto, T., Nasser-Ghodsi, N., Wolfe, M.S., Koo, E.H., Hyman, B.T., and Berezovska, O. (2010). Substrate docking to gamma-secretase allows access of gamma-secretase modulators to an allosteric site. *Nat Commun* 1**,** 130.

Urban, S., Lee, J.R., and Freeman, M. (2001). Drosophila rhomboid-1 defines a family of putative intramembrane serine proteases. *Cell* 107**,** 173-182.

Van Scherpenzeel, M., Moret, E.E., Ballell, L., Liskamp, R.M., Nilsson, U.J., Leffler, H., and Pieters, R.J. (2009). Synthesis and evaluation of new thiodigalactoside-based chemical probes to label galectin-3. *Chembiochem* 10**,** 1724-1733.

Vetrivel, K.S., Gong, P., Bowen, J.W., Cheng, H., Chen, Y., Carter, M., Nguyen, P.D., Placanica, L., Wieland, F.T., Li, Y.M., Kounnas, M.Z., and Thinakaran, G. (2007). Dual roles of the transmembrane protein p23/TMP21 in the modulation of amyloid precursor protein metabolism. *Mol Neurodegener* 2**,** 4.

Vetrivel, K.S., Zhang, X., Meckler, X., Cheng, H., Lee, S., Gong, P., Lopes, K.O., Chen, Y., Iwata, N., Yin, K.J., Lee, J.M., Parent, A.T., Saido, T.C., Li, Y.M., Sisodia, S.S., and Thinakaran, G. (2008). Evidence that CD147 modulation of beta-amyloid (Abeta) levels is mediated by extracellular degradation of secreted Abeta. *J Biol Chem* 283**,** 19489-19498.

Villa, J.C., Chiu, D., Brandes, A.H., Escorcia, F.E., Villa, C.H., Maguire, W.F., Hu, C.J., De Stanchina, E., Simon, M.C., Sisodia, S.S., Scheinberg, D.A., and Li, Y.M. (2014). Nontranscriptional role of Hif-1alpha in activation of gamma-secretase and notch signaling in breast cancer. *Cell Rep* 8**,** 1077-1092.

Walter, J., and Van Echten-Deckert, G. (2013). Cross-talk of membrane lipids and Alzheimer-related proteins. *Molecular Neurodegeneration* 8**,** 34.

Wang, J., Zhang, C.J., Zhang, J., He, Y., Lee, Y.M., Chen, S., Lim, T.K., Ng, S., Shen, H.M., and Lin, Q. (2015). Mapping sites of aspirin-induced acetylations in live cells by quantitative acid-cleavable activity-based protein profiling (QA-ABPP). *Sci Rep* 5**,** 7896.

Wang, R., Wang, B., He, W., and Zheng, H. (2006). Wild-type presenilin 1 protects against Alzheimer disease mutation-induced amyloid pathology. *J Biol Chem* 281**,** 15330-15336.

Wang, X., Huang, T., Zhao, Y., Zheng, Q., Thompson, R.C., Bu, G., Zhang, Y.W., Hong, W., and Xu, H. (2014). Sorting Nexin 27 Regulates Abeta Production through Modulating gamma-Secretase Activity. *Cell Rep* 9**,** 1023-1033.

Ward, A., Crean, S., Mercaldi, C.J., Collins, J.M., Boyd, D., Cook, M.N., and Arrighi, H.M. (2012). Prevalence of apolipoprotein E4 genotype and homozygotes (APOE e4/4) among patients diagnosed with Alzheimer's disease: a systematic review and meta-analysis. *Neuroepidemiology* 38**,** 1-17.

Weggen, S., Eriksen, J.L., Das, P., Sagi, S.A., Wang, R., Pietrzik, C.U., Findlay, K.A., Smith, T.E., Murphy, M.P., Bulter, T., Kang, D.E., Marquez-Sterling, N., Golde, T.E., and Koo, E.H. (2001). A subset of NSAIDs lower amyloidogenic Abeta42 independently of cyclooxygenase activity. *Nature* 414**,** 212-216.

Weihofen, A., Binns, K., Lemberg, M.K., Ashman, K., and Martoglio, B. (2002). Identification of signal peptide peptidase, a presenilin-type aspartic protease. *Science* 296**,** 2215-2218.

Weihofen, A., Lemberg, M.K., Friedmann, E., Rueeger, H., Schmitz, A., Paganetti, P., Rovelli, G., and Martoglio, B. (2003). Targeting presenilin-type aspartic protease signal peptide peptidase with gamma-secretase inhibitors. *J Biol Chem* 278**,** 16528-16533.

Weihofen, A., Lemberg, M.K., Ploegh, H.L., Bogyo, M., and Martoglio, B. (2000). Release of signal peptide fragments into the cytosol requires cleavage in the transmembrane region by a protease activity that is specifically blocked by a novel cysteine protease inhibitor. *J Biol Chem* 275**,** 30951-30956.

Wolfe, M.S. (2012). gamma-Secretase inhibitors and modulators for Alzheimer's disease. *J Neurochem* 120 Suppl 1**,** 89-98.

Wolfe, M.S., Citron, M., Diehl, T.S., Xia, W., Donkor, I.O., and Selkoe, D.J. (1998). A substrate-based difluoro ketone selectively inhibits Alzheimer's gamma-secretase activity. *J Med Chem* 41**,** 6-9.

Wolfe, M.S., Xia, W., Ostaszewski, B.L., Diehl, T.S., Kimberly, W.T., and Selkoe, D.J. (1999). Two transmembrane aspartates in presenilin-1 required for presenilin endoproteolysis and gamma-secretase activity. *Nature* 398**,** 513-517.

Wong, G.T., Manfra, D., Poulet, F.M., Zhang, Q., Josien, H., Bara, T., Engstrom, L., Pinzon-Ortiz, M., Fine, J.S., Lee, H.J., Zhang, L., Higgins, G.A., and Parker, E.M. (2004). Chronic treatment with the gamma-secretase inhibitor LY-411,575 inhibits beta-amyloid peptide production and alters

lymphopoiesis and intestinal cell differentiation. *J Biol Chem* 279**,** 12876-12882.

Wong, P.C., Zheng, H., Chen, H., Becher, M.W., Sirinathsinghji, D.J., Trumbauer, M.E., Chen, H.Y., Price, D.L., Van Der Ploeg, L.H., and Sisodia, S.S. (1997). Presenilin 1 is required for Notch1 and DII1 expression in the paraxial mesoderm. *Nature* 387**,** 288-292.

Wu, J., Petralia, R.S., Kurushima, H., Patel, H., Jung, M.Y., Volk, L., Chowdhury, S., Shepherd, J.D., Dehoff, M., Li, Y., Kuhl, D., Huganir, R.L., Price, D.L., Scannevin, R., Troncoso, J.C., Wong, P.C., and Worley, P.F. (2011). Arc/Arg3.1 Regulates an Endosomal Pathway Essential for Activity-Dependent beta-Amyloid Generation. *Cell* 147**,** 615-628.

Xia, X., Qian, S., Soriano, S., Wu, Y., Fletcher, A.M., Wang, X.J., Koo, E.H., Wu, X., and Zheng, H. (2001). Loss of presenilin 1 is associated with enhanced beta-catenin signaling and skin tumorigenesis. *Proc Natl Acad Sci U S A* 98**,** 10863-10868.

Xie, T., Yan, C., Zhou, R., Zhao, Y., Sun, L., Yang, G., Lu, P., Ma, D., and Shi, Y. (2014). Crystal structure of the gamma-secretase component nicastrin. *Proc Natl Acad Sci U S A* 111**,** 13349-13354.

Yan, Y., and Wang, C. (2007). Abeta40 protects non-toxic Abeta42 monomer from aggregation. *J Mol Biol* 369**,** 909-916.

Yang, G., Yin, Y.I., Chun, J., Shelton, C.C., Ouerfelli, O., and Li, Y.M. (2009). Stereo-controlled synthesis of novel photoreactive gamma-secretase inhibitors. *Bioorg Med Chem Lett* 19**,** 922-925.

Yang, T., Arslanova, D., Xu, X., Li, Y.M., and Xia, W. (2010). In vivo manifestation of Notch related phenotypes in zebrafish treated with Alzheimer's amyloid reducing gamma-secretase inhibitors. *J Neurochem* 113**,** 1200-1209.

Yang, Y., Hahne, H., Kuster, B., and Verhelst, S.H. (2013). A simple and effective cleavable linker for chemical proteomics applications. *Mol Cell Proteomics* 12**,** 237-244.

Yang, Y., and Verhelst, S.H. (2013). Cleavable trifunctional biotin reagents for protein labelling, capture and release. *Chem Commun (Camb)* 49**,** 5366-5368.

Yu, G., Nishimura, M., Arawaka, S., Levitan, D., Zhang, L., Tandon, A., Song, Y.Q., Rogaeva, E., Chen, F., Kawarai, T., Supala, A., Levesque, L., Yu, H., Yang, D.S., Holmes, E., Milman, P., Liang, Y., Zhang, D.M., Xu, D.H., Sato, C., Rogaev, E., Smith, M., Janus, C., Zhang, Y., Aebersold, R., Farrer, L.S., Sorbi, S., Bruni, A.,

Fraser, P., and St George Hyslop, P. (2000). Nicastrin modulates presenilin-mediated notch/glp-1 signal transduction and betaAPP processing. *Nature* 407**,** 48-54.

Zhang, J., Kang, D.E., Xia, W., Okochi, M., Mori, H., Selkoe, D.J., and Koo, E.H. (1998). Subcellular distribution and turnover of presenilins in transfected cells. *J Biol Chem* 273**,** 12436-12442.

Zhang, X., Hoey, R., Koide, A., Dolios, G., Paduch, M., Nguyen, P., Wu, X., Li, Y., Wagner, S.L., Wang, R., Koide, S., and Sisodia, S.S. (2014). Synthetic Antibody Fragment Targeting Nicastrin Affects Assembly and Trafficking of gamma-Secretase. *J Biol Chem*.

Zhang, X., Hoey, R.J., Lin, G., Koide, A., Leung, B., Ahn, K., Dolios, G., Paduch, M., Ikeuchi, T., Wang, R., Li, Y.M., Koide, S., and Sisodia, S.S. (2012). Identification of a tetratricopeptide repeat-like domain in the nicastrin subunit of gamma-secretase using synthetic antibodies. *Proc Natl Acad Sci U S A* 109**,** 8534-8539.

Zhang, Y.W., and Xu, H. (2010). Substrate check of gamma-secretase. *Nat Struct Mol Biol* 17**,** 140-141.

Zhao, G., Liu, Z., Ilagan, M.X., and Kopan, R. (2010). Gamma-secretase composed of PS1/Pen2/Aph1a can cleave notch and amyloid precursor protein in the absence of nicastrin. *J Neurosci* 30**,** 1648-1656.

Zhou, S., Zhou, H., Walian, P.J., and Jap, B.K. (2005). CD147 is a regulatory subunit of the gamma-secretase complex in Alzheimer's disease amyloid beta-peptide production. *Proc Natl Acad Sci U S A* 102**,** 7499-7504.

Zhu, M., Tao, Y., He, Q., Gao, H., Song, F., Sun, Y.M., Li, H.L., Wu, Z.Y., and Saffen, D. (2014). A common GSAP promoter variant contributes to Alzheimer's disease liability. *Neurobiol Aging* 35**,** 2656 e2651-2657.